Functional genomics of cartwheel proteins: Bld10 localizes to parental basal bodies and forms a protein complex

I n a u g u r a l - D i s s e r t a t i o n

zur

Erlangung des Doktorgrades

der Mathematisch-Naturwissenschaftlichen Fakultät

der Universität zu Köln

vorgelegt von

Nelli Vardanyan

aus Armavir, Armenien

Köln

2009

Berichterstatter:	**Prof. Dr. Michael Melkonian**
	Prof. Dr. Maria Leptin
Tag der mündlichen Prüfung:	**20.10.2009**

To my beloved husband

Abstract

In *Chlamydomonas reinhardtii* basal body formation occurs in a similar manner to centriole formation. Therefore, this organism provides an excellent model system for the study of the basal bodies/centrioles. The cartwheel with its ninefold symmetry and characteristic hub and spoke structure can be observed at the onset of basal body assembly. It is a highly conserved structure that determines the ninefold symmetry of centrioles/basal bodies. Although this structure has fascinated many scientists until now little is known about the cartwheel composition and function. To obtain knowledge about the cartwheel structural composition two key approaches were employed in this study: an isolation and purification approach and an affinity-based approach.

It is crucial to emphasize that to date no cartwheel structure has been purified from any eukaryote. To address this question, an attempt was made to purify the cartwheel structure biochemically by isolating the probasal bodies, which is predominantly comprised of cartwheels. It is important to stress the significance of the biochemical purification of the cartwheel structure as a novel concept, since it can provide a more direct way to study the whole cartwheel. To develop this enabling strategy three main parameters were tested: suitable *Chlamydomonas* cell wall deficient mutants, buffers and detergents. Despite progress made, isolation of the probasal bodies was not achieved.

Bld10p (175 kDa) is the first protein known to be localized to the cartwheel. By generating antibodies against this protein I aimed on one hand to identify the interacting proteins of Bld10 and on the other hand to have a closer look at the Bld10 localization. Therefore, polyclonal antibodies (against the C-terminal, the N-terminal and middle part) were raised in rabbits. Colocalization of Bld10 together with prominent cytoskeleton proteins such as centrin and tubulin helped to better understand the localization of the Bld10.

The present study reports two key findings. First, it has been determined by employing BN-PAGE followed by Western blotting that Bld10p forms a complex with molecular weight of about 600 kDa. Second, the immunolocalization data reveal Bld10p localization to parental basal bodies rather than to probasal bodies. Since the probasal bodies consist primarily of cartwheel we question the role of the Bld10 as a pivotal structural protein of the cartwheel.

Deutsche Kurzzusammenfassung

Bei *Chlamydomonas reinhardtii* erfolgt die Entstehung der Basalkörper in ähnlicher Weise wie die Bildung von Centriolen, weshalb dieser Organismus als gutes Modelsystem zu Erforschung dieser Strukturen dient. Das Cartwheel mit seiner 9-fachen Symmetrie und charakteristischen Struktur kann schon zu Beginn der Basalkörper-Entstehung beobachtet werden. Es handelt sich hierbei um eine hoch konservierte Struktur, die die 9-fache Symmetrie der Basalkörper bestimmt. Obwohl diese Struktur bis heute viele Wissenschaftler fasziniert, ist immer noch sehr wenig über ihre Zusammensetzung und Funktion bekannt. In der vorliegenden Arbeit wurden 2 unterschiedliche Ansätze verfolgt, um mehr über die strukturelle Zusammensetzung des Cartwheels herauszufinden: ein Isolierungs-/Reinigungs-Ansatz und ein Affinitäts-basierter Ansatz.

Es ist wichtig zu betonen, dass es bis heute bei keinem Eukaryoten gelungen ist, das Cartwheel zu isolieren. Um dieser Fragestellung nachzugehen, wurde beim Isolierungsansatz versucht, diese Struktur durch biochemische Methoden zu reinigen. Dazu sollten Probasalkörper isoliert werden, die zum größten Teil aus Cartwheel bestehen. Dieser Ansatz stellt ein neuartiges Konzept dar, das einen direkten Zugang zur Erforschung des gesamten Cartwheels ebnen könnte. Um diese Strategie entwickeln zu können, wurden 3 Hauptparameter getestet: geeignete *Chlamydomonas* Zellwand-Mutanten, sowie unterschiedliche Puffer und Detergenzien. Obwohl ein gewisser Fortschritt erzielt werden konnte, wurde keine Reinigung von Probasalkörpern erreicht.

Blp10p (175 kDa) ist das erste Protein, für das eine Lokalisierung am Cartwheel festgestellt wurde. Zunächst wurden Antikörper gegen unterschiedliche Bereiche von Bld10 hergestellt: gegen den C-terminalen, den mittleren und den N-terminalen Teil. Zum einen wurden diese Antikörper verwendet, um mögliche Interaktionspartner von Bld10 zu identifizieren. Andererseits sollte die Bld10-Lokalisierung genauer untersucht werden. Colokalisierungsexperimente mit bekannten Cytoskelettproteinen wie Centrin und Tubulin trugen zu einem besseren Verständnis der Bld10-Lokalisierung bei.

In der vorliegenden Arbeit wurden zwei entscheidende Entdeckungen gemacht. Zum einen konnte durch BN-PAGE mit anschließendem Western-Blot gezeigt werden, dass Bld10 einen Komplex von etwa 600 kDa bildet. Zum anderen zeigten die Bld10-Lokalisierungs-Studien eher eine Lokalisierung an den Basal- als an den Probasalkörpern. Da Probasalkörper

hauptsächlich aus Cartwheel aufgebaut sind, bestehen Zweifel an der Rolle von Bld10 als entscheidendem Strukturprotein des Cartwheels.

Table of contents

1. Introduction

1.1. *Chlamydomonas reinhardtii* as a model organism

Chlamydomonas reinhardtii occupies an important place in the eukaryotic world and presumably diverged from land plants about 1 billion years ago (Merchant et al., 2007). *Chlamydomonas reinhardtii* is a biflagellate unicellular photosynthetic alga, which serves as a powerful model of various morphological, physiological, cell-biological and genetic studies. The *Chlamydomonas reinhardtii* wild type cell is about 10 µm, with two anterior flagella (10 µm-12 µm), extending through specialized collar regions in the cell wall (Figure 1). The cell wall comprises seven layers and consists mainly of hydroxyproline-rich glycoproteins, but not cellulose. Cell wall-less mutants are widely used in different studies, including this PhD Thesis (see chapter 2.2.1). The only chloroplast (with one pyrenoid) occupies a large part of the cell, and surrounds partly the nucleus (Harris, 2001). The nuclear genome possesses 17 linkage groups, which likely correspond to 17 chromosomes (Merchant et al., 2007).

C. reinhardtii vegetative cells are haploid and under nitrogen deprivation haploid gametes are developed. There are two mating types (mt+) and (mt-), which can form a diploid zygospore, if they fuse. The zygospore undergoes meiosis during which four flagellated haploid cells are released; two of them are (mt+) and the other two are (mt-) (Harris, 2001).

Chlamydomonas is a eukaryote with haploid genetics, similar to yeast, but unlike yeast it has both chloroplast and flagella. In fact, tetrad analysis, which is a powerful tool in yeast and fungal genetics, was first described in *Chlamydomonas* (Pascher, 1918). Moreover, the genetic evidence that chloroplasts have a separate genome was as well obtained in *Chlamydomonas* (Sager, 1960). Besides, *Chlamydomonas* is the only organism in which transformation techniques have been developed for all three genomes: nuclear (Kindle et al., 1989; Kindle, 1990), chloroplast (Boynton et al., 1988) and mitochondrial (Boynton et al., 1988; Randolph-Anderson et al., 1993)

The laboratory strains of *Chlamydomonas reinhardtii* are presumably derived from field-isolated zygote isolated by G.M. Smith in Massachusetts in 1945 (Harris, 1989). Because of its ability to grow photoheterotrophically on a carbon source *Chlamydomonas reinhardtii* has emerged as a primary laboratory species of the genus *Chlamydomonas.* However, as it

was reported by Pröschold et al, numerous crosses and exchanges among laboratories brought confusion concerning strain genealogy more than 60 years after the first laboratory strain isolation (Pröschold et al., 2005).

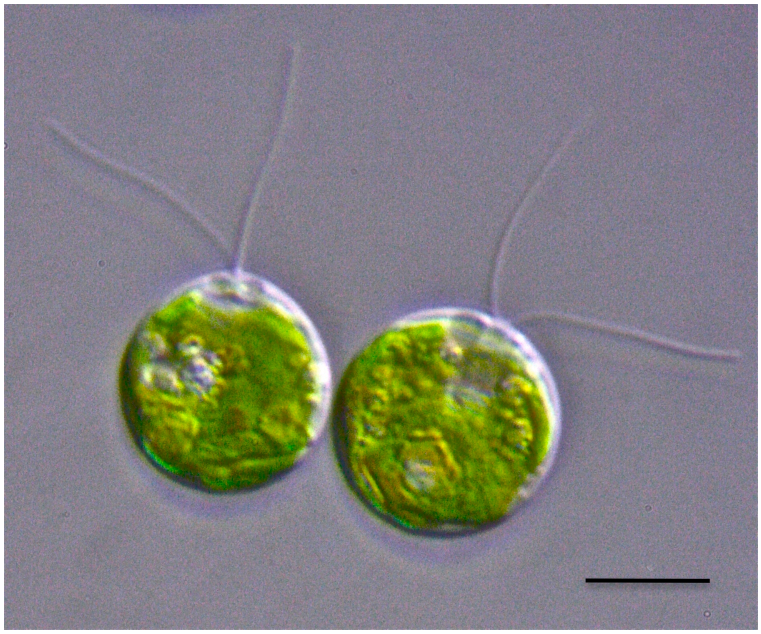

Figure 1. *Chlamydomonas reinhardtii cw92* mutant. Light microscopic image (differential interference contrast) of *cw92* cells. Scale bar, 5 µm.

A revolutionary breakthrough for *Chlamydomonas reinhardtii* as a model system was the generation of a comprehensive expressed sequence tag (EST) library that to date comprises about 200.000 ESTs (Asamizu et al., 1999; Asamizu et al., 2000; Shrager et al., 2003; Asamizu and Nakamura, 2004) and the sequencing of the 120-megabase nuclear genome by the Joint Genome Institute (Merchant et al., 2007). This enabled reverse genetics approaches in *Chlamydomonas reinhardtii,* like homologous recombination (Kindle et al., 1989; Sodeinde and Kindle, 1993; Zorin et al., 2009), gene silencing by RNA interference (Ruiz-Binder et al., 2002; Schroda, 2006; Schulz-Raffelt et al., 2007). However, homologous recombination is seems to be very inefficient in *Chlamydomonas*. Also, it has been implicated that the *Chlamydomonas* genome contains genes encoding Dicer and Argonaute nuclease (AGO) proteins, thereby determining its ability to perform RNA silencing (Cerutti and Casas-Mollano, 2006). Interestingly, it has been shown that *Chlamydomonas reinhardtii* has

miRNAs, which appear to be putative evolutionary precursors of miRNAs and types of siRNAs like those in higher plants. miRNAs and siRNAs similarity in an alga and in higher plants could be the indication that complex RNA-silencing systems evolved before multicellularity and were present in their common ancestor – most likely a primitive unicellular alga. This story becomes even more interesting considering the fact that miRNAs have been previously associated with developmental regulation and multicellularity (Molnar et al., 2007). However, *Chlamydomonas* genome has a very high GC content (over 65%), which cause various difficulties in genetical manipulations.

In addition, a recent data on *C. reinhardtii* proteomics provides data on the subcellular localization of the identified proteins and can be useful for adapting the publicly available targeting prediction tools to *Chlamydomonas* (Rolland et al., 2009).

Among many research problems being studied in this organism, like phototaxis, cellular division, cell-cell recognition, mitochondrial function and hydrogen production, two research areas have fundamental importance: chloroplast biogenesis and the assembly of basal bodies and flagella. Since *Chlamydomonas* is a photoheterotroph, mutations in photosynthetic genes are not lethal if an acetate source is provided. Many „ac“ mutants have been isolated and about 50 have been placed on the genetic map (Harris, 1989). *Chlamydomonas* possesses a pair of flagella to swim and recognize different conditions of environment. For flagellar formation and maintenance, transport of components from cytoplasm into the flagellum is necessary. This process is called intraflagellar transport (IFT) and was first identified in *C. reinhardtii* by the group of Joel Rosenbaum (Kozminski et al., 1993). After the discovery of IFT cellular machinery it became apparent that it is an evolutionary conserved process and is essential for the assembly of flagella in all eukaryotes (Rosenbaum and Witman, 2002; Scholey, 2008). Currently, many components of the core IFT machinery are known: at least 17 proteins make up the IFT particle. Most importantly, discoveries linking IFT to polycystic kidney disease (PKD), primary cilia dyskinesia (PCD) and other developmental phenotypes have shown that primary cilia and IFT are required for processes such as kidney tubule and retinal tissue development, limb bud morphogenesis and organ patterning (Cole, 2003; Blacque et al., 2008). Another syndrome connected with PCD, also known as immotile cilia syndrome, is hydrocephalus, which seems to be associated with defects in the central pair microtubules (Davy and Robinson, 2003; Lechtreck and Witman, 2007). Some rare human syndromes, including Senior-Loken syndrome, Jeune

syndrome, Bardet-Biedl Syndrome (BBS) are also characterized as cilia related disorders. Interestingly, patients with these syndromes might suffer from other clinical problems, such as obesity, hypertension and increased risk for diabetes (Rosenbaum and Witman, 2002; Boletta and Germino, 2003; Pazour and Witman, 2003). Flagella/cilia proteomic analyses have been completed in human cells (Ostrowski et al., 2002; Marshall, 2004), *Chlamydomonas* (Pazour et al., 2005) and trypanosomes (Broadhead et al., 2006). Remarkably, it has been shown that *Chlamydomonas* and animals have common genes, which are derived from the last plant-animal ancestor, many of which were lost in angiosperms, in particular those encoding flagella and basal body associated proteins. This is consistent with retaining flagella and basal bodies as cilia and centrioles in animals, respectively, and their absence in angiosperms (Merchant et al., 2007).

To summarize, basal bodies/centrioles are highly conserved in *Chlamydomonas reinhardtii*, which makes this organism an important model system to study these structures.

1.2. Microtubule organizing centers: centrosome, spindle pole bodies, basal apparatus

Centrosomes (from Latin for “central body”) are microtubule organizing centers of eukaryotic cells and presumably have evolved in multicellular organisms from the unicellular ancestor (Figure 2A) (Azimzadeh, 2004). The term “centrosome” was first described in late the 19th century by the early cell-biologists Boveri and van Beneden (Boveri, 1901). Since the centrosome was defined first by morphology rather than function various terms were used to describe this organelle until the term microtubule organizing center (MTOC) was introduced by Pickett-Heaps, which is now widely accepted by the scientific community (Pickett-Heaps, 1969). MTOC refers to all cellular structures that assemble and organize microtubule arrays. In different organisms the centrosome architecture can show a diversity of forms (Vogel et al., 1997; Graf et al., 1999) (Figure 2).

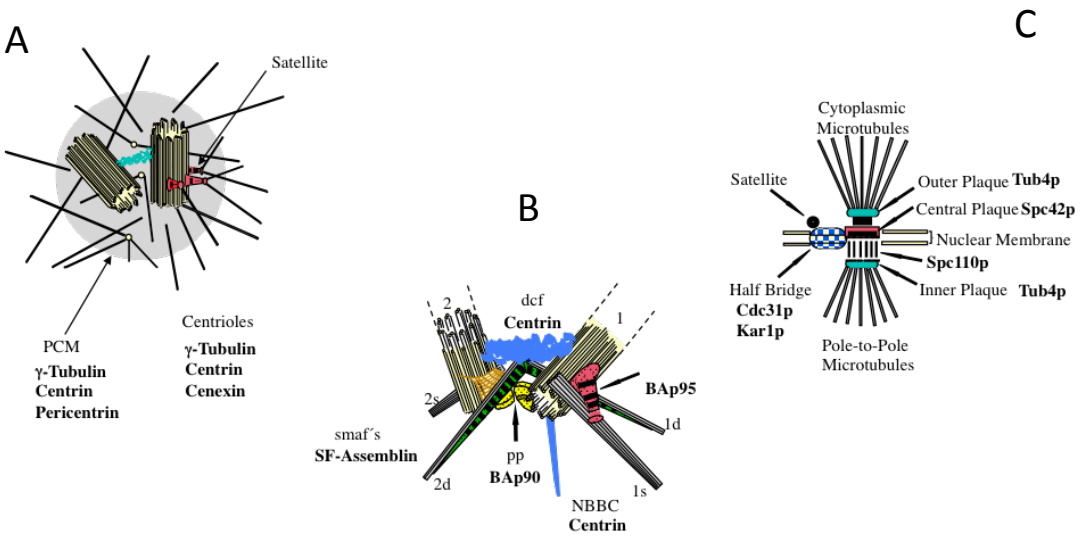

Figure 2. Microtubule organizing centers in mammals, algae and yeast. Three representative types of MTOC with their protein localizations. The mammalian centrosome **(A)** is composed of 2 centrioles and pericentriolar material (PCM). The algal basal apparatus **(B)** consists of the basal bodies, probasal bodies and arrays of fibers and microtubules. The centrin scaffold is colored blue. Yeast Spindle Poly Body **(C)** is a multilayer organelle, which does not contain centrioles. These layers are: an outer plaque, an electrondense central plaque, which is at the level of the nuclear envelope, and an inner plaque. The diagram was kindly provided by Dr. S. Geimer.

Hence, the centrosome is the microtubule organizing center of animal cells, whereas in yeast its equivalent is called “spindle pole body” (SPB) (Figure 2C). Most fungi have lost their ability to make centrioles and cilia; nevertheless they have evolved the morphologically distinct structure spindle pole body, which functions as a principal site of microtubule nucleation.

Despite the fact that common molecular mechanisms are likely to be involved in both cases, the centrosome from animal cells shows substantial complexity, in comparison with the simple organization of spindle pole bodies in fungi (Bornens, 2002). Although extensive research has been done towards understanding of SPBs, it is still not absolutely clear how they are related to centrioles. Some of the important components in these structures are highly conserved, which proves the fact that they are functional orthologs. Insights are coming from the studies of components like centrin, a calcium-binding protein identified in the flagellate green alga *Tetraselmis striata* (Salisbury et al., 1984). Centrins are highly conserved, ubiquitous proteins, known to be involved in assembly of centrosomes, SPBs, and the basal bodies (Salisbury, 1995; Salisbury et al., 2002).

Higher plants, in contrast, lack centrosomes or spindle pole bodies. Instead, the nuclear envelope itself appears to function as the main MTOC for microtubule nucleation and spindle organization during plant cell mitosis (Lambert, 1993). Microtubule arrays in plants include the radial array, which is connected with the nuclear envelope, the cortical interphase microtubules, the cortical preprophase band, the spindle and the phragmoplast. These structures, or at least some of them presumably comprise the MTOC (Schmit, 2002; Ehrhardt and Shaw, 2006). In addition, it has been shown that γ -tubulin, which is localized to these noncentrosomal structures has a pivotal role in nucleation and organization of microtubules in plants (Binarova et al., 2006; Pastuglia et al., 2006).

The centrosome probably contains more than hundred proteins (Urbani and Stearns, 1999). The animal centrosome occupies about 1 μ^3 space and is most often composed of two components: centrioles and electron dense pericentriolar material (PCM). Thus, the centrosome is not a membranous organelle and the PCM is a dynamic region, many components of which transit to and from the centrosome via microtubules or by diffusion (Zimmerman and Doxsey, 2000; Megraw et al., 2002; Kubo and Tsukita, 2003) It has been shown by a centriole removal experiment that centrioles have an effect on PCM organization (Bobinnec et al., 1998)

Many centrosome aberrations have been implicated in disease, particularly in cancer (Lingle et al., 2002; Tsang et al., 2009), and several genes have been found to regulate centrosome duplication (O'Connell et al., 2001; Meraldi and Nigg, 2002; Salisbury et al., 2002; Tsang et al., 2009). Centrosomes organize the poles of the mitotic spindle and if the cells contain more than 2 centrosomes, the spindle could become multipolar, which could randomize the chromosomes distribution and lead to aneuploidy. Aneuploidy is known to be a characteristic feature of malignant tumors (Loncarek and Khodjakov, 2009). To understand all this processes knowledge about the biochemical composition of centrosomes and protein-protein interactions within centrosomes is required.

In most mammalian cells as well as algae and protists the centriole has a diameter of about 200 nm and a length of about 400 nm and its microtubules are present in triplet arrangement (Dutcher, 2007). However, in other organisms the number of microtubules can vary. For instance, in *Drosophila* the microtubules are present in doublets in some tissues and triplets in others (McDonald and Morphew, 1993; Moritz et al., 1995; Callaini et al., 1997); in *Caenorhabditis elegans*, the microtubules are present as singlet microtubules

(Ward et al., 1981). Moreover, some species have basal bodies with six or ten triplets (Schrevel and Besse, 1975; Mansir and Justine, 1998). Interestingly, despite the differences in microtubule number in different organisms, the shape of the centrioles and ninefold symmetry are conserved even among distantly related organisms (Delattre and Gonczy, 2004; Strnad and Gonczy, 2008). Recently, Schmidt *et al* reported that the centriolar length in human cells can be regulated by the centriolar protein CPAP (the putative *sas-4* homolog) and CP110 (Schmidt et al., 2009) .

Centrioles are barrel-shaped evolutionary highly conserved organelles. Because of their localization in the middle of the centrosome, initially they were thought to be the microtubule-organizing structure, playing a crucial role in cell division. However, this theory was ruled out by clear demonstrations that many eukaryotes, including fungi and higher plants, completely lacking centrioles are still able to organize a bipolar mitotic spindle. Intriguingly, microsurgical removal of centrioles from animal cells still results in assembly of a mitotic spindle (Khodjakov et al., 2000; Hinchcliffe et al., 2001). This leads to the conclusion that the most important role of the centrioles is the formation of cilia and flagella. As an evidence serves the experiment, which shows that mutant flies lacking centrioles develop into morphologically normal adults, but nevertheless die shortly after birth, because their sensory neurons lack cilia (Basto et al., 2006). Wallace Marshall speculates that eukaryotes first evolved centrioles in order to make cilia which later was associated with the spindle poles and that during evolution the centriole slowly became a fundamental part of the centrosome (Marshall, 2007) Therefore, it was suggested that the PCM and not the centrioles is responsible for nucleation and organization of mitotic and interphase microtubules (Loncarek and Khodjakov, 2009) Some proteins of the PCM have been characterized, using autoimmune antibodies (Doxsey et al., 1994) or antibodies against mitotic extracts (Rao et al., 1989). One of the main components of the PCM and thus key player for microtubule organization is γ-tubulin. γ-tubulin was first described in *Aspergillu*s and was shown to be essential for microtubule formation in spindle pole bodies (Oakley and Oakley, 1989; Oakley et al., 1990). However, the mechanism of nucleation remains unknown. It has been reported by Wiese and colleague that γ-tubulin complexes might be regulated differently in different organisms despite the substantial conservation of MTOC (Wiese and Zheng, 2006). In *Chlamydomonas*, immunoelectron localization of γ-tubulin in interphase cells showed a pattern of 4 discrete dots, which is consistent with its function of

organization of microtubules in four rootlets that radiate from the basal bodies (Silflow et al., 1999). Thus, γ-tubulin plays a role in centriole formation (Fuller et al., 1995; Dammermann et al., 2004) and in nucleation of microtubules (Moritz et al., 2000). Presumably, this protein is required during centriole assembly because it nucleates centriolar microtubules (Loncarek and Khodjakov, 2009).

The functional equivalent of the centrosome in *Chlamydomonas reinhardtii* is a basal apparatus (Figure 2B). The basal apparatus comprises the basal bodies, probasal bodies and fibrous structures associated with the basal bodies (Melkonian, 1980) (Figure 3). The basal bodies, which are equivalent to the centrioles of mammalian cells (Lange and Gull, 1996) function as a template for the assembly of the axoneme - the cytoskeletal component of a flagellum. Flagellar root microtubules not only extend from the basal bodies and mediate interactions with different cell organelles, but also provide positional information to maintain the polarity of the flagellate cell.

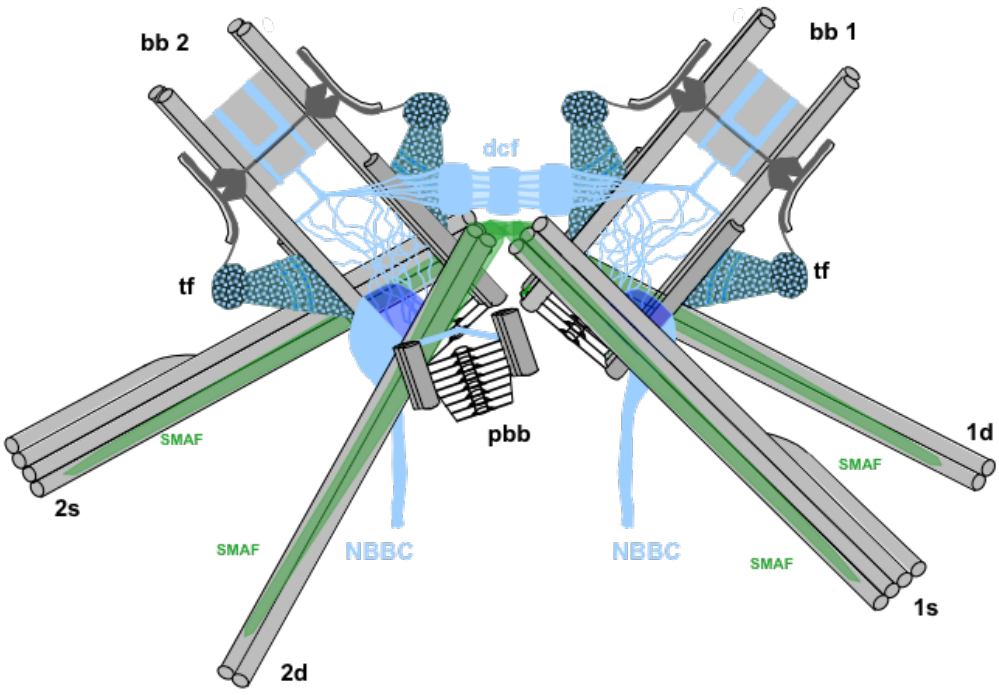

Figure 3. The detailed diagram of basal apparatus *Chlamydomonas reinhardtii* (Geimer and Melkonian, 2005). Basal apparatus with the two flagellum-bearing basal bodies in longitudinal sections (no. 1 for the older basal body and no. 2 for the younger basal body), including the transitional regions of the axonemes, one of the two probasal bodies (pbb) with cartwheel tiers, the distal connecting fiber (dcf) linking the two basal bodies, and the four flagellar roots with their microtubular (1s, 1d, 2s, and 2d; light gray) and fibrous SMAF (green) components. The centrin-containing structures (blue) form a scaffold that extends from the two NBBCs through the basal bodies to the transitional region of the axonemes and includes the transitional fibers (tf).

The function of the basal apparatus as an organizer of the mitotic spindle is less clear (Lechtreck and Grunow, 1999; Meraldi and Nigg, 2002), although a direct role for basal bodies during spindle pole initiation in flagellate green algae has been demonstrated (Lechtreck and Grunow, 1999). Basal bodies are associated with four specialized microtubule bundles known as rootlet microtubules. Two of them consist of four microtubules and the other two of two microtubules. The four-membered rootlet microtubule associated with the daughter basal body is shown to be adjacent to the eyespot. The latter can be used as a marker of the side of the cell with the daughter basal body (Dutcher, 2003). In addition to centrin fibers, which are present in the distal striated fiber, in the NBBC and in the stellate fibers of transition zone (Geimer and Melkonian, 2005), there are three other fiber systems in *Chlamydomonas*: one fiber system connects the daughter basal body to the mother and contains Vfl3 protein (Silflow et al., 2001); second system consists of the proximal striated fibers (Geimer et al., 1998(a); Geimer et al., 1998(b)); the last system are the striated microtubule-associated fibers (SMAF) (Figure 3), which are extending parallel to the rootlet microtubules and contain SF-assemblin (Lechtreck and Melkonian, 1991). SF-assemblin is the principal protein of the SMAF and was discovered in another flagellate green alga *Spermatozopsis similis* (Lechtreck and Melkonian, 1991).

In *Chlamydomonas*, basal body mutations can be recognized by the absence of flagella or their presence in an aberrant number (*bld* mutants are bald, without flagella; *uni* mutants are uniflagellate; *vfl* mutants have a variable number of flagella). *uni* mutants with single flagellum have ultrastructural defects in the transition zone (Huang et al., 1982). Besides, flagellar assembly defects in *uni* mutants are more severe in the probasal body than in basal body. The *uni* gene has been suggested to encode a new class of tubulin - δ-tubulin (Dutcher and Trabuco, 1998); the vfl1 and vfl3 proteins play an important role in the rotational orientation of the basal bodies (Silflow et al., 2001); the *bld2* gene encodes ε-tubulin (Dutcher et al., 2002); bld10p as well as bld12p (sas6) proteins are shown to be localized to the cartwheel (Matsuura et al., 2004; Nakazawa et al., 2007). It has been recently shown that the uni2 protein localizes at the distal end of basal body near to the transition zone (Piasecki and Silflow, 2009). *Bld1* cells have a mutation in the gene that encodes IFT52 (Brazelton et al., 2001).

In *Chlamydomonas* each flagellum is formed from a basal body, which acts as basal body in interphase and as a centriole in mitosis (Coss, 1974). It was first postulated by Henneguy and

Lenhossek in 1898 that basal bodies are equivalents to the mitotic centrioles (Henneguy, 1898; Lenhossek, 1898). Once centrioles have anchored to the cell membrane, they are known as basal bodies, which by extending form flagella/cilia. Therefore, many proteins involved in ciliogenesis accumulate in basal bodies, like for example, proteins involved in Bardet-Biedl syndrome (Li et al., 2004; Marshall, 2008) or Cep97 and CP110 proteins, which involve in cilia assembly regulation (Spektor et al., 2007). However, which mechanisms control the switch between basal body and centriole function still remain unknown.

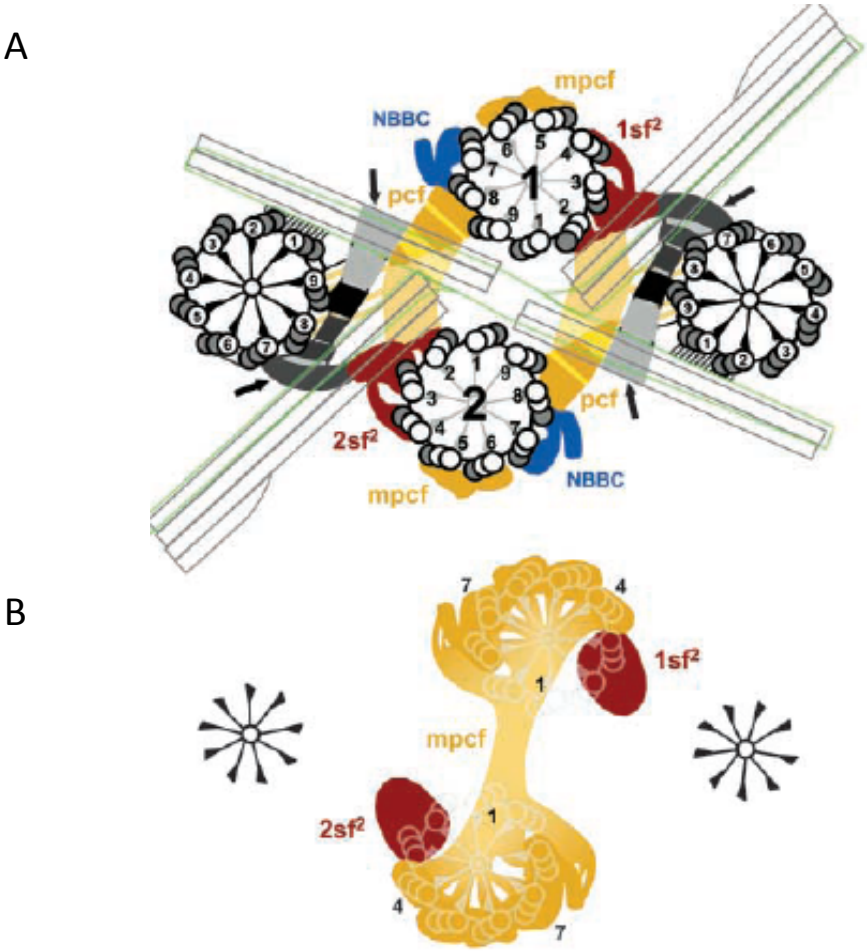

Figure 4. **Proximal part of the basal apparatus** (Geimer and Melkonian, 2004).
(A) The second set of s-fibers ($1sf^2$, $2sf^2$) connecting the bbs to their corresponding four-stranded microtubular roots (s-roots, 1s, 2s) is shown in red. The proximal connecting fibers (pcf, yellow) interconnect the bbs and also make contact with the adjacent pbb (with pbb triplets 8 and 9). The pbbs are attached by the lateral striated fiber (arrows) to their corresponding d-root and the sf^2 of the neighboring bb. In this region, the median proximal connecting fiber is attached to triplets 5 and 6 (mpcf, yellow).
(B) Structures lying below the proximal ends of the bbs (faintly outlined) are the median proximal connecting fiber (mpcf, yellow) and the proximal parts of the sf^2 (red). Of the pbbs, only the hub and spoke complex of the cartwheels are visible at this level.

In *C. reinhardtii* basal bodies duplicate once per cell cycle, as do centrioles in other cells (Dutcher, 2003). The new basal body will form at a right angle to the preexisting one. It has been suggested that mother centrioles are able to find their ways to the proper subcellular position, whereas daughter centrioles are unable to do so and rely on the mother for positional information. Authors assume that centrioles can play a significant role in propagation of cell geometry from one generation to the next (Feldman et al., 2007). Probasal bodies are present in G1, and the elongation occurs in G2 of the cell cycle. In mammalian cells duplication of centrioles occurs with the duplication of the DNA at the G1/S boundary (Dutcher, 2003). Although, it is likely that genes involved in duplication of centrioles in mammalian cells will also operate in *Chlamydomonas*, currently no mutations involved in the replication of the basal bodies of *C. reinhardtii* have been identified (Dutcher, 2003). The number of centrioles doubles, like the number of chromosomes. This exact duplication is very important, because it prevents formation of multipolar spindles and defects in chromosome segregation (Salisbury et al., 1999).

Currently, two main mechanisms of centriolar assembly are known: “templated” and “de novo”. Duplication of the centrioles near existing ones suggests the templating role of the old centriole, but centrioles can also develop *de novo* in cells lacking centrioles (Marshall et al., 2001; Khodjakov et al., 2002). For example, *C. reinhardtii* loses its centrioles in meiosis and later assembles them *de novo* (Cavalier-Smith, 1974).

1.3. Cartwheel – developmentally first ninefold symmetrical structure in basal bodies/centrioles

The cartwheel is a universal structure with ninefold rotational symmetry positioned at the proximal end of the basal bodies/centrioles (Figure 4, 5). The cartwheel is present in *Drosophila,* many protozoa, unicellular algae and in vertebrates. In vertebrates, the cartwheel is present in the procentriole but disappears from the mature centriole, whereas in algae and ciliated cells it is retained in the basal body throughout the cell cycle. The fact that in vertebrates it is present only in procentrioles/probasal bodies, whereas in algae it is preserved during the whole cell cycle makes algae suitable organism to study the cartwheel. In *C. reinhardtii* likewise cartwheel persists in mature basal body (Ringo, 1967; Cavalier-

Smith, 1974; O'Toole et al., 2003; Geimer and Melkonian, 2004) , whereas in human cells it disappear during centriole maturation (Alvey, 1986)

The first description that the cartwheel lies at the proximal end of the basal bodies/centrioles was made by Stubblefield and Brinkley in 1967, when very little was known about centriole structure and even less about procentriole structure (Stubblefield, 1967). The presence of cartwheel in two of three species of flagellate organisms has been shown by Gibbons and Grimstone (Gibbons and Grimstone, 1960). In *Chlamydomonas* the cartwheel structure was identified and described by Ringo (Ringo, 1967). Although adult centrioles may also contain cartwheel structure at their proximal end, it was suggested that cartwheels are a feature of procentrioles/probasal bodies, rather than centrioles/basal bodies (Alvey, 1986). While cartwheel is thought to nucleate the ninefold rotational symmetry, its counterpart – acorn, which is attached to distal end of the microtubular cylinder, might play an important role in the rotational asymmetry of the microtubular triplets (Geimer and Melkonian, 2004).

The cartwheel is composed of the central tubule-hub (diameter is about 25 nm) and a group of nine filaments – spokes, radiating from the hub and connected to the A-tubules by nine triangular electron-dense knobs (Cavalier-Smith, 1974; Geimer and Melkonian, 2004). In spite of the ninefold symmetrical structure characteristic to centrioles, cartwheel does not contain microtubules, instead, having nine radial spokes projecting from a central hub. During the assembly of the centriole/basal body, the cartwheel appears in the earliest stage, when its basement structure is assembled. Because the cartwheel structure displays ninefold symmetry, as does the mature basal body, this structure has been suggested to be the organizing center for the assembly of the triplet microtubules (Matsuura et al., 2004). Interestingly, the positions of the radial spokes appear to determine the number and the positions of centriolar microtubules (Matsuura et al., 2004; Hiraki et al., 2007; Nakazawa et al., 2007). In contrast, in *Paramecium* the cartwheel develops after the formation of microtubule blades, hence after the diameter and symmetry of the procentriole is established (Dippell, 1968).

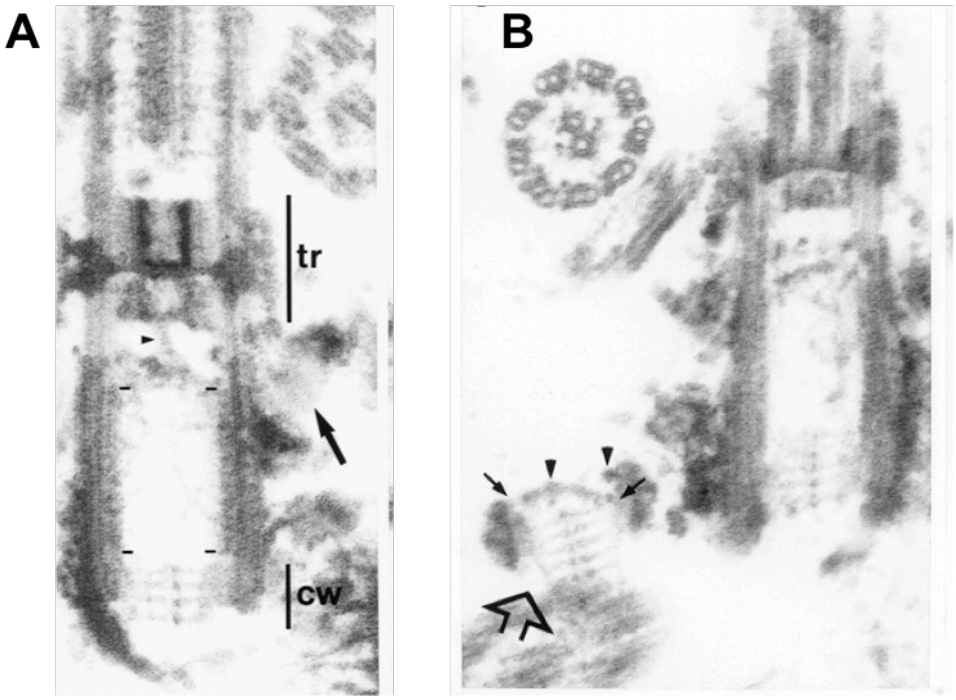

Figure 5. Transmission electron microscopy image (TEM) of the axoneme and basal body (Geimer and Melkonian, 2004).
(A) Median longitudinal section through the axoneme and bb showing the transitional region (vertical line labeled tr), the transitional fibers (large arrow), and the cartwheel (vertical line labeled cw).
(B) Longitudinal section through a bb and pbb (open arrow). The cartwheel of the pbb consists of six tiers. The acorn (marker for the rotational asymmetry) is seen as two asymmetrically positioned electron-dense dots in the pbb (arrowheads).

It was previously described in other flagellate green algae that the cartwheel of basal body has fewer tiers than the cartwheel in probasal body (Beech and Melkonian, 1993). In *Chlamydomonas*, statistical analysis of 53 longitudinal sections of probasal bodies revealed that the cartwheel of probasal bodies consist of four to seven tiers (Geimer and Melkonian, 2004) (Figure 5). Probasal bodies have an average length of 95 nm and the same diameter as basal bodies (about 210 nm) (Geimer and Melkonian, 2004).

To date two proteins have been shown to be localized to the cartwheel structure in *Chlamydomonas*: Bld10 (Matsuura et al., 2004) and SAS-6 (Nakazawa et al., 2007). It has been reported that Bld10p is localized at the tips of the cartwheel spokes and plays a key role in stabilizing the ninefold symmetry of the centrioles (Matsuura et al., 2004; Hiraki et al.,

2007). Mutations in *Chlamydomonas* Bld10p result in formation of a cartwheel with smaller and shorter spokes, eight symmetrically arranged triplets, unstable microtubule triplets (Hiraki et al., 2007), whereas mutation of the Bld10p ortholog in *Drosophila* causes defects in central pair of microtubules (Mottier-Pavie and Megraw, 2009). *bld10* mutation is not lethal in flies, but shows male sterile phenotype by the production of immotile sperm (Mottier-Pavie and Megraw, 2009). The human homologue of Bld10 is SEP135, which is likewise localized at proximal part of nascent centrioles (Kleylein-Sohn et al., 2007). RNAi studies in cell culture demonstrated that SEP135 is required for PCM integrity (Ohta et al., 2002; Uetake et al., 2004), for organization of centrosomes via centriolar C-NAP1 protein recruitment (Uetake et al., 2004), and the assembly of the additional procentrioles in Plk4-overexpressing cells (Kleylein-Sohn et al., 2007).

The second protein discovered in *Chlamydomonas* is a homolog of the human SAS-6 protein and called Bld12p. Mutations in Bld12p result in the absence of the central hub in the cartwheel, and in the formation of the structurally defective basal bodies (Nakazawa et al., 2007). In *Drosophila* depletion of DmSAS-6 leads to the formation of centrioles with reduced diameter and missing microtubule blades (Rodrigues-Martins et al., 2007).

1.4. The aims of the study

The cartwheel is a complex conserved structure that defines the ninefold symmetry of centrioles/basal bodies. Even though the cartwheel structure has fascinated many scientists, until now not much is known about the cartwheel composition and function. Therefore, knowledge about the protein composition of the cartwheel and protein-protein interactions within this structure is required. It is important to emphasize that no cartwheel structure has been yet purified in eukaryotes. In fact, the identification of the first cartwheel protein Bld10 was achieved by isolation of the basal body defective mutants, generated by insertional mutagenesis (Matsuura et al., 2004). Later, the same approach was used for the SAS-6 discovery, the second cartwheel protein in *Chlamydomonas* (Nakazawa et al., 2007). In *Chlamydomonas*, insertional mutagenesis has been used extensively and proved to be a very useful tool in functional genomics studies. However, we believe that biochemical isolation of the cartwheel structure with the further proteome analyses by mass spectrometry

represents an elegant approach to examine cartwheel protein composition. In *Chlamydomonas reinhardtii* probasal bodies are intact throughout the whole cell cycle. Probasal bodies like basal bodies are composed of nine microtubular triplets, but the number of cartwheel tiers in probasal bodies is higher than in basal bodies (Geimer and Melkonian, 2004). Given that the cartwheel is a very tiny structure, we assumed that isolation of probasal bodies, which predominantly is comprised of cartwheels could be a promising approach to achieve our goal. Thus, one of the aims of this PhD study was to address the following question: Is it possible to isolate and purify probasal bodies? To develop this enabling strategy I set out to investigate three important parameters. First, I have attempted to find out suitable cell wall deficient mutant of *C. reinhardtii* that would grow into a dense culture within a short period of the time. Second, I determined to test different buffers for their role to stabilize the cartwheel structure. Third, I intended to find out suitable nonionic detergent that would at one hand lyse cells, but on the other hand be mild enough not to destroy the cartwheel structure.

It is well-known fact that protein-protein interactions or protein complexes are essential in almost all cellular processes, from the metabolic to structural. Hiraki *et al* have claimed that the Bld10p is a core structural component of the cartwheel (Hiraki et al., 2007). Nevertheless, to date no interacting protein of Bld10p is discovered. Therefore, we aimed to elucidate complex protein interactions of Bld10p with neighboring proteins by using different *in vitro* affinity-based techniques, like co-immunoprecipitaion, far-western technique and Blue Native gel electrophoresis. For this purpose, I expressed heterologously partial C-terminal recombinant Bld10 protein, which was then used as an antigen to raise polyclonal antibodies in rabbits. Additionally, two other peptides were designed to produce polyclonal antibodies to cover N-terminus and middle part of the protein. The antibodies were used to study the localization of the Bld10p by immunofluorescence analyses and as a tool to find out interaction partners of Bld10p.

2. Materials and Methods

2.1. Chemical substances

Acetic Acid (CH_3COOH)	Roth
Acetone (CH_3COCH_3)	Merck
Acrylamide: N,N'-Methylenbisacrylamide (37,5:1**)** Rotiphorese Gel 30	Roth
Agar	Fluka
Agarose	PeqLab
Amido Black 10B	Serva
6-Aminocaproic Acid ($C_6H_{13}NO_2$)	Serva
Ammonium Chloride (NH_4Cl)	Fisher
Ammonium Molybdate Tetrahydrate ($(NH_4)_6\ Mo_7O_{24}$ x $4H_20$)	AppliChem
Ammonium Persulfate ($(NH_4)_2S_2O_8$	Sigma
Brij 58	Sigma
Boric Acid (H_3BO_3)	Roth
5-Bromo-4-Chloro-3-Indole Toluidine Phosphate (X-Phosphate)	Roth
5-Bromo-4-Chloro-3-Indole-β-D-Galactopyranoside (X-Gal)	Roth
Bromophenol Blue ($C_{19}H_{10}Br_4O_5S$)	Sigma
Calcium Chloride ($CaCl_2$ x $2H_2O$)	Merck
Chloroform ($CHCl_3$)	Roth
Cobalt (II) Chloride Hexahydrate ($CoCl_2$ x $6H_2O$)	Merck
Copper Sulphate Pentahydrate ($CuSO_4$ x $5H_2O$)	Merck
Deoxycholic Acid ($C_{24}H_{40}O_4$)	Sigma
4',6-Diamidino-2-phenylindole (DAPI)	Invitrogen
1,4-Diazabicyclo [2.2.2] octane (DABCO)	Sigma
N,N-Dimethylformamid (DMF)	Sigma
Dimethylsulfoxide (DMSO)	Merck
Dithiothreitol (DTT Plus one)	Amersham
DNA-Sample Buffer (6x)	Fermentas
DNA-Standard: Mass Ruler^{TM}DNA Ladder Mix	Fermentas
Iron Sulfate ($FeSO_4$ x $7H_2O$)	Merck

Epon 812	Serva
Ethanol (C_2H_5OH)	AppliChem
Ethidium Bromide ($C_{21}H_{20}BrN_3$)	AppliChem
Ethylenediaminetetraacetic acid disodium salt (Na_2-EDTA)	Merck
Ethylenglycol-bis(2-aminoethylether)-N,N,N',N'-tetraacetic acid (EGTA)	Sigma
Fish Gelatin	Sigma
Formaldehyde (CHOH)	Sigma
Formaldehyde (EM-grade), 16%	Serva
D(+)-Glucose Monohydrate ($C_6H_{12}O_6$ x H_2O)	Merck
Glutaraldehyde ($C_5H_8O_2$) (EM-grade), 25%	Serva
Glycerol, 87% (Plus one)	Amersham
Glycine (NH_2CH_2COOH)	ICN
Hydrochloric acid (HCl)	Roth
4-(2-hydroxyethyl)-1-piperazineethanesulfonic acid (HEPES)	Roth
Iodacetamide	Fluka
IPG-Buffer	Amersham
Isobutanol ($C_4H_{10}O$)	Baker
Isopropanol (C_3H_8O)	Merck
Isopropyl-β-D-thiogalactopyranosid (IPTG)	AppliChem
Magnesium Chloride Hexahydrate ($MgCl_2$ x $6H_2O$)	Merck
Magnesium Sulfate Heptahydrate ($MgSO_4$ x $7H_2O$	Roth
Mangan (II) Chloride Tetrahydrate ($MnCl_2$ x $4H_2O$)	Sigma
2-Mercaptoethanol (C_2H_6OS)	Sigma
Methanol (CH_4O)	AppliChem
3-Methyl-1-Butanol ($C_5H_{12}O$)	Sigma
4-Nitro Blue Tetrazolium Chloride (NBT)	Roth
Nonidet P-40 (NP-40)	Roche
Octyl Glucoside (n-octyl-beta-D-glucoside)	Sigma
Osmium Tetroxide (OsO_4)	Plano
PEG 400	Sigma
Pioloform	Plano
Phenylmethylsulfonylfluorid (PMSF)	Sigma

Poly-L-Lysine Solution	Sigma
Potassium Chloride (KCl)	Merck
Polyoxyethylen Sorbitan Monolaurate (Tween 20)	Sigma
Ponceau-S	Sigma
Di-Potassium Hydrogenphosphate Trihydrate (K_2HPO_4 x $3H_2O$)	Merck
Potassium Hydrogenphoshate (K_2HPO_4)	Merck
Propylene Oxide (C_3H_6O)	Serva
SDS-Protein Standards: PageRuler Protein Ladder	Fermentas
PageRuler Prestained Protein Ladder	Fermentas
Serva Blue G-250 (Coomassie Brilliant Blue)	Serva
Silver Nitrate ($AgNO_3$)	Roth
Sodium Acetate Trihydrate (CH_3COONa x $3H_2O$)	Merck
Sodium Azide (NaN_3)	Merck
Sodium Carbonate (Na_2CO_3)	Merck
Sodium Citrate Dihydrate ($C_6H_5Na_3O_7$ x $2H_2O$)	Merck
Sodium Chloride (NaCl)	Merck
Sodium Dihydrogen Phosphate Dihydrate (NaH_2PO_4 x $2H_2O$)	Merck
di-Sodium Dihydrogen Phosphate Dihydrate (Na_2HPO_4 x $2H_2O$)	Merck
Sodium Dodecyl Sulfate (SDS)	Serva
Sodium Hydroxide (NaOH)	Merck
Sodium Thiosulfate Pentahydrate ($Na_2S_2O_3$ x $5H_2O$)	Roth
Sucrose	MPBiomedicals
N,N,N',N'-Tetramethylethylenediamine (TEMED)	Roth
Tris ($C_4H_{11}NO_3$)	Roth
Triton X-100	Sigma
Trizol-Reagent	Invitrogen
Tryptone	AppliChem
Tween 20	Sigma
Uranyl Acetate ($UO_2(CH_3COO)_2$ x $2H_2O$)	TAAB
Urea $(NH_2)_2CO$ (Plus one)	Amersham
Yeast extract	Difco
Zink Sulfate Heptahydrate ($ZnSO_4$ x $7H_2O$)	Merck

2.1.1. Antibiotics

Ampicillin	ICN
Carbenicillin	Sigma
Chloramphenicol	Sigma
Tetracycline	AppliChem

2.1.2. Antibodies

2.1.2.1. Primary antibodies

Polyclonal Antibody C	Davids GmbH
Polyclonal Peptide Antibody N	Davids GmbH
Polyclonal Peptide Antibody M	Davids GmbH
Monoclonal Mouse Anti α-Tubulin (DM-1A)	ICN
Monoclonal Mouse Anti α-Tubulin (B-5-1-2)	Sigma
Monoclonal Mouse Anti-His-Tag	Novagen
Monoclonal anti-centrin antibody (BAS 6.8)	(Ruiz-Binder et al., 2002)

2.1.2.2. Secondary antibodies

Goat Anti-Rabbit-IgG (H+L), Alkaline Phosphatase Conjugate	Sigma
Goat Anti-Mouse IgG (H+L), Alkaline Phosphatase Conjugate	Sigma
Goat Anti-Rabbit IgG Cy3-Conjugate	Dianova
Goat Anti-Mouse IgG Cy3-Conjugate	Dianova
Goat Anti-Rabbit IgG FITC-Conjugate	Sigma
Goat Anti-Mouse IgG FITC-Conjugate	Sigma

2.1.3. Enzymes

EcoRV (10U/µl)	Gibco BRL
NotI (10U/µl)	Fermentas

T4 DNA-Ligase (1U/µl)	Gibco BRL
High Fidelity PCR Enzyme Mix (5U/µl)	Fermentas
Taq-Polymerase (5U/µl)	Biotherm

2.1.4. Kits

Big Dye Terminator v.1.1 Cycle Sequencing Kit	ABI
BugBuster Protein Extraction Reagent	Novagen
Colloidal Blue Staining Kit	Invitrogen
c*O*mpleteMini, Protease Inhibitor Cocktail Tablets	Roche
Coomassie Plus – The Better Bradford™Assay Kit	Pierce
His-Bind Kit	Novagen
pGEM-T Easy Vector System	Promega
pETBlue-2 Perfectly Blunt Cloning Kit	Novagen
QIAprep Spin Miniprep Kit	Qiagen
RevertAid™ H Minus First Strand cDNA Synthesis Kit	Fermentas
Wizard® SV Gel and PCR Clean-UP System	Promega
ProFound™ Co-immunoprecipitation Kit	Pierce
Gentle Ag/Ab Binding and Elution Buffer	Pierce

2.1.5. Primers

2.1.5.1. Sequencing primers

T7	5'-TAATACGACTCACTATAGGG-3'
SP6	5'-CATTTAGGTGACACTATAG-3'
pETBlue UP	5'-UPTCATAACGTCCCGCGAAA-3'
pETBlue DOWN	5'-GTTAAATTGCTAACGCAGTCA-3'

2.1.5.2. Restriction sites primers

2 NotI_rev	5'-TAGCGGCCGCCTGCACCTGGCCTTGTCC-3'

2 EcoRV_for	5'-TAGATATCCGATCGGCTCACCTCGGAG-3'
6 EcoRV_for	5'-TAGATATCGGTCGGCGGATAAGGAGAAC-3'
6 NotI_rev	5' TAGCGGCCGCCAGGAACTGGGTATCGTCCA-3'
7 EcoRV_for	5'-TAGATATCGCAGCAATGCGCGAAGCAA-3'
7 NotI_rev	5'-TAGCGGCCGCCCTGCTGTAACGCTCCTC-3'
NotI-3_rev	5'-TAGCGGCCGCCAGGAACTGGGTATCGT-3'
EcoRV-1_for	5'-TAGATATCGGTGCAAAAGCTCGTAGAGG-3'

2.1.5.3. Primers for the *Bld10* partial cDNA synthesis

bld1_for	5'-GGTGCAAAAGCTCGTAGAGG-3'
bld2_rev	5'-CAGCAGGAACTGGGTATCGT-3'
bld3_for	5'-AGAGTATGAGGCCGATGTGG-3'
bld4_rev	5'-AAGGAGGCTACCTGCTCCTC-3'
bld5_for	5'-CGTTTGATCGGCTCACCT-3'
bld6_rev	5'-CCTGCACCTGGCCTTGTC-3'
mid1_for	5'-GTCGGCGGATAAGGAGAAC-3'
mid2_rev	5'-GACCTGCTGTAACGCTCCTC-3'
KM1_for	5'-CGCGGATCCCTGCGGCGTGTTTATGAGGC-3'
KM2_rev	5'-CCGGAATTCCCCTGTTACGGTCCACCATG-3'

2.1.6. Membranes, filters, dialysis

D-Tube™Dialyzer Maxi, MWCO 12-14 KDa	Novagen
D-Tube™Dialyzer Midi, MWCO 6-8 KDa	Novagen
Immobilon-P PVDF-Membrane (0,45 µm)	Millipore
Cellulose acetate membrane (12200)	Sartorius
Steril Filter Minisart (pore size 0,2 µm)	Sartorius

2.1.7. Standard buffers and solutions

Amido Black Staining Sol.:	90% (v/v) Methanol
	10% (v/v) Acetic Acid
	0,1% (w/v) Amido Black 10B
Amido Black Destaining Sol.:	90% (v/v) Methanol
	10% (v/v) Acetic Acid
Anode Buffer (BN-PAGE):	50 mM Bis-Tris

Prepare 1 liter as a 10x stock, adjust pH to 7,0 with HCl and store at 4^0C.

AP-Buffer:	100 mM Tris-HCl, pH 9,5
	100 mM NaCl
	5 mM $MgCl_2$
Base Buffer (BN-PAGE):	20 mM Bis-Tris
	5 mM 6-Aminocaproic Acid
	20 mM NaCl
	10% Glycerol
	Adjust pH with HCl to 7,0. Store at 4^0C
Binding Buffer:	0,2 M NaH_2PO_4, pH 7,0
	0,05% Sodium Azide
Blocking Buffer (WB):	3% Fish Gelatin in TBS-Tween or
	1% BSA in TBS-Tween
Blocking Buffer (IMF):	Na-PBS Buffer with
	0,05% (v/v) Tween 20
	3% (w/v) BSA
	0,1% (v/v) Fish Gelatin
	pH 7,4
BN-LysisBuffer (BN-PAGE):	1 x Base Buffer
	8 M Urea
	1 x Protease Inhibitor cocktail
	1 mM PMSF
	1% Coomassie Blue G250

Cathode Buffer (BN-PAGE):	15 mM Bis-Tris
	50 mM Tricine
	0,02% Coomassie Blue G250

Prepare 1 liter as a 10x stock, adjust pH to 7,0 with HCl and store at 4 ^{0}C.

Coomasie Staining Solution:	10% (v/v) Acetic Acid
	50% (v/v) Methanol
	0,1% (w/v) Serva Blue G-250
Coomasie Destaining Solution:	7% (v/v) Acetic Acid
	10% (v/v) Methanol
Glycine-Elution Buffer (Affinity purification of IgGs):	0,2 M Glycine
	1 mM EDTA
	adjust pH to 2,5 with HCl
Elution Buffer (Protein A chromatography):	0,1 M Sodium Citrate
	0,05% Sodium Azide
	pH 3,0
Fixative (whole-cells IMF):	4% paraformaldehyde, EM Grade
	10 mM HEPES buffer (pH 7,0)
	5mM EGTA
	3 mM $MgSO_4$
	25 mM KCl
	0,1% NP40
	pH 7,0
LB-Medium:	5 g/l Yeast Extract
	5 g/l NaCl
	10 g/l Trypton
	pH 7,0; adjust the pH with NaOH
MT-Buffer:	30 mM HEPES
	15 mM KCl
	5 mM EGTA
	pH 7,0; adjust the pH with KOH
MT^{Mg2+}-Buffer:	Regular MT Buffer with 5 mM $MgSO_4$

MT Lysis Buffer with Triton X-100:	MT Buffer with
	1%, 2%, 3%, 4% Triton X-100
MT Lysis Buffer with NP-40:	MT Buffer with
	1%, 2%, 3%, 4% NP-40
MT Lysis Buffer with Brij 58:	MT Buffer with
	1%, 2%, 3%, 4% Brij 58
MT Lysis Buffer with Deoxycholic Acid:	MT Buffer with
	1%, 2%, 3%, 4% Deoxycholic Acid
Phosphate-Buffered Saline (PBS Buffer):	150 mM NaCl
	8,1 mM Na_2HPO_4
	1,5 mM NaH_2PO_4
	pH 7,4; adjust the pH with NaOH
PBS-Tween:	PBS-Buffer with 0,05% (v/v) Tween 20
NBT Stock Solution:	75 mg NBT in 1 ml 70% (v/v) DMF
Neutralization Buffer (Affinity purification of IgGs):	300 µl TBS-T + 1% BSA
	100 µl 1M Tris (pH 9,0)
	100 µl 10 x TBS-T
Ponceau S-Staining Solution:	3% (v/v) Acetic Acid
	0,2% (w/v) Ponceau-S
Protein SDS Sample Buffer (4x):	250 mM Tris-HCl
	4 mM EDTA
	40% (v/v) Glycerin
	8% (w/v) SDS
	2% (v/v) 2-Mercaptoethanol
	0,2% (w/v) Bromophenol Blue
	pH 6,8
Resolving Gel Buffer:	1,5 M Tris-HCl
	0,8% (w/v) SDS
	pH 8,8
Stacking Gel Buffer:	0,5 M Tris-HCl
	0,8% (w/v) SDS
	pH 6,8

SDS Running Buffer:	25 mM Tris
	192 mM Glycine
	0,1% (w/v) SDS
Stabilizing Buffer:	5% (w/v) DABCO in 1:2 Na-PBS and Glycerol mixture
TAE Buffer (50x):	2 M Tris
	5,7% (v/v) Acetic Acid
	50 mM EDTA
	pH 8,0
TBS Buffer:	50 mM Tris
	150 mM NaCl
	pH 7,5; adjust the pH with HCl
TBS-Tween:	TBS Buffer with 0,05% (v/v) Tween 20
TE Buffer:	10 mM Tris-HCl
	2 mM EDTA
	pH 7,4
Transfer Buffer (Western blotting):	96 mM Glycine
	12 mM Tris
	10% (v/v) Methanol
X-Gal Stock Solution:	50 mg X-Gal in 1 ml DMF
X-Phosphate Stock Solution:	50 mg X-Phosphate in 1 ml DMF

2.2. Strains and culture conditions

2.2.1. *Chlamydomonas reinhardtii* cell wall deficient mutants

To make the cell disruption less complicated and the isolation procedure more efficient, cell wall deficient mutants of *Chlamydomonas reinhardtii* were used in this study. Davies and colleague isolated and genetically analyzed mutants with altered cell walls (Davies and Lyall, 1973). Seventy-nine mutants were classified into three morphological groups: *Class A* - walls are not attached to the plasma membrane, however produced in more or less normal quantities. Besides, walls may show abnormal structure and are shed into the medium; *Class B* – although walls appear normal in EM, cells show a typical "amoeboid" shape and colonies have characteristics of wall deficient mutants; *Class C* – cell walls are absent or produced in greatly reduced quantity compared to wild-type cells (Harris, 2008). To date, neither biochemical characterization of these mutants was done, nor the genes affected by these mutations have been identified.

Four different strains of *Chlamydomonas reinhardtii* cell wall-less mutants were tested in this work (*cw92, cw2,* (+) and (-) mating types of *cw15*) that fall into different classes of cell wall deficient mutants. Mutant *cw2* which belongs to *(Class A)* appeared to have only central triplet of the wall structure, *cw15 (Class C)* fails to assemble the central triplet and *cw92 (Class C)* has very little residual wall material (Harris, 2008).

Cells were cultured in 50 ml flasks. These cultures served as an inoculum to inoculate 500 ml to 600 ml Marburg flasks. Cultures were grown in Sueoka high salt medium (HSM) (Sueoka, 1960; Lien and Knutsen, 1976) at 15°C with a light/dark cycle of 14/10 hours and a photon flux density of 20-40 µE m^{-2} $second^{-1}$ (1:1 ratio of Osram, L 58 W/25 universal white and Osram, L58 W/31 warm white).

2.2.2. Culture medium (HSM)

HSM stock solutions	Final concentration
1. NH_4Cl	0,5 g/l
$MgSO_4 \times 7H_2O$	0,2 g/l
2. $CaCl_2 \times 2H_20$	0,015 g/l
3. $K_2HPO_4 \times 3H_2O$	1,44 g/l
KH_2PO_4	0,72 g/l
4. H_3BO_3	0,5 mg/l
5. $MnCl_2 \times 4H_20$	0,5 mg/l
6. $ZnSO_4 \times 7H_20$	0,2 mg/l
7. $(NH_4)_6 Mo_7O_{24} \times 4H_2O$	0,02 mg/l
8. $FeSO_4 \times 7H_2O$	6,9 mg/l
Na_2-EDTA (Triplex III)	9,3 mg/l

Adjust pH to 6,95 with HCl

Note: to prepare stock solution number 8, chemical agents should be dissolved in 80 ml distilled water and heated with stirring until complete solubilization is achieved. After cooling down, it was refilled with water to 100 ml.

2.2.3. Medium sterilization

Medium was autoclaved for 20 min at 121°C and stored at 15°C until usage. 10 l culture bottles were sterilized by tyndallization (3 h, 100°C) 3 times with 24 hours cooling intervals.

2.3. Molecular biological techniques

2.3.1. Total RNA isolation

For total RNA isolation 500 ml of *C. reinhardtii cw92* culture was used. Cells were centrifuged at 500 *x g* (DuPont, Sorvall, RC 5B, SLA-600TC, 1700 rpm, 10 min). The pellet was then resuspended in a couple of ml of medium. To prevent contamination, the following steps were carried out under sterile conditions (clean bench). Cells were crashed thoroughly using a mortar and pestle under liquid nitrogen. 0,25 ml samples were combined with 0,75 ml of Trizol Reagent in 2 ml Eppendorf microtubes and incubated for 5 min at room temperature. Trizol reagent helps to maintain the integrity of the RNA, while disrupting cells and dissolving cell components. 0,2 ml of chloroform was added to each Eppendorf microtube, shaken vigorously by hand for 15 sec and incubated at room temperature for 2-3 min. Samples were centrifuged at 12000 *x g* for 15 min, 4°C (1K15, Sigma centrifuge, 11500 rpm) which separates the mixture into a lower red, chloroform phase, an interphase, and a colorless upper aqueous phase (about 60% of the total volume). RNA remains exclusively in the aqueous phase. The upper aqueous phase was transferred to a fresh microtubes. The RNA was precipitated from aqueous phase by mixing it with 0,5 ml isopropyl alcohol. The mixture was incubated 10 min at RT and centrifuged at 12000 *x g* for 10 min, 4°C (1K15, Sigma centrifuge, 11500 rpm). The RNA precipitates, forming a gel-like pellet on the side and bottom of the tube. Supernatants were removed and the RNA pellets were washed with 1ml 75% ethanol. Samples were mixed by vortexing and centrifuged at 7500 *x g* for 5 min at 4°C (1K15, Sigma centrifuge, 9100 rpm). Finally, RNA pellets were air-dried and stored at -80°C.

2.3.2. Reverse Transcriptase (RT)-PCR

2.3.2.1. cDNA first strand synthesis

For synthesis of first strand cDNA "RevertAid^{TM} H Minus First Strand cDNA Synthesis Kit" (Fermentas) was employed according to the manufacturer's instructions. As a template served total RNA isolated from *cw92* mutant of *C. reinhardtii* (see chapter 2.3.1). The frozen total RNA pellet was diluted in 80 µl DEPC-water and RNA concentration level was measured

by photometer (BioPhotometer, Eppendorf,). DEPC-water can be prepared by addition of 0,1% diethylpyrocarbonate (DEPC) to water, which is mixed thoroughly, and then autoclaved to destroy DEPC by causing hydrolysis of DEPC. Oligo$(dT)_{18}$ primers along with 1,5 µg RNA were used for cDNA synthesis. cDNA is stored at -20°C.

2.3.2.2. PCR amplification of first strand cDNA

The first strand of cDNA can be directly used as a template in PCR. In this work PCR is performed to produce partial cDNA, which later can be used for heterologous expression of antigens followed by antibody production.

The standard reaction:

2,5 µl	10x buffer (Biotherm with $MgCl_2$)
1,5 µl	DMSO
2,5 µl	cDNA
2,5 µl	dNTPs
2 µl (20pmol)	forward primer
2 µl (20pmol)	reverse primer
11,7 µl	ddH_20
0,3 µl	Taq-polymerase (Biotherm)
25 µl	**Total volume**

The cycling conditions:

Initial denaturation:	5 min at 95°C
Processed for 30 cycles:	
denaturation:	1 min at 95°C
annealing:	2 min at 55°C (t can vary depending on the Tm of the primer)
elongation:	3 min at 68°C
final elongation:	7 min at 68°C

Cooling down at 8°C

PCR products were analyzed on a standard 1% agarose gel, containing ethidium bromide and visually inspected for products under UV light.

2.3.3. Vectors

For the standard PCR product cloning pGEM®-T Easy Vector Systems (Promega) were used. For the partial cDNAs cloning pETBlue-2 Vectors (Novagen) were used. The pET System is a system developed for the cloning and expression of recombinant proteins in *E. coli*. The pETBlue vectors are designed to identify recombinants by traditional blue/white screening. pETBlue-2 provides a vector-encoded ATG start codon, has an expanded multiple cloning site (MCS) and C-terminal HSV-Tag and His-Tag sequences.

2.3.4. Ligation

Before ligation all products were purified either from gel or directly from PCR reaction with the help of the "Wizard SV Gel and PCR Clean-Up System".

2.3.4.1. Ligation with the vector pGEM®-T Easy

The ligations were performed with the help of pGEM®-T Easy Vector Systems (Promega). All procedures were conducted according to the manufacturer's instructions. To calculate the amount of PCR product (insert), necessary for the ligation reaction, the following equation is used: *ng of vector x kb size of insert : kb size of vector x insert:vector ratio = ng of insert*

The ligation reaction:

1 µl	vector (50 ng)
5 µl	2 x ligation buffer
1 µl	T4 DNA ligase
x µl	insert
add deionized water to a final volume	
10 µl	**Total volume**

Note: The molar ratio 3:1 insert:vector has been used successfully.

2.3.4.2. Ligation with pETBlue-2

Before performing the ligation reaction the vector was digested with restriction enzymes NotI and insert with restriction enzymes NotI and EcoRV (see chapters 2.3.5.1 and 2.3.5.2) The molar ratio 3:1 insert:vector has been used for the ligation reaction.

The ligation reaction:

2 µl	5 x ligation buffer (Gibco BRL)
1 µl	T4 DNA ligase (Gibco BRL)
x µl	Vector
x µl	Insert
add deionized water to a final volume	
10 µl	**Total volume**

2.3.5. Restriction

All restriction reactions were performed at 37°C for 90 min. To deactivate NotI enzyme samples were incubated for 20 min at 65°C. Heating does not deactivate EcoRV. To remove small DNA fragments after restriction reactions microspin columns were used (MicroSpin S-400 HR Columns, Amersham).

2.3.5.1. Restriction of the purified PCR product (insert)

PCR products were digested with restriction enzymes NotI and EcoRV, which will enable the ligation of the PCR products with vector pETBlue-2. The reaction buffer (React3, Invitrogen) provides high reactivity for both enzymes. The PCR product was purified prior to restriction reaction.

Restriction reaction (insert):

1 µl	10 x Buffer
1 µl	NotI (10U)
1 µl	EcoRV (10U)
6 µl	PCR product (400 ng)
1 µl	ddH_20
10 µl	**Total volume**

2.3.5.2. Restriction of the pETBlue-2 vector

Restriction digest of the pETBlue vector was performed in parallel with the insert restriction digest. Ligation was performed overnight at 4°C (see chapter 2.3.4.).

Restriction reaction (vector):

1 µl	10 x Buffer
1 µl	NotI (10 U)
2 µl	vector (50 ng/µl)
6 µl	ddH_20
10 µl	**Total volume**

2.3.6. Polymerase chain reaction (PCR)

The PCR reactions were run in a Primus 96 plus thermocycler (MWG Biotech, Ebersberg, Germany) and in a T personal thermocycler (Biometra, Göttingen, Germany).

2.3.6.1. PCR reaction with the plasmid DNA as a template

To introduce restriction enzyme recognition sites (NotI and EcoRV) for the following cloning of the partial cDNA into the expression vector (pETBlue-2), PCR with the plasmid DNA as a template was performed**.**

Standard reaction:

2,5 µl	10x buffer (Fermentas)
2,5 µl (100-300 ng)	Plasmid with insert
1,5 µl	DMSO
2,5 µl (2mM)	dNTPs
2 µl (20pmol)	forward primer (EcoRV-1_for)
2 µl (20pmol)	reverse primer (NotI-3_rev)
11,7 µl	ddH_20
0,3 µl	Polymerase (“High Fidelity PCR Enzyme Mix”, Fermentas)
25 µl	**Total volume**

The cycling conditions:

Initial denaturation:	5 min at 95°C
Processed for 30 cycles:	
denaturation:	45 sec at 95°C
annealing:	30 sec at 55°C
elongation:	1 min at 68°C
final elongation:	7 min at 68°C

Cooling down at 8°C

2.3.6.2. Reamplification

To obtain a clear sharp band reamplification of PCR was conducted. Prior to reamplification, either the PCR reaction was directly purified or the faint-blurred band was excised and purified with the help of PCR clean-up kit following manufacturer's instructions (PCR Clean-Up Kit).

The PCR reaction:

2,5 µl	10 x Buffer (Biotherm with $MgCl_2$)
1,5 µl	DMSO
1,5 µl	cDNA
2,5 µl	dNTPs
2 µl (20 pmol)	forward primer
2 µl (20 pmol)	reverse primer
12,7 µl	ddH_20
0,3 µl	Taq-Polymerase (Biotherm)
25 µl	**Total volume**

PCR conditions are described in chapter 2.3.2.2.

2.3.6.3. PCR reaction with the first strand cDNA as a template

In this reaction first strand partial cDNA was used as a template that later served to heterologously express protein for antibody production. PCR reaction and conditions are given in chapter 2.3.2.2.

2.3.7. DNA-sequencing

PCR products were sequenced either directly, using the same primers as for PCR or after amplification in a vector system, using the vector specific primers T7 and SP6. All sequencing reactions were done by the sequencing service facility at the University of Cologne (Cologne Center of Genomics) in an ABI 3100 16 capillary sequencer. For the sequencing reaction the Big Dye Terminator DNA Sequencing Kit version 1.1 (ABI, Applied Biosystems, Foster City, USA) was employed. Sequencing reactions were run as described below:

Sequencing reaction:

0,5 µl	Plasmid
0,2 µl	Primer
0,5 µl	Big Dye Version 1.1
1,3 µl	ddH_20
2,5 µl	**Total volume**

The reactions were run in a thermocycler by MWG-Biotech (Primus 96 Plus). The following cycling conditions were used:

The cycling conditions:

Initial denaturation:	2 min at 94°C
Processed for 35 cycles:	
denaturation:	20 sec at 94°C
annealing:	30 sec at 50°C
elongation:	2 min at 60°C
final elongation:	6 min at 60°C

Cooling down at 8°C

Reactions were stored at 4°C until usage. Before sequencing tubes were filled up with 17,5 µl of deionized water to a total volume of 20 µl.

2.3.8. Bacterial strains

JM109 strain of *E.coli* competent cells was used for the standard cloning (Promega). JM109 is used to select the recombinant DNA using the activity of β-galactosidase. Protein expression is accomplished by transforming the recombinant pETBlue plasmid into the host strains Tuner™ (DE3) pLacI followed by induction with IPTG (Novagen).

2.3.9. Transformation

2.3.9.1. *E.coli* JM109 strain transformation

Transformation using heat shock was performed using commercial *E.coli* JM109 competent cells (Promega) according to the manufacturer's instructions with slight modifications. 50 µl of cells were mixed well with 2 µl of plasmid DNA (see chapter 2.3.4.1.), then chilled on ice for 10 min. Cells were heat-shocked by placing the tube in a water bath (42°C) for 45-50 sec and immediately chilled on ice for 2 min. 950 µl of SOC medium was added to the transformation reaction and incubated for 90 min at 37°C under constant agitation. The transformed bacterial cells were grown on LB-agar plates containing 50 µg/ml ampicillin as well as 70 µg/ml X-Gal and 20 µg/ml IPTG, which allow the selection of the recombinant clones by blue–white screening.

2.3.9.2. *E.coli* NovaBlue strain transformation

After ligation (see chapter 2.3.4.2) pETBlue-2 vector was transformed into NovaBlue competent cells (Novagen). NovaBlue (K-12 strain) is a suitable initial cloning host due to its high transformation efficiency and blue/white screening capability. 1 µl plasmid was mixed with 50 µl of competent cells and chilled on ice for 5 min. 30 sec heat shock reaction was performed in a water bath at 42°C. Cells were chilled on ice for 2 min, and then 250 µl of

SOC medium was added. Finally, cells were plated on LB-agar plates containing 50 µg/ml ampicillin, 12,5 µg/ml tetracycline, 70 µg/ml X-Gal and 20 µg/ml IPTG.

2.3.9.3. *E.coli* Tuner^{TM}(DE3)pLacI strain transformation

The correct sequence and reading frame of isolated plasmids from transformed Nova Blue cells were verified by sequencing. Clones were transformed to the expression strain Tuner^{TM}(DE3)pLacI, which enables adjustable levels of protein expression in a culture. 1 µl of 1:50 diluted plasmid preparation were mixed with 20 µl competent cells and incubated on ice for 5 min. Tubes were heat-shocked in a water bath for 30 sec at 42°C, then placed on ice for 2 min. 80 µl SOC medium was added to the tube and it was incubated under constant agitation for 60 min at 37°C. Finally, cells were plated on LB-agar plates containing 1% glucose, 50 µl/mg carbenicillin and 34 µl/mg chloramphenicol.

2.3.10. Plasmid preparation (Miniprep)

To extract and purify plasmid DNA from *E.coli* cell suspensions miniprep was performed. Positive clones were transferred in 4 ml LB medium supplemented with respective antibiotics and grown under constant agitation overnight at 37°C. The isolation was performed using QIAprep Spin Miniprep Kit (Qiagen) and a microcentrifuge following manufacturer's instructions. To enhance the DNA concentration miniprep protocol was slightly modified. The DNA was diluted in 35 µl of deionized water, instead of 50 µl. DNA concentration was estimated by measuring the absorbance at 260 nm (BioPhotometer, Eppendorf). Plasmids were stored at -20°C.

2.3.11. Agarose gel electrophoresis

To separate and analyze DNA agarose gel electrophoresis was used. The DNA is visualized in the gel by addition of ethidium bromide. 1% agarose (w/v) was diluted in TAE buffer. The solution was heated to boiling in the microwave to dissolve the agarose. To minimize production of ethidium bromide vapors, it is important to cool down dissolved agarose. Ethidium bromide (final concentration 0,5 mg/ml) was added to the dissolved agarose and

mixed. Electrophoresis was performed for 1 hour at 100 V constant voltage. After electrophoresis the gel is illuminated with an ultraviolet lamp to view the DNA bands. Gels were documented with the help of Digit Store Duo System.

2.3.12. DNA Ladder/Marker

DNA ladder is applied to an agarose gel as a reference to estimate the size of unknown DNA molecules. The following DNA Ladder was used: Ready-to-use MassRuler™ DNA Ladder Mix (Fermentas) with the fragments size of 10000, 8000, 6000, 5000, 4000, 3000, 2500, 2000, 1500, 1031, 900, 700, 600, 500, 400, 300, 200, 100, 80 base pairs (bp).

2.4. Biochemical and protein techniques

2.4.1. Protein expression from partial cDNA

Hetereologous expression of antigens was performed in the prokaryotic host *E.coli* with the help of the pETBlue-2 system (Novagen) according to the manufacturer's instructions. The partial cDNA was expressed by the induction of the T7 promoter. A single colony (clone) (see chapter 2.3.9.3) was inoculated in 4 ml of starter culture (LB medium containing 1% glucose, 50 µl/mg carbenicillin and 34 µl/mg chloramphenicol). The glucose was added to the medium to reduce target protein expression prior to induction. The culture was incubated at 37°C with shaking at 250 rpm to an OD_{600} of 0,6 to 1,0 and stored at 4°C. Next day the culture was pelleted (Hettich, ROTIXA/K, 3000 rpm, 5 min) and fresh culture medium was added. The culture was transferred to 100 ml of the same LB medium and agitated at 37°C until OD_{600} is approximately 0,6-1,0. OD_{600} was monitored during growth by removing aliquots aseptically. Prior to induction, cultures were split into two 50 ml cultures. The induction was achieved by the addition of 250 µM IPTG to the growing culture. IPTG is added only to one of the 50 ml cultures and the other culture was used as an uninduced control. Both cultures were incubated 3-4 hours at 37°C on a shaker (250 rpm). Cells were collected by centrifugation (Hettich, ROTIXA/K, 3000 rpm, 12 min) and pellets were stored at -20°C until cell disruption is performed. To obtain more recombinant protein from bacterial

cultures, the volume of the culture was increased to 2 liters. To quickly examine the expression of the target gene analysis of total cell protein (TCP) on a SDS-PAGE was performed

2.4.2. Purification of the recombinant protein

2.4.2.1. Bacterial cell disruption

BugBuster protein extraction reagent was used for gentle disruption of the cell wall of *E.coli* to release proteins following the manufacturer's protocol. Bacterial pellets were resuspended in BugBuster reagent by gentle pipetting using ca. 2,5 ml reagent per 50 ml culture and incubated on a shaking platform for 20 min at RT. Insoluble cell debris (inclusion bodies) were removed by centrifugation at 16000 *x g* (Sigma, 1K15, 13375 rpm, 20 min, 4 °C). The pellet was saved for the examination on SDS-PAGE or if necessary for inclusion body purification. The supernatant was transferred to a fresh tube and can be directly loaded onto Ni-NTA His-Bind resin (Novagen).

2.4.2.2. Purification of the recombinant protein using Ni - column

To purify recombinant protein Ni-charged His-Bind Resin kit was used (Novagen) according to the manufacturer's protocol. The column holds 2,5 ml settled resin and can be used to purify up to 20 mg of target protein. The soluble extract was loaded onto a column. 10 fractions with 1,5 ml volume were eluted after several washing steps and the eluates were examined on a SDS-PAGE.

2.4.3. Polyacrylamide gel electrophoresis

Proteins are separated using polyacrylamide gel electrophoresis (PAGE) to characterize individual proteins in complex samples or to examine multiple proteins within a single sample. PAGE was used both as an analytical tool to provide information on mass, purity or presence of a protein and as a preparative tool to obtain a pure protein sample. There are several forms of PAGE, which can provide different types of information about proteins. In

this work SDS-PAGE (both analytical and preparative), Blue Native PAGE (BN-PAGE) and 2D/BN-SDS PAGE were employed.

2.4.3.1. SDS-Polyacrylamide gel electrophoresis

Sodium dodecyl sulfate-polyacrylamide gel electrophoresis (SDS-PAGE) was used to separate individual proteins according to their molecular mass (Laemmli, 1970). In SDS-PAGE, proteins are treated with sodium dodecyl sulfate (SDS) - an ionic detergent that denatures proteins by disrupting non-covalent bonds in them, and applies a negative charge to each protein in proportion to its mass. Thus, the charge of all proteins is made roughly equal and proteins are separated according to mass.

Acrylamide mixed with bisacrylamide forms a crosslinked polymer network when the polymerizing agents are added. The polymerization of the gels was reached by adding ammonium persulfate (APS) as a trigger of radicals formation and N,N,N',N'-Tetramethylethylenediamine (TEMED), which helps APS to produce free radicals faster. Samples were mixed with SDS-sample buffer, heated at 100°C for 5 min, centrifuged briefly (Heraeus Pico 17 microcentrifuge, Thermo Scientific) and cooled down on ice for 5 min.

2.4.3.2. Minigels

Minigels were often used to perform SDS-PAGE. The gels have a height of 6,5 cm (ca. 0,5 cm sealing gel, 4,5 cm resolving gel, 1,5 cm stacking gel), 8 cm width and 0,1 cm depth. To prevent leakage, glass plates were tightly covered on the bottom with sealing tape Parafilm, and sealed with the help of the sealing gel, which is composed of 1,5 ml acrylamide (Rotiphorese 30, Roth), 10 µl TEMED and 15 µl APS (10%). In this work 8% and 12,5% gels were used. To separate small proteins a 12,5% gel was used with the following composition: 1,35 ml resolving buffer, 1,55 ml ddH_20, 2,1 ml acrylamide, 10 µl TEMED and 20 µl APS (10%). To resolve large proteins an 8% gel was used. To prepare 8% gel 1,35 ml resolving buffer, 1,33 ml acrylamide, 2,32 ddH_20 and finally 10 µl TEMED and 20 µl APS (10%) were mixed. After addition of polymerizing agents, solution was immediately poured between the plates, leaving space for the stacking gel. The Isobutanol layer was applied on top, followed by 45 min incubation. Isobutanol prevents contact with the oxygen, which could inhibit

polymerization. After polymerization isobutanol was poured off and the top of the resolving gel was rinsed abundantly with water. A 4% Stacking gel was prepared by mixing 0,95 ml stacking buffer, 2,1 ml ddH_20, 0,47 ml acrylamide, 10 µl TEMED and 20 µl APS (10%), then poured on top of the polymerized resolving gel. The comb was inserted straight, avoiding bubble formation. The stacking gel polymerized in 20 to 30 minutes. Samples as well as protein ladder were loaded on a gel. Minigels were run at a constant current of 25 mA per gel for about 1 hour (PowerPac 1000 Power Supply, Bio-Rad). The minigel glass plate assembly apparatus was made in the Mechanical Tools-Workshop of the Botanical Institute, University of Cologne.

2.4.3.3. Preparative gels

To obtain pure recombinant protein after purification on His-Tag Ni^{2+}-charged column (see chapter 2.4.2.2) preparative gel electrophoresis was performed. Preparative gels have 16 cm height (ca. 0,5-1 cm 1% agarose, 12 cm resolving gel, 3-4 cm stacking gel). Standard SDS-PAGE (12,5% gel resolving and 4% stacking gel) with a single large lane and one lane for protein marker was prepared. The gel was run 45 min at a constant current of 15 mA per gel, then 5 to 6 hours at 35mA per gel. After electrophoresis and Coomassie staining the protein band was accurately excised and subjected to electroelution.

2.4.3.4. Native precast gradient gels

Blue native electrophoresis was performed with commercial precast 4-16% Native PAGE™ Novex® Bis-Tris 1mm, 10 well gels (Invitrogen).

2.4.3.5. Blue native polyacrylamide gel electrophoresis

Blue native polyacrylamide gel electrophoresis (BN-PAGE) was performed with modifications according to a protocol of Schägger et al (Schagger and von Jagow, 1991). This technique enables the identification and analysis of protein complexes by separation under native conditions. Cytoskeletons were isolated as described in chapter 2.4.10. All the following centrifugations were performed at 4°C, 20 min at top speed (21000 *x g*). At the final step of

cytoskeleton isolation protocol samples were resuspended in 1,5 ml MT buffer and centrifuged. This step was repeated one more time. Then the pellet was resuspended in MT buffer containing 0,8% octyl glucoside (n-octyl-beta-D-glucoside) and centrifuged. This step was performed to replace Triton X-100 ions with the milder detergent octyl glucoside and to remove monovalent cations. The procedure was repeated again. After centrifugation samples were resuspended in base buffer, containing 0,8% octyl glucoside and centrifuged. Solubilization was performed in sample solubilization buffer (Base buffer, urea, protease inhibitors cocktail, PMSF) for 1 hour at RT, resuspending the pellet each 15 min by pipetting. Centrifugation was performed and the supernatant was mixed with Coomassie to a final volume 1% and loaded on a native gel (Native PAGE, Novex Bis-Tris Gel System, Invitrogen) along with ready-to-use native marker (NativeMark™ Unstained, Invitrogen). Samples were loaded in the dry wells and in each well samples were overlaid with Cathode Buffer. For the BN-PAGE XCell *SureLock*™ Mini-Cell vertical electrophoresis system (Invitrogen) was employed. The inner chamber was filled with Cathode Buffer and the outer chamber with Anode Buffer. The BN-PAGE was run at 100 V constant voltage until the samples had entered the separating gel, then the voltage was increased to 180 V and run until the dye front reached the end of the gel. The gel run took ca. 4 hours. The gels were stained with Colloidal Coomassie Stain (Invitrogen) for 6-12 hours and destained with deionized water for 4-5 hours.

2.4.3.6. 2D BN/SDS-PAGE

To separate protein complexes into its monomeric components, second-dimension SDS-PAGE was run after performing first-dimension BN-PAGE. To make the loading of the gel-slice easier double spacers and double combs (sealed together with a thin Parafilm slice) were used. This makes the gel thicker and allows the BN-PAGE gel slice slip between the plates more easily. Standard 8% SDS-PAGE with the single large lane and one lane for protein marker was prepared. The BN gel lane was excised, incubated for 10 min in 4-5 ml SDS-sample buffer, then boiled in the microwave for 15 sec and finally incubated in hot SDS-sample buffer for another 20 min. Then gel-slice was loaded over stacking gel, sealed with 1% agarose and overlayed with SDS-sample buffer. The gel was run 2-3 hours at 25 mA and stained using Silver staining.

2.4.4. Protein ladders/markers

To assess the relative molecular weight (MW) of a protein on a gel, protein MW markers are run in the outer lanes of the gel for comparison. A standard curve can be constructed from the distances migrated by each marker protein. The distance migrated by the unknown protein is then plotted, and the molecular weight is interpolated from the standard curve. The following protein markers were used in this study:

- PageRuler™ Prestained Protein Ladder (Fermentas) with MW of 170, 130, 100, 70, 55, 40, 35, 25, 15, 10 and two reference bands - orange at ~70 kDa and green at ~10 kDa.
- PageRuler™ Unstained Protein Ladder (Fermentas) with MW of 200, 150, 120, 100, 85, 70, 60, 50, 40, 30, 25, 15, 10 kDa.
- NativeMark™ Unstained ready-to-use Protein Standard with MW of 1048, 720, 480, 242, 146, 66, 20 kDa.

2.4.5. Protein determination techniques

To measure protein levels, standard protein assays were used.

2.4.5.1. Bradford assay

To determine the protein concentration quantitatively, a ready-to-use protein determination kit was employed (Coomassie Plus - The Better Bradford™ Assay Kit, Pierce, Rockford, IL, USA). The kit is based on the standard Bradford method (Bradford, 1976) and was used according to the Standard Test Tube Protocol. Protein concentrations are estimated by reference to the absorbances obtained for a series of standard protein dilutions with the linear working range with BSA of 125-1000 µg/ml. The assay was performed in a test tube with the following steps: 50 µl of standard/sample were combined with 1,5 ml of assay reagent, mixed well and incubated for 10 min at RT. Absorbance was measured at 595 nm (Shimadzu, UV-2450, UV-VIS Spectrophotometer)

2.4.5.2. Neuhoff assay

The advantage of this method is that protein samples can be used in a mixture with SDS-sample buffer (Neuhoff et al., 1979). Samples were heated at 100°C for 5 min and 5 µl of each sample was loaded on a cellulose-acetate membrane. Membrane with dried sample was transferred into Amidoblack staining solution and incubated for 5 min at RT. The stained membrane was gradually destained in destaining solution and dried at RT. After drying, the membrane was incubated in 1 ml DMSO solution with the constant shaking. The absorption was measured at 630 nm (Shimadzu, UV-2450, UV-VIS Spectrophotometer). As a control served the membrane, which was treated the same way as the probe, but loaded with the SDS-probe buffer only. Calibration curve in a range 0,5-5 µg/µl was employed with the help of BSA.

2.4.5.3. Amidoblack staining of PVDF-membranes

To check the protein level nonquantitatively after the transfer from the gel to the PVDF-membrane, staining with amidoblack staining solution was performed (Batteiger et al., 1982). After the transfer membrane was incubated for 5 min in a staining solution, then 5-10 min in a destaining solution. Finally, the membrane was dried on a standard filter paper.

2.4.5.4. Ponceau staining of PVDF-membrane

For quick and easy visualization of proteins transferred to PVDF membranes following SDS-PAGE, staining with the help of Ponceau S reagent was conducted. This is a rapid and reversible staining method for locating protein bands on Western blots. It is less sensitive than Coomassie Blue and produces reddish pink stained bands, which are easily removed by washing. The PVDF membrane was incubated in a Ponceau S-Staining Solution for 3-5 min. Finally, the stain was reversed with water washes.

2.4.6. Gel staining

2.4.6.1. Coomassie staining

To visualize protein bands standard Coomassie staining was used. After electrophoresis gels were soaked in a Coomassie staining solution for 10-15 min. The gel was then destained to remove the background prior to drying and/or documenting. Destaining solution should be changed several times until the protein bands are seen without background staining of the gel.

2.4.6.2. Colloidal blue staining

To visualize Blue Native PAGE, staining with the help of a more sensitive method - the Colloidal Blue Staining Kit was performed (Invitrogen). It is about five times more sensitive than traditional Coomassie. Staining of NuPAGE Novex Bis-Tris Gels, as well as Tris-Glycine Gels was performed according to the protocol recommended by the manufacturer.

2.4.6.3. Silver staining

To visualize bands of low protein concentration, a silver staining protocol was employed. This method can detect very low amounts of proteins and is at least 10 times more sensitive than Coomassie staining.

Gels were first fixed overnight in aqueous 10% acetic acid and 40% ethanol solution. Next day they were incubated 30 min in 0,2% (w/v) aqueous sodium thiosulphate ($Na_2S_2O_3$) sensitizing solution, which consist of 0,5 g $Na_2S_2O_3$, 17 g sodium acetate, 75 ml ethanol and dd$H_2$0 filled up to 250 ml. The gels were washed thoroughly with water 3 times for 5 min. Then they were incubated in staining solution containing 0,25% (w/v) silver nitrate ($AgNO_3$) for 60 min. Gels were washed twice thoroughly with deionized water for 2 min, then developed in aqueous solution containing 2,5% (w/v) sodium carbonate (Na_2CO_3), and 0,04% (v/v) formaldehyde. The development of the gels was stopped by transferring the gels to 1,5% EDTA solution.

2.4.7. Dialysis

Dialysis against 5 mM ammonium bicarbonate was carried out to neutralize pH and to remove Tris and Glycine from the protein solution after electroelution (see chapter 2.4.8.). For dialysis D-Tube Dialyzer Maxi Kit, Novagen, with the molecular cut off 12-14 kDa was used. All steps were done according to the manufacturer's instruction protocol.

2.4.8. Electroelution

To further purify the electrophoresed protein from polyacrylamide gel (see chapter 2.4.3.3), elution of the protein from the gel matrix was done. The electroelution device enables protein removal from the gels and it's concentration in a small volume. In this technique, protein-containing gel pieces are placed in an electroelution chamber, where the proteins are eluted from the gel matrix into a buffer solution using an electrical field and captured against a dialysis membrane (BT2-Elutrap-Membranes dry, Whatman) with an appropriate molecular weight cut off. Excised gel pieces were placed in a chamber filled with SDS Running Buffer. The elution was performed at 4°C for 24-48 hours using 120 V constant voltage. To remove aggregated proteins from the dialysis membrane, the electroelution device was run with reversed polarity for 20-30 sec. The electroelution chamber was made in the Mechanical Tools-Workshop of the Botanical Institute, University of Cologne.

2.4.9. Lyophilisation

Lyophilisation, or freeze-drying, is a method for the preservation of proteins in a dehydrated form. Following freezing at -80°C for ca. 4 hours, dialyzed protein was lyophilized in a special vacuum device (Alpha I-5; Christ). The procedure can last 24 to 48 hours, depending on the amount of liquid. The lyophilized protein served as an antigen for raising polyclonal antibodies in rabbits

2.4.10. Cytoskeleton isolation (with flagella) of *Chlamydomonas reinhardtii*

It was shown that the cytoskeletons can be released from cells in a complex that includes the flagella, the basal bodies, the rootlet microtubules, the structures linking the basal bodies to the nucleus (nucleus-basal body connectors), and chromatin containing nuclear remnants (Gould, 1975; Wright et al., 1985). In this work cytoskeletons were isolated from *C. reinhardtii cw92* mutant cells. 500-600 ml of culture with the cell density of about 2 x 10^6 per ml was used for this purpose. To pellet cells down, 10 min centrifugation at 490 *x g* was performed (Du Pont, Sorvall, RC 5B, GS-3 rotor, 1700 rpm). The pelleted cells were then gently resuspended in 50 ml MT (microtubule stabilizing) buffer and distributed into 50 ml falcon tubes. The suspension was centrifuged approximately 7 min at 280 *x g*, 4°C (swing-out centrifuge Hettich, ROTIXA/K, 2200 rpm). The pellet was again gently resuspended in MT Buffer, and then lysed by mixing it 1:1 (v/v) with 4% Triton X-100 solution in MT buffer. Lysis was performed on ice, 10-15 min with stirring at low speed (to avoid foam formation). Lysis was confirmed microscopically. Lysed cells were centrifuged 30 min at 280 *x g*, 4°C using the swing-out Hettich centrifuge. Cytoskeletons (ca. 5 ml) were pelleted over a starch pellet and could be removed using a glass Pasteur pipette. They were then resuspended in 45 ml MT buffer and centrifuged 15 min at the same speed. The supernatant was discarded and the pellet was resuspended in MT buffer and centrifuged 25 min at the same conditions. The pellet was then resuspended in 6 ml MT buffer and distributed into Eppendorf microtubes. Cytoskeletons were centrifuged at 4°C, 21000 *x g*, 20 min (1K15, Sigma centrifuge). If some residual starch was still present, one or two more centrifugation steps were required to wash out starch remnants. Cytoskeleton pellets were stored at -20°C for further analyses.

2.4.11. Attempt to develop an isolation protocol for *Chlamydomonas reinhardtii* probasal bodies

C. reinhardtii mutants *(cw92, cw15-)* culture (10 l) was harvested early in the morning with the help of tangential flow filtration (The Pellicon cassette systems, Filtertype HVLP 000 C5, pore size 0,45 µm) or by centrifugation (Du Pont, Sorvall, RC 5B, GS-3 rotor, 1700 rpm). Cell density was about 1-2 x 10^6 per ml. To further concentrate cells, 15 min centrifugation was performed at 490 *x g* (Du Pont, Sorvall, RC 5B, GS-3 rotor, 1700 rpm). The pelleted cells were then gently resuspended in 250-300 ml MT (microtubule stabilizing) buffer and centrifuged

again using the same conditions as described above.

To deflagellate cells, cells were treated with 2,5% acetic acid for 15-20 seconds until a pH of 4,5 is reached. The mixture should be stirring for 90-120 sec. To raise the pH to 7,0-7,4 0,5 M KOH was added quickly. The whole procedure should be completed within 2 min. To keep the cells intact, the pH value should not undershoot pH 4,5 or overshoot pH 7,4. Deflagellation was confirmed microscopically. Deflagellated cells were distributed into 50 ml falcon tubes and centrifuged approximately 5 min at 220 *x g* 4°C (swing-out centrifuge Hettich, ROTIXA/K, 1800 rpm). The supernatant was discarded, whereas the pellet was gently resuspended in MT Buffer and centrifuged again as described above.

Lysis was performed on ice by mixing the cells 1:1 (v/v) with 4% detergent (Triton X-100, NP40) solution in MT buffer, and stirring for 10-15 min at low speed (to avoid foam formation). Lysis was confirmed microscopically. Lysed cells were carefully added to 5 ml 50% sucrose in a 50 ml falcon flask and centrifuged at 4°C, 900 *x g*, 20 min, (the swing-out Hettich centrifuge ROTIXA/K, 2800 rpm). The interphase, which had a characteristic yellowish/whitish color, was removed very carefully with a Pasteur pipette and diluted in MT buffer. Samples were taken at this stage for electron microscopical analysis.

To further fractionate interphase extract discontinuous sucrose gradient was used. Sucrose solutions were prepared in MT buffer with the addition of 0,05% (w/v) sodium azide. Sucrose solutions were stored at -20°C. The discontinuous sucrose density gradient is prepared by layering decreasing sucrose densities solutions upon one another. The following concentrations and volumes of sucrose were used: 5 ml 50%, 9 ml 40%, 10 ml 30%, 6 ml 20%. Interphase extracts were loaded very carefully onto sucrose gradient and centrifuged at 12400 *x g* for 2 hours (Du Pont, Sorvall, RC 5B, HB-4, 8700 rpm, 4°C, without brake). The sample was removed directly beneath 30%/40% interphase, diluted 1:1 with 2x MT Buffer and centrifuged for 1 hour (Du Pont, Sorvall, RC 5B, SS-34 Rotor, 4°C, 17000 rpm)

2.5. Immunological techniques

2.5.1. Antibodies

2.5.1.1. Antigen production

To produce antigen in order to raise polyclonal antibodies in rabbits, overexpression of partial cDNA in *E.coli* was performed (see chapter 2.4.1.). The recombinant protein was first purified using Ni-column (see chapter 2.4.2.2.) then further purified by preparative SDS-PAGE (see chapter 2.4.3.3.). The protein band was excised, electroeluted (see chapter 2.4.8.), dialyzed (see chapter 2.4.7.) and lyophilized (see chapter 2.4.9.).

2.5.1.2. Immunization

Rabbit antiserum production, peptide synthesis and affinity purification of 2 peptide antibodies (abM and abN) were carried out by Davids Biotechnologie (Röntgenstr. 3, 93055, Regensburg). Antisera were obtained by injection of the immunogen (antigen) into a rabbit in combination with an adjuvant to increase the immune response. Preimmune bleed was collected on the first day, which was followed by immunization. The quality of peptides used for the immunizations and affinity matrix production was tested by mass spectrometry for the right mass and RP-HPLC to get a fraction of 83-95% purity. Approximately 800 µg of antigen C was required for the immunization of two rabbits. Two rabbits were injected for antibody C and one rabbit for antibody M and antibody N production respectively. The antibody response was enhanced by subsequent booster injections of the antigen on the 14^{th} and 28^{th} day. Once a sufficiently high titer had been reached, the antiserum was prepared by blood collection followed by serum preparation, with subsequent purification of antibodies from the serum if required. The antiserum was delivered containing preservative 0,02% Sodium-Azide. Preimmune and immune sera (abC) were aliquoted and stored at -80°C. Affinity-purified abM and abN were aliquoted as well and stored at -80°C.

2.5.1.3. Purification of IgGs from immune and preimmune sera

To concentrate and enrich antigen-specific antibodies and lower background by removing non-specific proteins, IgG purification from immune and preimmune sera using Protein A chromatography was performed. Before starting the experiment, all buffers, solutions and sera were sterilized by filtration (pore size 0,2 µm). Sterilized sera were desalted using PD-10 desalting column (GE Healthcare; 8,3 ml bed volume). First, the column was equilibrated with 25 ml Binding buffer. Then 2,5 ml serum was loaded on the column. The flow-through was discarded and the IgGs were eluted in 3,5 ml Binding buffer. Then purification using protein A column was performed (HiTrap rProtein AFF, GE Healthcare; 1 ml column volume). To equilibrate the column 10 ml of Binding buffer were run through column, followed by 2 ml of desalted serum. A washing step using 10 ml Binding buffer followed. Finally, IgGs were eluted in 2 ml Elution buffer. Since the elution buffer is highly acidic, quick neutralization using Tris-HCl pH 9,0 is required (ca. 150 µl for 2 ml volume). The eluate was aliquoted and stored at -80°C. The protein concentration was determined using standard Bradford assay (see chapter 2.4.5.1.).

2.5.1.4. Affinity purification of IgGs (western strip technique)

For affinity purification of IgGs antigen was immobilized on a PVDF membrane, which served as a ligand to purify protein-specific antibodies from sera. First, standard 12,5% SDS-PAGE was run with antigen C loaded on it. Then transfer from the gel to membrane was performed (see chapter 2.5.2.). After the transfer was completed, proteins were stained with Ponceau S dye (see chapter 2.4.5.4.) The protein band of respective size was excised and incubated 1 h at RT in TBS-T buffer containing 1% BSA (prehybridization). Then strips were incubated overnight at 4°C on a shaking platform in a hybridization solution containing 700 µl TBS-T with 1% BSA and 300 µl of immune serum. Next day, the strips were washed 4-6 times at RT in TBS-T buffer containing 1% BSA. The strips were incubated for 2 min at RT on a shaking platform with 500 µl Glycine-Elution buffer. After this incubation the Glycine-Elution buffer was removed and immediately mixed with the 500 µl of neutralization buffer. To confirm neutralization pH was checked immediately. Antibodies were aliquoted and stored at -80°C.

2.5.2. Western blotting

To detect specific proteins (antigens) in a given sample or extract the Western blotting (also called immunoblotting) immunological analytical technique was used (Towbin et al., 1979). In this method the antibody-antigen interaction specificity enables identification of a target protein in a complex protein mixture. Tankblot detection system as a most suitable method for my goal was used in this work. The tankblot is recommended particularly for blotting of large molecules or of proteins, which are difficult to transfer. During tank blotting proteins are transferred in a vertical buffer tank between electrodes arranged on the sidewalls. The tankblot chambers were made in the Mechanical Tools Workshop of Botanical Institute, University of Cologne. The first step in a Western Blotting procedure is to separate the macromolecules using PAGE. After electrophoresis, the separated molecules are transferred or blotted on PVDF (polyvinylidene difluoride) membrane. PVDF is highly hydrophobic and therefore should be wet in methanol before it is used. The PVDF membrane was moistened in 100% methanol for 10-20 sec then washed for 2 min in deionized water to remove excess methanol and finally soaked in transfer buffer. Fleece and Whatman filter paper were as well soaked in transfer buffer. The tankblot device was chilled by a special integrated chamber filled with ice. Transfer was performed using constant 100 V voltage. The duration can vary from 1 to 3 hours. The following order was used for the blotting:

Cathode (+)

- Fleece
- Whatman filter paper
- PVDF membrane
- Gel
- Whatman filter paper
- Fleece

Anode (-)

After transfer, the membrane was stained with Ponceau S reagent. The membrane can be stored at -20°C and used later or used directly. Blocking of non-specific bindings is achieved by incubating the membrane overnight at 4°C in a blocking buffer (3% fish gelatin or 1% BSA in TBS-Tween solution). The membrane was next incubated on a shaker for 90 min with primary antibody (1:1000-1:10000 dilutions in blocking buffer), then washed several times

for 5 min with TBS buffer and finally incubated with secondary antibody (anti-rabbit or anti-mouse IgG alkaline phosphatase conjugates diluted 1:2000 in blocking buffer). Membrane was washed thoroughly with TBS buffer and detected colorimetrically by incubation in the following solution (10 ml AP-buffer, 50 µl NBT-stock solution, 40 µl X-phosphate stock solution). The reaction was stopped by washing away the dye with deionized water and finally the membrane was air-dried on a filter paper.

2.5.3. Far-western blotting

Far-western blotting is a technique to identify protein-protein interactions. In this method antibody detectable protein ("bait") is used to detect target ("prey") protein on the membrane. The cytoskeleton preparations were separated using SDS-PAGE, then transferred to a PVDF membrane. After transfer the membrane was blocked in a blocking buffer (3% fish gelatin or 1% BSA in TBS-Tween solution) and then incubated with heterologously expressed antigen C ("bait") (1:1000 dilution in blocking buffer). Then incubation with primary antibody C and following incubation with secondary antibody takes place. Colorimetrical detection was performed as described in chapter 2.5.2. and finally the reaction was stopped by washing the membrane with deionized water.

2.5.4. Western blotting of 1-D BN gels and 2D-SDS gels

After the first dimension BN electrophoresis and the second dimension 2D-BN/SDS electrophoresis gels can be blotted onto a PVDF membrane. The gel was incubated twice in SDS-running buffer for 30 min, which helps to remove Coomassie and gives a negative charge to the proteins. Then the gel was equilibrated in Transfer Buffer for 30-40 min and transferred to the PDVF membrane. Transfer was performed for 2 hours at 100 V. The following steps were carried out as described in chapter 2.5.2.

2.5.5. Indirect immunofluorescence of isolated cytoskeletons with flagella

2.5.5.1. Preparation of diagnostic slides

Multi-well diagnostic slides (Roth) were scrupulously cleaned with detergent, thoroughly rinsed with deionized water, treated with methanol, finally rinsed with dH_20 and air-dried. One drop (ca. 30 µl) of Poly-L-Lysine was applied onto the center of each well and incubated for 10 min at RT. Poly L-Lysine provides higher adhesion, reducing the chances of tissue or cell loss during processing. Slides were placed in a covered chamber, filled with water to avoid drying.

2.5.5.2. Cytoskeleton isolation, fixation, labeling and mounting

50ml of cells (*cw92*) were used to isolate cytoskeletons from *cw92* mutant with the following immunofluorescence assay**.** Cells were centrifuged 10 min at 290 *x g*, 4°C (Heraeus Sepatech Labofuge Ae)**.** Pellets were resuspended in MT^{Mg2+} - buffer. In order to keep the cells intact, a cut blue pipette tip was used. Subsequently, centrifugation was done at the same conditions as described above. Cells were resuspended in MT^{Mg2+} - buffer (ca. 200 µl). Cell density was controlled microscopically followed by incubation on ice for 5 min. Samples were treated 1:1 with 4% Triton in MT^{Mg2+} - buffer and incubated for 20 min on ice. Lysis was confirmed microscopically.

Cytoskeletons were fixed on ice for 15 min using a 1:1 dilution with 6% formaldehyde in MT $+Mg^{2+}$-buffer. Fixed cytoskeletons were placed onto slides and incubated 30 min at room temperature. The incubation was performed in a box covered inside with wet tissue papers. The slide was rinsed with PBS buffer and then blocked for 30 min in blocking buffer at 37°C. It was then washed with PBS buffer and carefully air-dried.

For the labeling, primary antibodies were diluted in blocking buffer (dilution range 1:50 to 1:500). Samples were incubated for 90 min at 37°C with primary antibodies. Following the incubation, the slide was thoroughly rinsed with PBS buffer to remove excess antibody solution and air-dried. To avoid bleaching, all further steps were performed under limited light conditions. Incubation with secondary antibodies (Goat Anti-Rabbit IgG Cy3-Conjugate, Goat Anti-Mouse IgG Cy3-Conjugate, Goat Anti-Rabbit IgG FITC-Conjugate, Goat Anti-Mouse IgG FITC-Conjugate) was performed 90 min at 37°C. For the double labeling, in which two

antigens are to be localized, it is necessary to use primary antibodies raised in different species (i.e., rabbit and mouse) and the appropriate secondary antibodies conjugated to distinct fluorochromes to achieve desired discrimination between two primary targets. Finally, slide was rinsed with PBS buffer and air-dried.

For mounting 4 µl of 5% DABCO in PBS/Glycerol (1:2) was placed onto the centre of each well of the slide. Mounting medium is used to reduce bleaching of the fluorochrome as well as to avoid drying and resist evaporation. The slide was covered with cover slide very carefully and then sealed with simple nail polish. The slide was stored in darkness at 4°C.

2.5.5.3. Observation

To examine fluorescence, Nikon Fluorescence microscope (Eclipse E-800 with 100 x PlanApo-Oil immersion objective) was employed. Documentation was done with the help of a digital camera (Visitron System RT Monochrome) and MetaMorph image processing software (Version 6.3r4).

2.5.6. Indirect immunofluorescence of isolated deflagellated cytoskeletons

Chlamydomonas cells shed their flagella in response to many stressful conditions to minimize exposure to environmental stress. In this work pH shock was used for flagellar amputation. Cells can be deflagellated at any density or stage of growth.

While *C. reinhardtii* culture (ca. 50 ml) is stirring gently on ice on a magnetic stirrer, 2,5% acetic acid was added dropwise within 15-20 seconds until a pH of 4,5 was reached. The mixture should be stirring approximately 90-120 seconds. To raise the pH to 7,0-7,4 0,5 M KOH was added dropwise. The whole procedure should be completed in 2 min. To avoid killing the cells, the pH value should not undershoot pH 4,5 or overshoot pH 7,4. Deflagellation is confirmed microscopically. The following steps were performed as described in chapter 2.5.5.

2.5.7. Indirect immunofluorescence of whole cells

Chlamydomonas cw92 cells (50 µl) were collected and centrifuged at 290 *x g* for 10 min. Pellets were resuspended in MT^{Mg2+} - buffer and centrifuged at 290 *x g* for 10 min. Then, cells were lightly resuspended in MT^{Mg2+} - buffer and fixed in 3 volumes of the fixative for 30 min on ice. The multi-well slides were prepared as described in chapter 2.5.5.1. Fixed cells were placed onto slides and incubated for 30 min. Slides were washed thoroughly with the PBS buffer. Then, cells were permeabilized in -20°C MeOH for 10 min and air-dried. Note, that MeOH should be at -20°C overnight to ensure that it is cold. The slide was rinsed with PBS buffer and then blocked for 30 min in blocking buffer in humidified chamber at 37°C. It was then washed with the PBS buffer and carefully air-dried. For the labeling, primary antibodies were diluted in blocking buffer (dilution range 1:50 to 1:500). Samples were incubated for 90 min at 37°C with primary antibodies. Following the incubation, the slide was thoroughly rinsed with PBS buffer to remove excess antibody solution and air-dried. To avoid bleaching, all further steps were performed under limited light conditions. Incubation with secondary antibodies (Goat Anti-Rabbit IgG Cy3-Conjugate, Goat Anti-Mouse IgG Cy3-Conjugate, Goat Anti-Rabbit IgG FITC-Conjugate, Goat Anti-Mouse IgG FITC-Conjugate) was performed 90 min at 37°C. Finally, slide was rinsed with PBS buffer and air-dried. The mounting was performed as described in chapter 2.5.5.2. The slide was stored in darkness at 4°C.

2.5.8. Post-Embedding Immunogold Labeling Technique

2.5.8.1. Embedding of Isolated Cytoskeletons from *Chlamydomonas* in LR Gold

Cytoskeletons were isolated from *Chlamydomonas* according to the protocol of Wright *et al* (Wright et al., 1985). Pellet of isolated cytoskeletons was resuspended in MT^{Mg2+} buffer in a 1,5 ml tube and centrifuged at about 16000 *x g* for 10 minutes, 4°C. The pellet should be approximately 1 mm thick. Pellet was fixed in MT^{Mg2+} buffer containing 0,1-0,25% glutaraldehyde and 2-3% formaldehyde, pH 7,2 for 40-60 min at 15°C. After 15 minutes of incubation the pellet was carefully released from the wall of the microfuge tube. A glass Pasteur pipette with its tip drawn out and melted shut is a good tool for this purpose. The

pellet was washed with two changes of MT^{Mg2+} buffer, 5 minutes each and dehydrated with a graduated series of ethanol. Next, the pellet was infiltrated with LR Gold. Depending on the size of the pellet, the last infiltration step should be extended to up to 24 hours with one or two changes in between. For embedding, the pellet was transferred into a gelatin capsule. Like many acrylic resins oxygen inhibits polymerization of LR Gold. It is unavoidable to trap some air when closing the capsule, but the trapped air bubble should be kept as small as possible by overfilling the capsule with LR Gold to convexity before closing it. Polymerization is carried out at -25°C under UV light for at least 48 hrs.
Ultrathin sections were cut with diamond knife (35° knife angel; Diatome, Biel, Switzerland) using ultramicrotome EM UC6 (Leica Microsystems, Vienna, Austria).

2.5.8.2. Immunogold Labeling

After sectioning, the slot grids (pioloform covered gold gilded copper grids) were transferred to drops of a freshly prepared saturated solution of sodium metaperiodate and incubated for 2-4 minutes. It has been found that treatment with sodium metaperiodate can partially restore protein antigenicity on thin sections of osmicated material (Bendayan and Zollinger, 1983). The grids were washed extensively by transferring them across 4 changes of distilled water and 2 changes of Na-PBS, 5 minutes each. Then, the grids blocked for 30-60 minutes with blocking buffer. The grids were transferred to drops of the primary antibody diluted in blocking buffer (1:300) and incubated for about 90 minutes at RT. The grids were washed extensively by transferring them across 5 changes of PBS, 5-10 minutes each. The grids were incubated on drops of the secondary antibody (Goat anti-Rabbit IgG (H+L) (Human Abs.) British BioCell International, Cardiff, UK), 10 nm gold conjugate conjugated to colloidal gold diluted in blocking buffer (1:30) for about 90 minutes at RT. Next, the grids were washed extensively by transferring them across 5 changes of PBS, 5-10 minutes each and incubated for 8 minutes on a drop Na-PBS containing 1% glutaraldehyde. This step is to chemically fix bound antibodies in place as they might be released by the low pH of the uranyl acetate solution used for post staining. The grids were washed extensively by transferring them across 4 changes of distilled water, 5 minutes each and then blotted dry by touching the edge to a piece of filter paper.

Subsequently, the grids were poststained with 2% uranyl acetate in distilled water for about 20 minutes and lead citrate for 2-4 minutes. Contrasting was performed according to the protocol from Reynolds (Reynolds, 1963). As a control served sample with secondary antibody only.

2.6. Transmission electron microscopy (TEM)

2.6.1. Copper grid covering

Copper mesh grids (3,05 mm mesh grids, Plano, Göttingen) were covered with the thin layer of 0,25% (w/v) pioloform. A clean microscope slide was soaked into pioloform solution in chloroform, which formed a thin film upon drying. It was then carefully transferred to a beaker with deionized water. The floating film was overlaid with copper grids. The copper grids were withdrawn from the water surface with the help of a parafilm strip and air-dried.

2.6.2. Fixation and embedding

Isolated cytoskeletons (see chapter 2.4.10.) were fixed in 2,5% glutaraldehyde in MT buffer for 20 min on ice. Then, the same volume of 4% tannic acid solution (w/v) was added and the whole was incubated for 25 min at RT. After this incubation the cytoskeletons were sedimented. The pellets were washed twice in MT buffer and osmicated for 20 min in 2% (m/v) osmium tetroxide in MT buffer. Pellets were washed twice in MT buffer and then transferred into agar (Agar Noble, 2% (w/v) in dH_20).

The pellets were dehydrated with the following steps: 50% ethanol and 70% ethanol with an incubation time of the 15 min on ice, 70% and 90% ethanol with the 15 min incubation time at -20°C. Finally, agar blocks were incubated overnight in 100% ethanol at -20°C. Next day incubation with 1:1 ethanol/propylenoxide (v/v) and 2 incubations in propylenoxide (at -20°C, 15 min each) were performed. Subsequently, the embedded pellet was transferred into 1:1 epon/propylenoxide (v/v) and incubated for 12-20 h at RT in an Eppendorf tube. The following day; to let propylenoxide evaporate Eppendorf tube was incubated with an open lid under sterile hood. After propylenoxide was evaporated, agar blocks were embedded in fresh Epon. To achieve hardening of the Epon block, the agar blocks with surrounding Epon

were placed into a rubber mold and baked for 12-24 hours at 65°C.

2.6.3. Preparation and staining of ultrathin sections

The Epon block was trimmed with a razor blade to remove excess Epon material and get close to the embedded pellet. Ultrathin serial sections (60 nm) were cut with a diamond knife (Delaware Diamond Knives, Wilmington, Delaware, USA) on a RCM MT 6000-XL microtome (RMC, Tuscon, Arizona, USA). The Epon block was trimmed with a glass knife to form a small trapezoid, surrounding the embedded pellet. Thin sections were transferred from the dH_20-filled tank to the pioloform film of the prepared mesh grids. For the staining, the grids carrying the thin sections were inserted in a rubber grid holder, covered with the drop of 2,5% uranyl acetate and incubated 20-25 min at RT, protected from light. Uranyl acetate was washed out with water and the grids were air-dried. The grids were then covered with a drop of lead citrate and incubated 3 min. The lead citrate was washed out with water.

The lead citrate solution was made according to the following recipe: 2,1 ml sodium citrate solution (4,15 g in 50ml dH_2O) was mixed with 2,1 ml lead citrate solution (3,13 g in 50 ml dH_2O)

The white precipitate was dissolved with 0,8 ml 1M NaOH. Finally the solution was aliquoted and stored at 4°C. Uranyl acetate was also stored in aliquots at 4°C. Both lead citrate and uranyl acetate are centrifuged 5 min at 15800 *x g* (Eppendorf-Centrifuge 5415C, 14000 rpm, RT) right before usage.

2.6.4. Electron microscopy and documentation

Micrographs were taken with a Philips CM10 Transmission Electron Microscope (TEM) and documented photographically using a plate camera of 65x90 mm with Scientia film (23D56 P3 AH, Agfa Gevaert, Leverkusen)

2.7. Databases and software

2.7.1. NEBcutter v. 2.0

To determine if given restriction enzymes cleave a particular DNA sequence, NEBcutter v2.0 (New England Biolabs) online software was used. The sequence could be input as a text file, FASTA file, or GenBank number. The software can be found under the following address: http://tools.neb.com/NEBcutter2/index.php

2.7.2. Sequence alignment software

To read and edit chromatographs obtained from the sequencing service facility at the University of Cologne (Cologne Center of Genomics) Chromas and GeneDoc editor software were used. These software allow manual editing and adding a wide range of attributes to multi-sequence alignments, export sequences in plaint text, reverse and complement the sequence and chromatogram, display translations in 3 frames along with the sequence, and so on.

2.7.3. *Chlamydomonas* genome database

Chlamydomonas genome sequence as well as gene models are available at JGI, the Joint Genome Institute (Merchant et al., 2007) genome database. In this work Version 2.0; Version 3.0 as well as the latest Version 4.0 were utilized. The following links can lead to all 3 versions of genome database:

http://genome.jgi-psf.org/cgi-bin/browserLoad/49e3832322afd07856057038

http://genome.jgi-psf.org/cgi-bin/browserLoad/49e383961780c79466d1cf24

http://genome.jgi-psf.org/Chlre4/Chlre4.home.html

2.7.4. BLAST

Sequences were compared using Blast (**B**asic **L**ocal **A**lignment **S**earch **T**ool) of NCBI (The National Center for Biotechnology Information) public database. The web page is the following:

http://blast.ncbi.nlm.nih.gov/Blast.cgi

2.7.5. EXPASY

To analyze protein sequences and structures EXPASY (**Ex**pert **P**rotein **A**nalysis **Sy**stem) proteomics software was used. It provides access to a variety of databases and analytical tools dedicated to proteins and proteomics. The software can be found under the following address:

http://www.expasy.ch/

2.7.6. COILS

Prediction of coiled coil regions in proteins was done with the help of COILS program (Lupas et al., 1991). This program calculates the probability that the sequence will adopt a coiled-coil conformation. It can be used online under:

http://www.ch.embnet.org/software/COILS_form.html

2.7.7. MHCPred

To find out how many epitopes an antigen could possibly posses and where they are located, MHCPred software was used (Guan et al., 2003). This program predicts the binding affinity of major histocompatibility complex (MHC) class I and II molecules. The software can be found under the following address:

http://www.jenner.ac.uk/MHCPred/help.htm

2.7.8. Primer3

For designing PCR primers Primer3 online software was used. Primer3 has many different input parameters that can be controlled, which allows designing primers specific for one's goal. The software can be found under the following link:
http://biotools.umassmed.edu/bioapps/primer3_www.cgi

3. Results

3.1. Developing an isolation protocol to purify the cartwheel structure

One of the aims of my PhD thesis was to develop an isolation protocol to purify the cartwheel structure. Since probasal bodies have longer cartwheels than basal bodies, we assumed that the isolation of probasal bodies and comparison of their protein composition with that of mature basal bodies would help to identify novel cartwheel proteins. Different cell wall deficient mutants, buffers and detergents were employed during the development of an isolation protocol for probasal bodies. To facilitate the isolation of the cytoskeletons several cell wall-less mutants of *Chlamydomonas reinhardtii* were used. During the study the following mutants (*cw2*, *cw15+*, *cw15-*, *cw92*) were employed A detailed description of the strains and culture conditions can be found in chapter 2.2.1.

Different cell wall deficient mutants showed different cell growth. For instance, in 10 days *cw92* cell number reached from original approximately 2 x 10^5 cells per ml to 5 x 10^6 cells per ml. *cw2* and *cw15+* strains showed a slightly lower cell number (4 x 10^6) after 10 days growth compared to *cw92*. Interestingly, relatively slowly growth (2 x 10^6) of *cw15-* mutant has been observed after 10 days of incubation. Light microscopic observations showed that most of the cells of *cw15-* lack flagella.

To study the lysability of mutants five different nonionic detergents were used: Nonidet P40 (NP-40), Triton X-100, Brij58, Tween 20 and deoxicholic acid. Several concentrations of these detergents were tested, starting with very low (0,5%) to high (4%). The experiments were examined and documented by phase contrast light microscopy. 4% Nonidet P40 and 4% Triton X-100 (end concentration 2%) appeared to demonstrate the best lysability results, i.e. by treating cells with these detergents and using the above mentioned concentration the cells were completely lysed and cytoskeletons were retained. Based on cell growth and lysability data I have decided to use *cw92* as a model system in my studies.

Another important step towards developing an isolation protocol is the selection of an appropriate buffer. Two buffers were used in this study: TE buffer (Tris-EDTA buffer) and MT buffer (microtubule-stabilizing buffer). As it is shown in the purification protocol of basal

bodies modified in our lab (Brachhold, 2007) by using TE buffer probasal bodies are detached from basal bodies. Moreover, the cartwheel structure in basal bodies as well was not observed in EM preparations.

Electron micrographs of isolated cytoskeletons show that by employing MT buffer probasal bodies are still intact and attached to basal body (Figure 6) whereas by using TE buffer the probasal bodies are detached and no cartwheel structures has been observed (Brachhold, 2007) (results not shown). Because MT buffer helped to retain the basal bodies together with the probasal bodies, all following experiments were performed with the MT buffer.

Although the presence of probasal bodies as well as the cartwheel structure of basal bodies was verified by electron microscopy in ultrathin sections of embedded cytoskeleton preparations, further purification steps were necessary to obtain pure probasal bodies. Further experiments to purify complex of basal and probasal bodies with the following detachment of probasal bodies from basal bodies were not successful.

Even though progress has been made towards isolation of probasal bodies, purification needs to be improved. Importantly, it was shown that only by using MT buffer and low percentage non-ionic detergents such as NP-40 and Triton X-100 the intact structure of the cartwheel could be preserved.

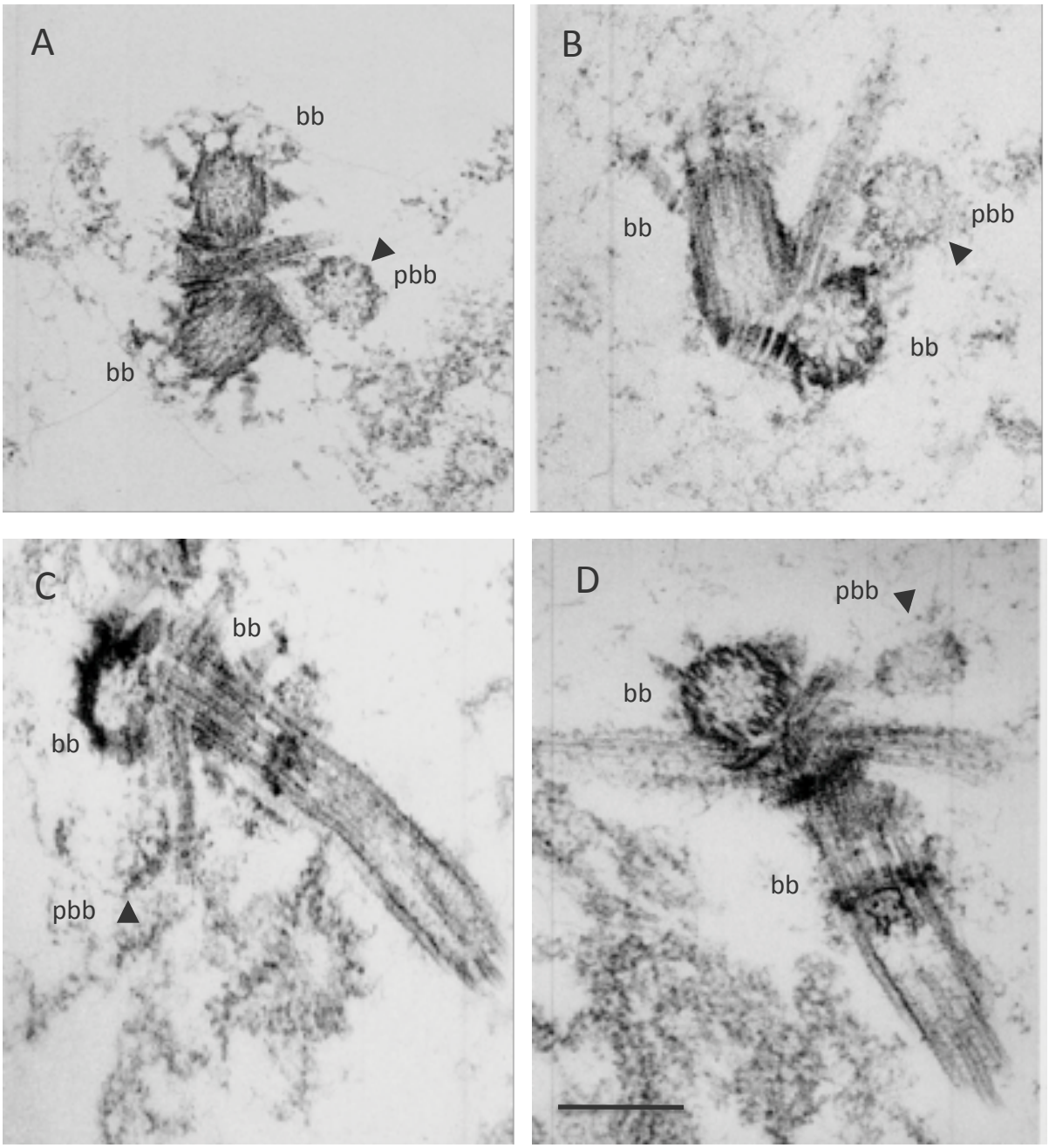

Figure 6. Transmission electron microscopy image of the basal and probasal bodies in *cw92* isolated cytoskeletons.
(A, B) Cross-sectional view of the basal bodies (bbs) and a probasal body (pbb) (arrowhead).
(B) The cartwheel structure with the characteristic hub and spoke complex is observed in one of the bbs and a pbb.
(C, D) The longitudinal section of the bbs and a pbb (arrowhead). Scale bar, 250 nm.

3.2. Generating antibodies against cartwheel protein Bld10

An alternative approach to study cartwheel proteins could be to use an already known cartwheel protein as an antigen to raise antibody against it. This antibody can be used for different affinity-based applications. When I have started to work on this project the only cartwheel protein known was Bld10p (Matsuura et al., 2004). Currently, another cartwheel protein (SAS-6) has been identified in *Chlamydomonas* (Hiraki et al., 2007).

3.2.1. RT-PCR to obtain *bld10* partial cDNA

To amplify partial cDNA from total RNA RT-PCR (reverse-transcription polymerase chain reaction) was performed. The *bld10* gene has a single ORF of 4923 bp that encodes 1640 amino acids of Bld10 protein (Matsuura et al., 2004). Clearly, the cloning of the whole length DNA would be very complicated, especially considering the fact that the *Chlamydomonas* genome has high a GC content. Therefore, 3 pairs of primers that would cover parts of the molecule were designed, i.e. N-terminus, C-terminus and middle part. I anticipated, that the estimated size of the PCR products should not be over 1500 bp (Figure 7A). To check whether nucleotide sequences of the products were in frame and corresponded exactly to the amino acid (aa) sequence the DNA sequence was translated and compared (blasted) with aa sequence in *Chlamydomonas* genome database (JGI). Following primers were designed to obtain partial PCR products: Bld1_for and Bld2_rev primers generate PCR product A (1119 bp). Product A was positioned in the N-terminal part of the molecule. PCR product B (1350 bp) was generated by the Bld3_for and Bld4_rev primers and localized in the middle part of the molecule. PCR product C (807bp) was generated by the primers Bld5_for and Bld6_rev and positioned in the C-terminal part of the molecule.

A

```
   1 atggccatcg atgtagaccg aactctcgcg gtcctccggc gcaagctgga ggcccttggc
  61 tactccgacc cgcttgaacc ggcgagcttg cagctggtgc aaaagctcgt agaggacttg
 121 gtgcacacca cggacagcta cacggccgtg aagcagcaat gcgcgaagca agctcaggag
 181 atagcagcgt tcgacacacg gctggagtca gtgcggcagg actcggtgcg gctgcagtcg
 241 gagaacagcc agctgcacgt ccttgtaatg cagcacgcgg agcggcacga gcgggaggcg
 301 cgggagcact acacggcggt gaagcggctg gaggacacca tcgcagagct gtcctactgg
 361 aagcacgctg ctgcggagaa actggcgtcg gcggataagg agaacgcggg gctgcggaag
 421 cggtgcgagg agctggccaa gctcacggac cgccttgcct cgggcgctgc gaccccgcag
 481 tccgtggcgc ccaagatttc ctcgcgcagc cccatccggg ttgcgcctcc tccctctccg
 541 ccgcggcccc gtcaggccac tgtggatgtg ctgcaggccg ctaacggcag gatcctgtcg
 601 ctgcagcggc aactggccga cgccaccgca gagctgcagg agctgcggca gcgcgtggcg
 661 gaggacgagg accagatccg gcggcgggac gtggagatcg accgcctggg cactcgggcg
 721 gggacggaca ccaacgtgct ggcgctgcgg gcacgcaacg aggccaatga gagcatgatc
 781 ctgcagctca acggcacggt ggaatccctg gcggcccggg tccgtgagct ggaggccgtg
 841 gaggtgcggt gtgaagagct gcaggggggca ctgcgccgcg cggagatgga ccgcgaccag
 901 gcagaggagc gttacagcag gtctgcacgc gaccacgacg ccctgtctcg tgaggtgttg
 961 ggcctacgcc gcgacttggc ggctctgcag gacaccaaca acagggcggc ggggctgctg
1021 gcggcagacg cggcgggggc tagtacaccg gacacaaccg caggggcccc ggcgctgcgg
1081 cagcgactgg ctgactctcg ggcggacgtg gagaggctga gcgggcagtt ggcggcggcg
1141 gacatggagc ggagaaacct ggcgcagcag ttgtccgcct tgcgctcgga gctggacgat
1201 acccagttcc tgctggcgga ggcacagagc cgcgccgctg ggctggcggc agcgcaggca
1261 gtggcggaga gcgaggcgcg acggctggct ggcgaggcgg cggcacgtga ggggcggctg
1321 cgggagctgg acagccaact ggcggtggtg ctgtccgacc tggaggcgcg gcaggcgggc
1381 tttgcagcgc tggagaagga ccgcgcggag gccaatgcca gggctgagga gctggctcgg
1441 cgcctggatg aggtggagcg ctctgcggcg tctgagcgcg cggctgcggc ggcggcacag
1501 cagtcggtgt cgcggctgga ctccgagctg agggtggtgc ggggcagcgc agccgcgttg
1561 gaggcagagg cggcggcatt gaggcaggag ctccaggacg tgtctgtggg caaggtgcgt
1621 gccacgtcgg cgctgagcag cacagaggac gaggctgttc gcgcgcggca gcaagcagaa
1681 gcgctccgga tgcagctgac ggccgagcgc cgcgctgcgg aggagctgcg ggcgggccac
1741 gacacgctgc agctcgaggt ggaccggctg ggcggccagc tggcgctgca gcaacaggag
1801 gcggagctgc tgcggcagca actggctgcg gcgcgggggcg agctggcagc cagcgaggcg
1861 gcggccagcg gcgccgagca gaagctgtcg gggttaggag cgctttcgca acggctggaa
1921 gagatgggcg agcaggcgcg ccgcgcacag gcggccaccg ctgaggctga ggcagaagct
1981 gtgcgactgc gggcggcggt ctccgaagcc aaggaggggc aggcgcgggc ggagcggggc
2041 ctgcgggagg cgaggcggga ggtcgagggc gcgcgggagg cagaggcgct ggtccgggcg
2101 cagctgcgtg aggttgaggc acaggcggaa gggacgtcca aggcactcaa ggcagcagag
2161 gccgaccgtg accgcgcgct gatggacgcg cgcctggccg ccggcgacct ggcgtcattg
2221 cgcgatcagc tggcggcgga gacgtcctcg gcggcagacg cgggcagcac cgcacggcag
2281 atggcggcgc ggctatcagc ggcggagcgg gcggcggctg cggcgcagga ggagcgcgag
2341 cgggcagcgg tggcggctga ggaggcggaa gcggcggctg cagcagctcg gggtcgcgag
2401 gaggaggccc gtgcccaggg ccgcgagtgg gcggagcgcg ctcggcgagc agaggcactg
2461 gtggcagagt atgaggccga tgtgacacag ttgcgcgcgg cccgtgactc ggatgcggcg
2521 gcgctgcgct ctctggagga cactgtggcg gcggctcggc gggacctgga cgccggcgc
2581 agtgaggtgg agcagctgac cactctgagc ctgaggggtg acgccactgt gcaggagtac
2641 atggcaaacc tcaaggccat gtccactgat ctacgtgccg ccgaaatgcg cgccgctgac
2701 ctggcgggtg aggcggcggc ggcacaggac gcggccgcca gctggcgcag tgaggcggag
2761 cagctgcggg gcctgctgcg gcagatggat gcggacaggg acaacctgca gcacgagctg
2821 gatgccaagg cagagcggct ggtggcgcaa gagcagcagc tagcaggggc gcaggcagca
2881 gagcaggagg cagccaggct gttggcgctg gctgagggcc gcttggcgct gacggacaac
2941 cgcgcgcggg agggcgaggc agaagctgcg gcagtgcggg cgcagctggc ggcggcgctg
3001 gacagtgtgc gggcgctgag cggcgagggc gaggcgctgc gtgaggagct gcgggcggtg
3061 agcgaggacc tggaggcgct ggtgcgagag aaccaagtag tgggcggcga gctggcggcg
3121 gtggcggcgc agcgggacag cgcggcagag gaggcgcggc ggctgggcgg gcggcgggcg
3181 agtgcggagc agctgctacg ggccaaggag gcggaggcgg aggacctgcg gcgtgtttat
3241 gaggcgttgg cggcggagca ccggcggctg cagggcggtg ttggggctct ggagcgggag
3301 ggtgccatgc gcgaggcggc gctgcaggcc aaggcggcgg aggtgtccag tctggctgag
3361 tcacagcggg ctgcacaggc caccatcaac cagtatgtca tggacctgca ggcgtttgag
3421 cggcaggtgg actcgctgtc gcggcagctg agccaggcag aggcagacgg cgaggagctg
3481 gtgcggcagc gtgaggcgct gctggaggag atacgcgcgg cgcagcaggt gcggctgggt
3541 ctggagcggc accgtgagga gctgcagcgg caggtggcgt cactcgacag ccaggtggcc
3601 atcggccgcg cccggctgga ggactccaac agcgaggctg ccagcctcaa ccagcgcctg
3661 gctatggaac gaagcagggt tgcggagctg gagggtctgc tggcgggcat gcgggcgcgc
3721 gagttccgca gcgactttcgc cagcgaccgg gcaggcggcc agctggcggt catggtggac
3781 cgtaacaggg cgctggagga gcaggtagcc tccttgcagc accaggtggg ggcgctgcag
3841 gcctcgcggg aggcgcagga ccgcgagctg tcccgactgc gtggcgaggc gctggcgctg
3901 gcggccagca ccgcggccag cctggaggga cgcacagcag ctgcgggcgg cgcagcggcg
3961 ggtgcggcca aggaccaggc cgcggcgttg gatcggctca cctcggagcg ggacgccgct
4021 caggacgagg cagcccggct gcgggggggct ctggcggctg ccgaggcagc ggccgcctcg
4081 gcgtctacag ccgccgccgt gtccatccca gctgctggct ctgggtctga ggctgctgcg
4141 gtgctgcggg tccgctgctc cgagctggag cgccgcaaca cggagctgat gcaggagctg
4201 cgcacgctgc aggacacgtg ccggcagcag gagtcgctgc tgtctgcggc acagaacgag
4261 ctgagtgcgc tgcaggcaga gcaccggcgg ctggtggagc tggtggcgcg gctggaccag
4321 gacaaggcag cggcggcagc agaggccgcc gccgcccggc agcaggtcgc aacggccacc
4381 cggcgtgtag ccactgcgga acaggaggcg gcggcgggcg cggcgcggct gcagtcgcag
4441 ctgagggacg agcaaggccg gcggcgccag gccgagcgcg acttcctgga gctgctgtcc
4501 agcattgagg gagcgggcgg cgaggcggcg gcggcggcag ttgcggccgc tcacggcgag
4561 ggcgcggcgg agctggccag caggcgcttg cgcgagctgc agacccaggt ggatgctctt
4621 gaggccgaga aggcgggtct ggaggaggcc acgcagcgca cccgcgccac cctgggagcc
4681 atgtcgggac agatggcagc catacaggcc gagtatgacg ccactaatac tgcactggcg
4741 ggtctggcgg gggccatggc ggccggcgcg caggacaag gccaggtgca ggggcccgct
4801 gggaccgcgc ctgctgctgc cgcaggcgcg ccggggccac agccgggtca ggcgcaggcg
4861 gggggctttg gcgggggcga cggtggcggc agcatcagcc tctcgggggg gccgcgtcgg
4921 tag
```

B

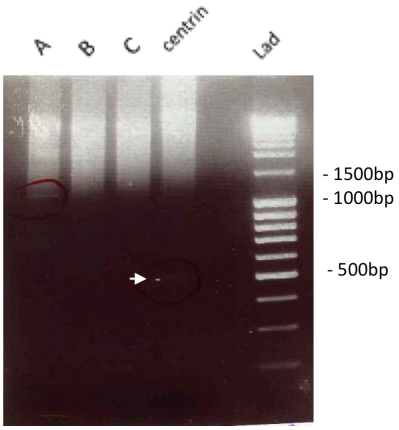

C

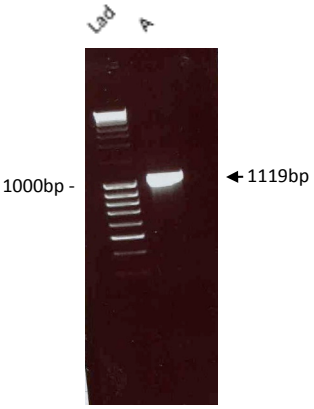

Figure 7.

(A) cDNA sequence of *bld10*. The colored and underlined sequences correspond to the respective primers. Bld1_for and Bld2_rev primers are shown in red and generate the PCR product A (1119bp). Bld3_for and Bld4_rev are demonstrated in pink and produce the PCR product B (1350bp). Bld5_for and Bld6_rev are depicted in green and generate the PCR product C (807bp). Primers KM1_for and KM2_rev (Matsuura et al., 2004) are depicted in blue. Primers mdl1_for and mdl2_rev are displayed in yellow and were later used to verify that the sequence of the partial cDNA was correct.

(B) RT-PCR of the products A, B, C and centrin (positive control). Only product A produces a faint band (black arrowhead), whereas the other products show no band. Centrin (white arrowhead) also produces faint band.

(C) The reamplification of the product A. After the reamplification a clear sharp band is observed.

As a positive control in RT-PCR primers for centrin were used that generate the product of about 500 bp. The PCR showed faint bands of centrin and product A (Figure 7B) The PCR for the products B and C did not work. To obtain more PCR product product A was reamplified, which after visualization showed thick band on a gel (Figure 7C).

3.2.2. Cloning strategy

Here, a cloning strategy for the production of the partial bld10 recombinant protein (product A) tagged with a polyhistidine sequence is presented (Figure 8). First, product A was cloned into the pGEM®-T Easy vector and the plasmid was transformed into JM109 competent cells. After the plasmid isolation the DNA sequence of product A was verified by sequencing. Because product A has relatively long sequence, extra primers were designed to cover the whole length. After having overlapping fragments of the whole product A, the sequence was verified by sequencing. To introduce restriction sites PCR with restriction enzyme primers EcoRV-1_for and NotI_3 rev was performed. Additionally, the absence of these restriction sites within the insert was checked by using NEB cutter software. The PCR product was cloned into expression vector pETBlue-2. The pETBlue-2 provides a vector-encoded ATG start codon. Then the plasmid was transformed into Nova Blue competent cells. Nova Blue cells (K-12 strain) serve as an initial cloning host, because it has high transformation efficiency, and a capability of blue/white screening. After transformation into Nova Blue competent cells and blue-white screening 4 clones were picked and subjected to sequencing. Overall four primers were used for the sequencing: pETBlue UP, pETBLue Down and the internal primers mdl1_for and mdl2_rev. The sequence of only 1 clone was correct; the other three clones had shown some errors in the chromatogram. Subsequently, the plasmid was transformed from the correct clone into expression strain Tuner™ (DE3) pLacI cells (Figure 8).

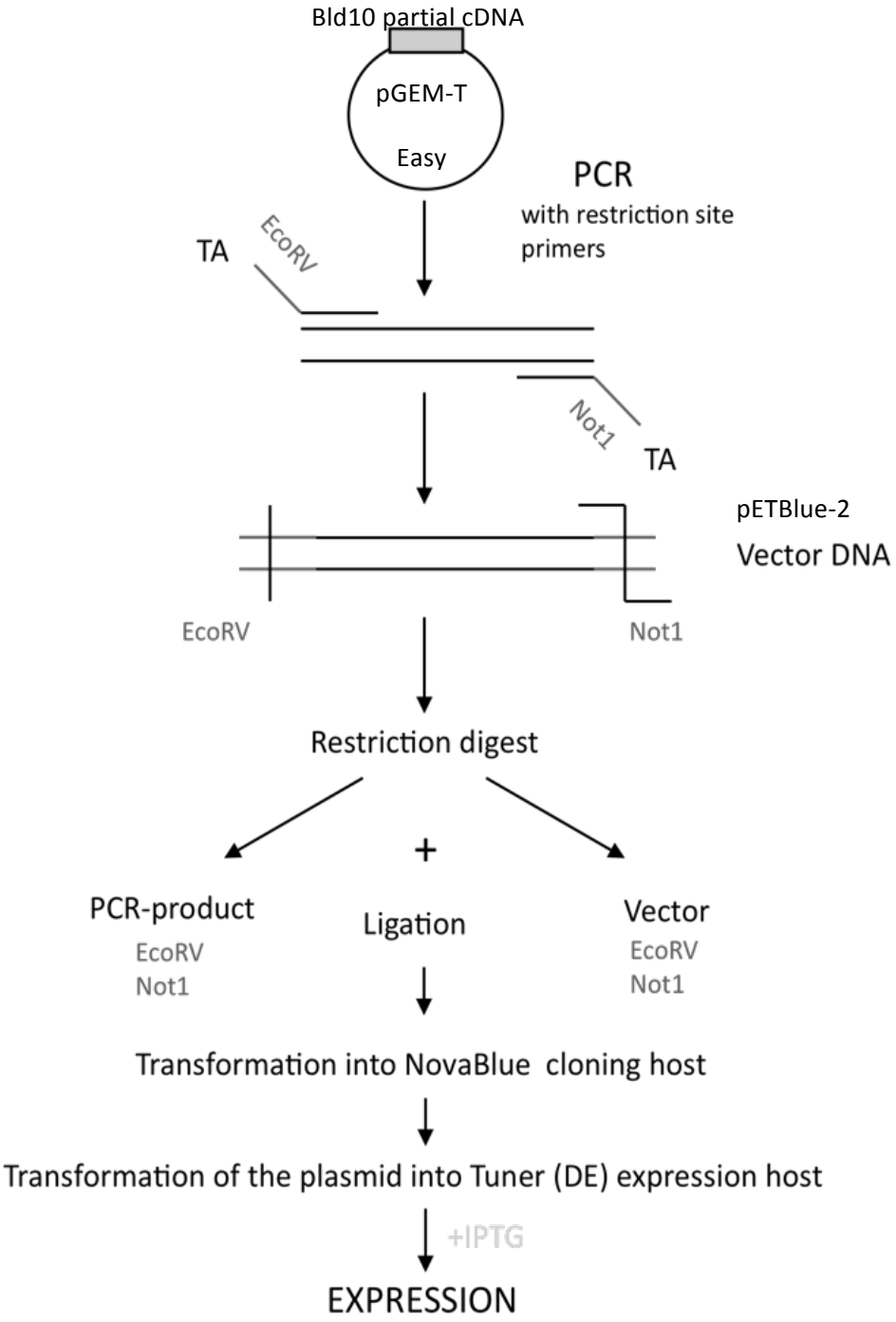

Figure 8. Schematic diagram of the cloning strategy.

3.2.3. Hetereologous protein expression of the partial Bld10p (product A)

After the target plasmid was established in Tuner^{TM} (DE3) pLacI cells, expression of the target DNA (product A) was induced by the addition of the 250 µM IPTG to a growing culture. To assess the expression of the target protein induced and uninduced cell cultures, as well as soluble and insoluble fractions of the induced culture were loaded on a SDS-polyacrylamide gel followed by Coomassie staining. Product A has a molecular weight of approximately 45 kDa. After the IPTG induction the thick band expected to be observed. Surprisingly, no detectable induction was observed on SDS-PAGE (Figure 9).

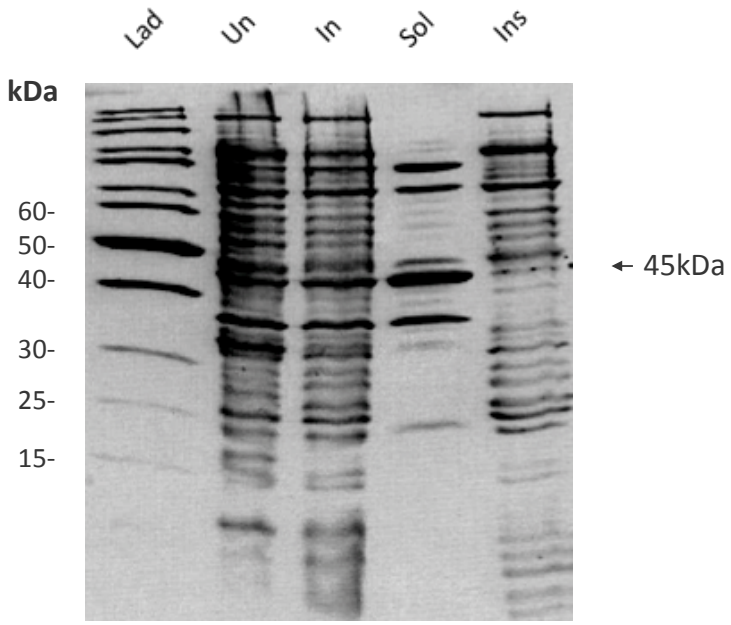

Figure 9. Protein expression of product A. The first two lanes after the ladder represent the total cellular proteins of the uninduced and the induced bacterial cultures respectively. The fourth lane is the soluble fraction of the induced bacteria and the fifth lane is the insoluble fraction (inclusion bodies) of the induced bacteria. Samples were run on a 12,5% SDS-polyacrylamide gel, and stained with Coomassie. Approximately 10 µg/lane protein was loaded on a gel.

Further induction experiments using different clones also did not produce overexpression of the recombinant protein (results not presented). To prove whether the insert is still incorporated within the plasmid in induced bacterial culture, restriction digest with the help of restriction enzymes NotI and EcoRV was performed, where uninduced culture served as a

positive control. Surprisingly, both induced and uninduced cell cultures showed no difference in outcome i.e. the digest showed that the insert was still present in the induced culture.

3.2.4. Cloning of different partial *bld10* cDNA sequences

Owing to the fact that the partial *bld10* product – product A was not expressed in detectable amounts, a new set of experiments was conducted starting with the synthesis of the first strand cDNA. For the RT-PCR the same primers with the same and different combinations were used (Figure 7A). As it is shown in Figure 7B two pair of primers, which generate product B and product C did not produce any band after RT-PCR. Because here I intended to test different PCR conditions these primers were as well employed. Primers Bld3_for and Bld4_rev produce product B (1350 bp), Bld5_for and Bld6_rev – product C (807 bp), mdl1_for and mdl2_rev – product D (660 bp), km1_for and km2_rev – product E (565 bp), Bld3_for and Bld6_rev – product F (2326 bp), mdl1_for and Bld2rev – product G (828 bp) and finally Bld1_for and mdl2_rev – product H (827 bp). The primers km1_for and km2_rev were used by the group of M. Hirono to amplify the cDNA sequence with the following heterologous expression of the protein and the antibody production (Matsuura et al., 2004) The RT-PCR with all above mentioned primers did not reveal bands on a agarose gel (result not shown). However, the positive control (centrin) did work. The following reamplification reaction produced some non-specific bands (result not shown). In order to get rid of non-specific bands, the reamplification was performed using higher annealing temperature of 59°C.

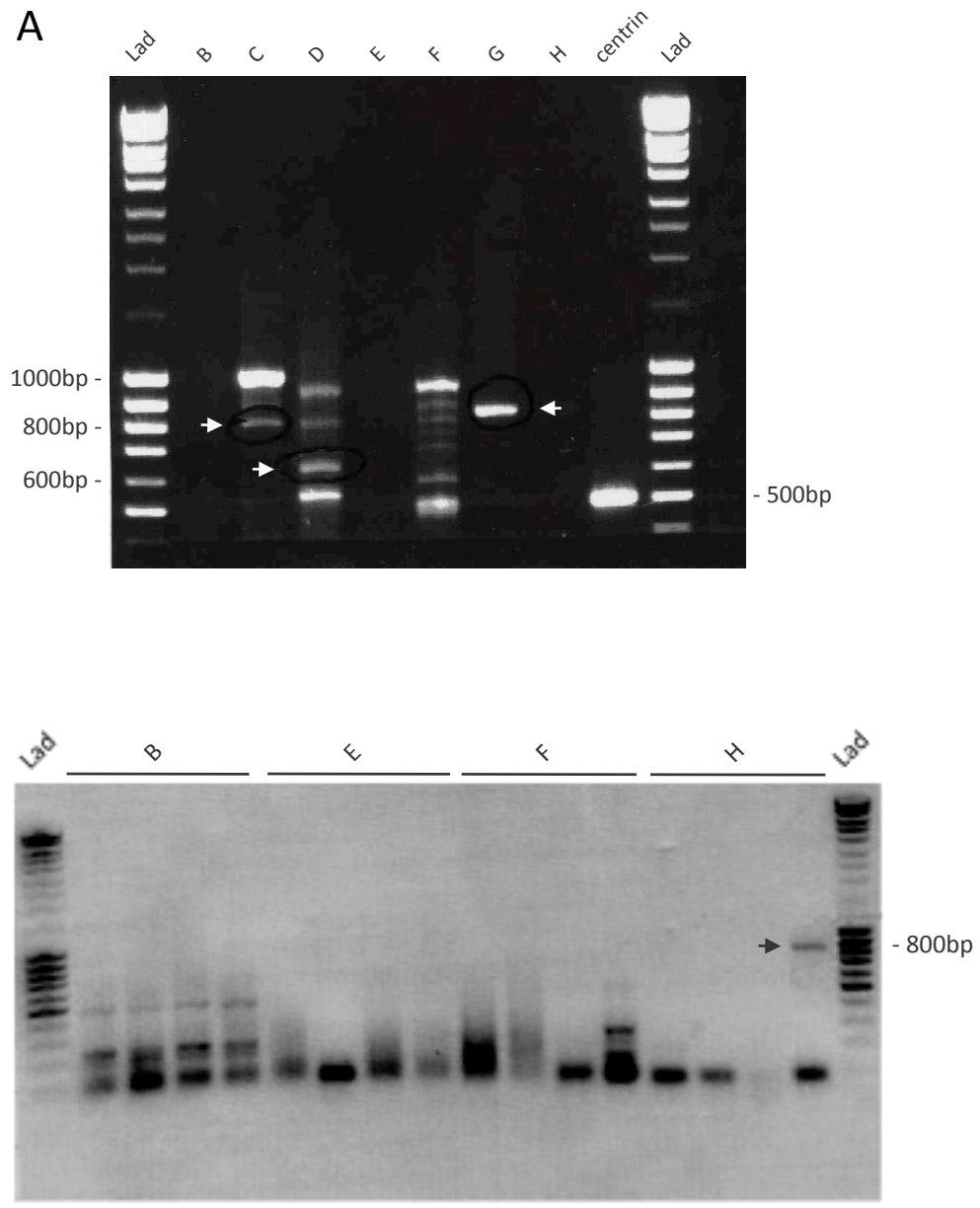

Figure 10.
(A) Reamplification with the annealing temperature of 59°C. The lane numbers correspond to the products numbers. Arrowheads depict the product bands of the expected size.
(B) Reamplification of the products B, E, F, H using different DNA concentrations. From left to right the DNA amounts are increasing from 1 µl, 1,2 µl, 1,5 µl and 2 µl respectively for each product. Only one replicon (2 µl DNA) of product H produced a band of the correct size.

In this case, along with the non-specific bands only PCR of products C, D and G showed bands of the expected sizes (Figure 10A). Separate PCRs with the annealing temperature of 59°C and 65°C were conducted for product E, because of high Tm of the primers.

Interestingly, none of these PCR reactions worked. Moreover, the reamplification also did not produce any products.

In order to get PCR products for the products B, E, F, H as well I performed PCR reaction using 4 replicas, using the following different DNA amounts: 1 µl, 1,2 µl, 1,5 µl, 2 µl. The PCR did not produce any bands, but the reamplification reaction worked for the product H (Figure 10B).

Thus, only products C, D, G, and H were cloned and transformed into JM109 competent cells. The transformation did not work for product D. The sequences of the other three products (C, G and H) were verified by sequencing. Subsequently, primers with restriction sites were designed following the cloning strategy outlined in a chapter 3.2.2. (Figure 8). Then PCR was performed followed by the cloning in vector pETBlue-2. The vector was transformed in Nova Blue competent cells and the sequence was verified by sequencing. Three clones of product C, two clones of product G, three clones of product H were sequenced. Both chromatograms (forward and reverse) of the product G sequences revealed an incorrect sequence. Only one clone from products C and H respectively was correct. Remarkably, the sequence of the product C was truncated compared to the original one. Although the sequence was in the correct reading frame, 80 aa were missing from the original cloned sequence. Subsequently, the transformation of the plasmids from the clones of these two products (C and H) into Tuner^{TM} (DE3) pLacI cells was performed. After the induction with 250 µM IPTG the total cellular proteins of the induced and uninduced bacteria as well as their soluble and insoluble fractions were loaded on a gel. Again, no overexpression of the recombinant protein was detected on a gel (Figure 11A).

3.2.5. Expression of the partial Bld10p (product C)

To obtain the expression of the Bld10 partial recombinant protein numerous experiments were tried out to optimize conditions for successful expression. Because the bacteria that contained plasmid with product H showed very slow growth and relatively low OD_{600} all further experiments were performed only with the bacteria containing product C. In order to obtain expression of partial Bld10p I tested different IPTG concentrations from 50 µM to 500 µM, used freshly prepared IPTG, different temperatures for bacterial incubation starting

with 16°C up to 37°C and different incubation times harvesting the bacteria 1 to 4 hours after incubation.

Neither of these experiments produced expected results. To observe whether the recombinant protein is present in the bacterial culture and did not degrade right after induction Western blotting using His-monoclonal antibody was performed. This His-Tag antibody is a mouse monoclonal antibody directed against the His-Tag sequence. The antibody recognizes five uninterrupted histidine residues. In this experiment induced bacterial cultures grown 3 hours at 23°C, 28°C and 37°C were used. In all induced cultures a band at the expected size of 23 kDa was detected, which proofed the presence of the recombinant protein in the cultures (Figure 11B).

Later, I also demonstrated by the Western blotting that the recombinant protein was in the soluble cytoplasmatic fraction of the bacterial culture rather than in the insoluble fraction, known as inclusion bodies (result not shown). Evidently, the fact that the recombinant protein was expressed at very low amounts made it impossible to detect it on a polyacrylamide gel. Therefore, I aimed to purify the target protein and determine the target protein level. The purification was performed with the help of His-Tag, i.e. by using the Ni-column in order to isolate the recombinant protein. Cell extract was prepared by using BugBuster extraction reagent, which is an alternative method to mechanical cell disruption methods. This reagent gently disrupts the *E.coli* cell wall and liberates the proteins.

After the BugBuster treatment, the soluble fraction of the extract can be directly loaded onto the His-Bind Resin. The column was loaded with soluble extract and afterwards the flowthrough was collected. Several washing steps by using binding buffer and washing buffer were performed to wash away other proteins. When unbound proteins are washed away, the recombinant protein is recovered by elution with imidazole. Almost two liters of culture were cultivated in order to obtain a maximal amount of target protein. After the purification with the His-Bind Ni-charged column, the samples were loaded on a SDS-polyacrylamide gel. As it is shown in Figure 12 the target protein level was significantly enhanced and made it attainable to detect it on a SDS-PAGE. It is important to emphasize that only after the purification of the target protein with the help of Ni-column, it was possible to detect the recombinant protein on the gel.

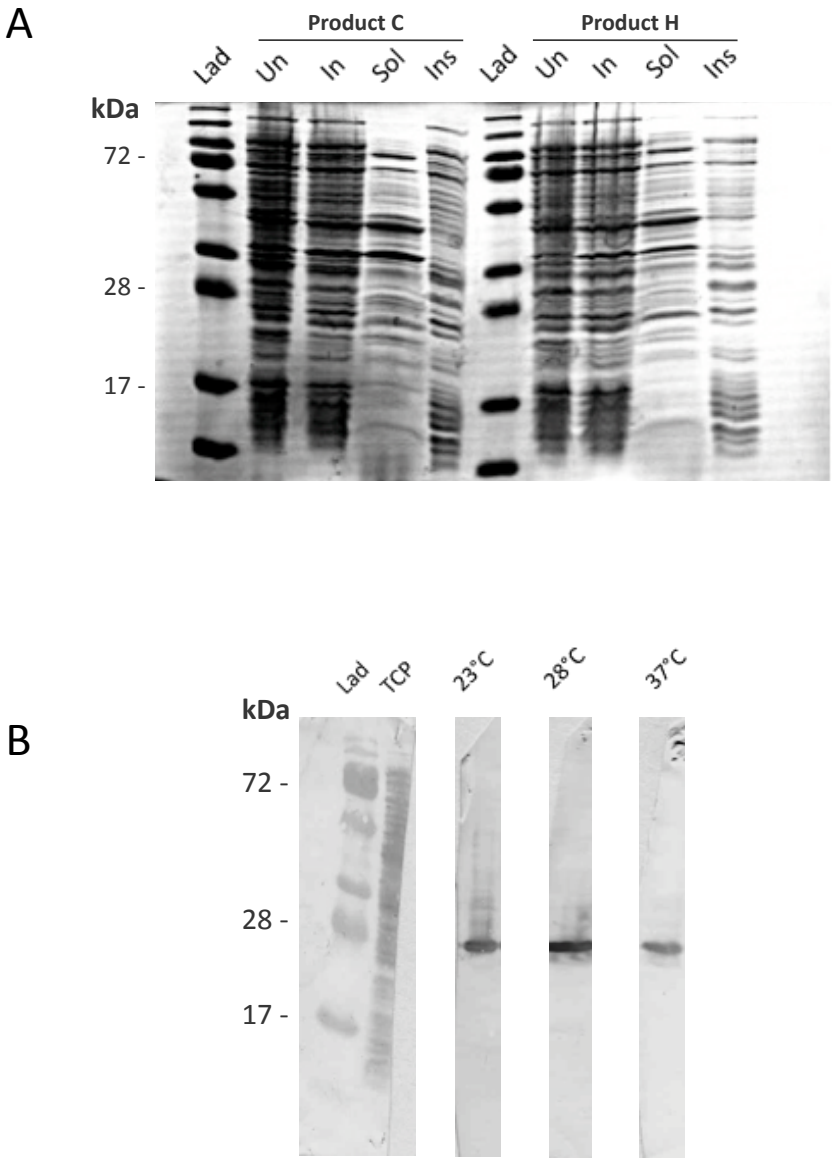

Figure 11.
(A) Protein expression of the products C and H. The first two lanes after the ladder represent the total cellular proteins of the uninduced and the induced bacterial cultures of the product C and H respectively. The fourth lane is the soluble fraction of the induced bacteria and the fifth lane is the insoluble fraction (inclusion bodies) of the induced bacteria. No prominent band was observed. Approximately 10 μg of the protein per lane was loaded Samples were run on 12,5% SDS-polyacrylamide gel, and stained with Coomassie.
(B) Western blotting of the induced bacterial culture incubated at 23°C, 28°C and 37°C. The ladder and bacterial TCP (total cellular protein) are stained with amidoblack. As a primary antibody His-tag monoclonal ab (1:2000) was used. All three samples showed positive results.

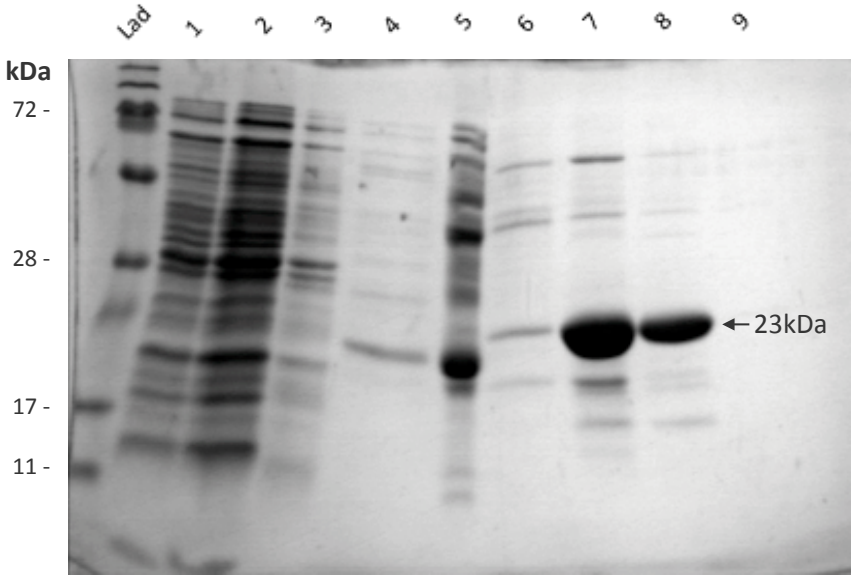

Figure 12. The protein expression of the product C after the purification with His-Bind Ni-charged resin. Lane 1 – flowthrough; lane 2 – combined washing fraction 1 and 2 after treating with binding buffer; lane 3 – combined washing fraction 3 and 4 after treating with binding buffer; lane 4 – combined washing fraction 1 and 2 after treating with washing buffer; lane 5 – combined washing fraction 3 and 4 after treating with washing buffer; lane 6 – elution fraction 1; lane 7 – elution fraction 2; lane 8 – elution fraction 3; lane 9 – elution fraction 4. Approximately 10 µg of the protein per lane was loaded. Samples were run on 12,5% a SDS-polyacrylamide gel, and stained with Coomassie. The recombinant protein was eluted in fractions 2 and 3.

All other attempts to change parameters, such as the temperature or IPTG concentration did not change the outcome. After the successful detection of the recombinant protein (product C) on the SDS-polyacrylamide gel, I tried to use the same strategy for the product A, i.e. to purify the target-protein by Ni-charged column. Interestingly, no overexpression or very little expression has been observed in this case (results not shown).

Several harvests with 2 liters of bacteria had to be performed in order to get enough protein/antigen for the antibody production. Approximately 1 mg of protein was necessary for the immunization of two rabbits. As it is depicted in Figure 12 the eluate with the target protein contained, along with target protein, also some other proteins in minor quantities. However, in order to get a specific antibody it was necessary to obtain pure protein. Therefore, a preparative gel was used to further purify the product. After electrophoresis, the band was excised and electroeluted. Then, the eluate was dialyzed and the protein concentration was estimated and finally frozen. Finally, lyophilisation was performed. About 800 µg of protein was obtained after several harvests that was used to generate polyclonal antibody against the recombinant product C.

3.3. Three anti-Bld10p antibodies

The product C was localized at the C-terminal part of the molecule. Remarkably, this partial protein was the only product of Bld10p, which could be heterologously overexpressed in bacteria. Because of its C-terminal end localization it has been named antigen C and the respective antibody – anti-C antibody. The molecular weight of the antigen C is approximately 23 kDa. Antigen C was injected in two rabbits, which induces B-cells to produce immunoglobulins (IgG) specific for the antigen. These antibodies are polyclonal, since they are derived from different cell lines, i.e. they are a mixture of IgGs secreted against a specific antigen, each recognizing a different epitope. Once a high titer of antibodies was achieved, polyclonal IgGs from sera were ready to be used in laboratory experiments. The IgGs were purified from the sera with the help of protein A column. Additionally, for more specificity, affinity purification of the IgGs was conducted by using a Western strip technique.

In order to obtain specific antibodies against other important regions of the molecule, such as the N-terminal part and the middle part of the molecule two specific polyclonal anti-peptide antibodies were generated. These polyclonal antibodies were raised against synthetic peptides. The main advantage of using synthetic peptides for the antibody production is that specific epitopes can be targeted. The selection of the peptide sequences of Bld10p was guided by the coiled-coil nature of the protein. The design of peptides was defined based on the presence of epitopes, localization of the peptide, hydrophobicity, series of specific amino acids. The peptide sequences were blasted using BLASTp and sequences with the minimal homology were selected to avoid non-specific antibody binding. Bld10p is a coiled-coil protein. Therefore, it was crucial to find a region with minimal coiled-coils. To check coiled-coil regions I employed special software called *Coils*. With the help of this software two peptides were designed: the N-terminus peptide contained 18 aa, whereas middle part peptide contained 19 aa.

The antigen localized in the N-terminal part was called antigen N and the corresponding respective antibody later called anti-N antibody. The antigen localized in the middle part of the molecule was called antigen M and the corresponding antibody was named anti-M antibody. The sequences and localizations of all three antibodies are demonstrated in Figure 13. Only one rabbit was used for the immunization with each of the peptide antigens.

To assess the quality of the IgGs, antibodies were tested by Western blotting against their specific antigens. As a negative control served the corresponding preimmune sera. Because of the presence of some nonspecific bands, it was necessary to affinity purify the antibodies. For the purification of the antibody C Western-strip technique was used. The antibodies N and M were purified by using affinity matrix conjugated with antigen.

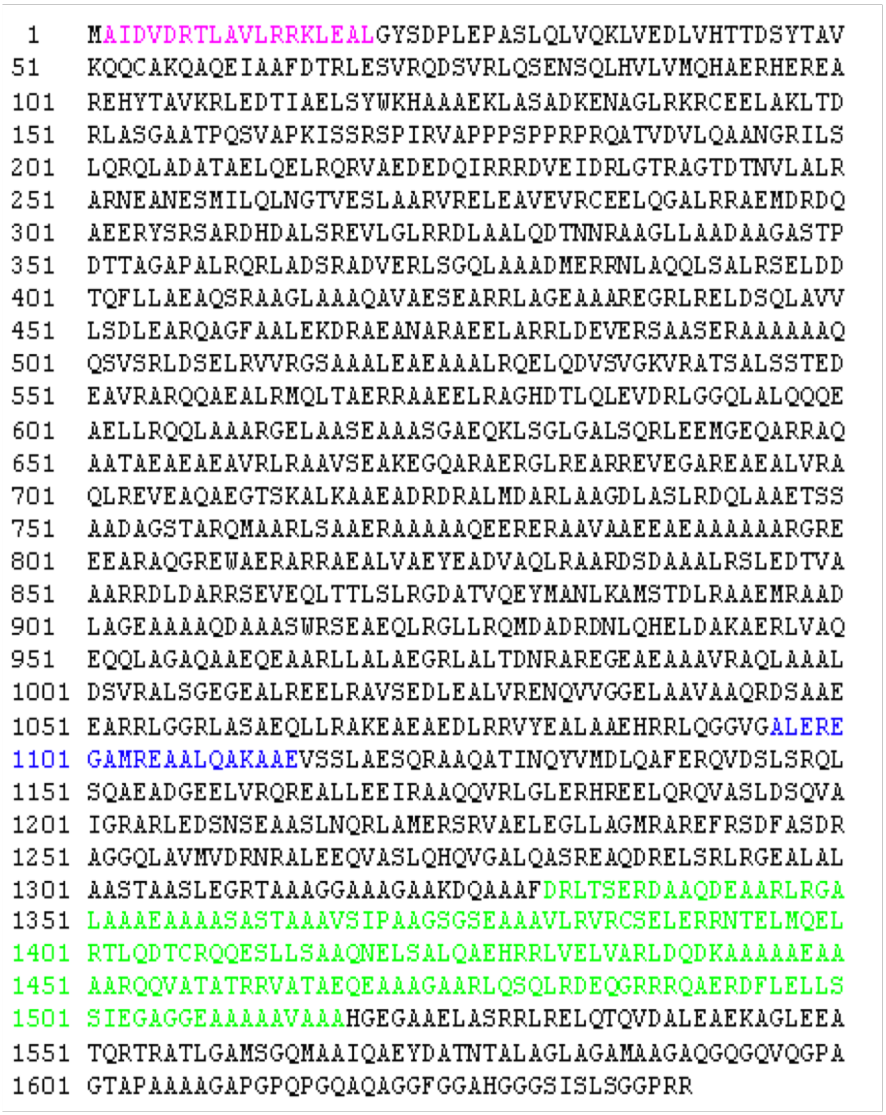

Figure 13. Localizations of the antigens on the aa sequence of Bld10. N-terminal peptide antigen, i.e. antigen N is highlighted in pink. The blue sequence represents middle part of the antigen, i.e. antigen M. The heterologously expressed antigen C is depicted in green.

3.3.1. The Western blotting detection of antigen C

To control the specificity and quality of the anti-C antibody Western blotting analyses against its own Ni-column purified antigen were performed. First, anti-C antibody was affinity purified from the sera of both rabbits (rabbit 1, rabbit 2) by the Western strip technique. Numerous experiments were performed to find out the optimal dilution for the antibody C. Based on the outcome of these experiments the optimal dilution for antibody C was determined as 1:1000. As it is demonstrated in Figure 14A the antibody C produced

strong signal of the expected size (23 kDa). As a negative control served purified preimmune IgGs of both rabbits. Next, I tested the antibody C on isolated cytoskeleton preparations (Figure 14B). Also on cytoskeleton preparations a single signal was detected at the expected size of 175 kDa. Thus, these experiments have proved that antibody C is specific to Bld10p.

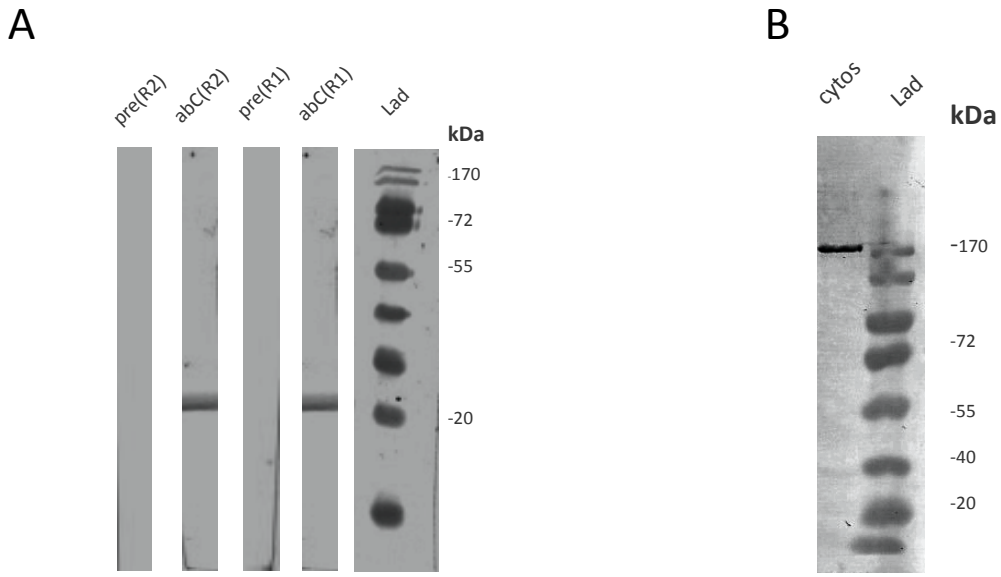

Figure 14. Western blotting with the antibody C.
(A) Testing the antibody C against its own heterologously expressed antigen. First abC(R1) and third abC(R2) lane left of the ladder represent affinity purified antibody C (as a primary antibody) from rabbit one and two respectively. Both lanes detect a signal of the expected size (23 kDa). The second pre(R1) and forth pre(R2) lane left of the ladder show Western blot with the purified preimmune IgGs of rabbit one and two respectively. In contrast, preimmune IgGs detect no signal.
(B) Testing the anti-C antibody (1:1000) (R1) against isolated cytoskeleton preparations of *cw92.* A signal of the expected size (175 kDa) is detected in cytoskeleton preparations.

3.3.2. Immunolocalization of Bld10p with anti-C antibody

To examine the subcellular localization of Bld10p indirect immunofluorescence experiments on whole cells as well as isolated cytoskeletons were performed with affinity purified polyclonal antibodies. To better understand the localization of Bld10p, double fluorescence labeling was utilized. Thus, antibodies against prominent cytoskeleton proteins like centrin and tubulin were used together with anti-C antibody. To achieve the discrimination between the two primary antibodies in case of double localization it is necessary to use primary antibodies raised in different species (here: rabbit and mouse) and the suitable secondary antibodies conjugated to distinct fluorochromes. In whole cell experiments as a secondary antibody for anti-C antibody goat anti-rabbit IgG FITC-conjugate (fluorescein isothiocyanate)

and for anti-α-tubulin goat anti-mouse IgG Cy3-conjugate were employed. The nucleus was stained with DAPI (4',6' diamidino-2 phenylindole), which binds strongly to DNA. The optimal dilution for antibody C was determined as 1:300. Despite the chloroplast autofluorescence immunofluorescence on whole cells shows Bld10p localization at the position of basal bodies (Figure 15). However, because of autofluorescence it was difficult to determine the exact localization of Bld10p. Next, localization studies were performed on isolated cytoskeletons. As a secondary antibody for anti-C antibody goat anti-rabbit IgG Cy3-conjugate and for anti-α-tubulin and anti-centrin goat anti-mouse IgG FITC-conjugate were used. The immunofluorescence analyses on isolated cytoskeletons in contrast have demonstrated clear localization in basal bodies (Figure 16). One dot (rarely 2 dots) was visible in both anti-centrin and anti-α-tubulin colocalization experiments. This dot was usually localized to one basal/probasal body. IgGs from preimmune sera were used as negative control. As it is shown, no fluorescence at the basal bodies was observed.

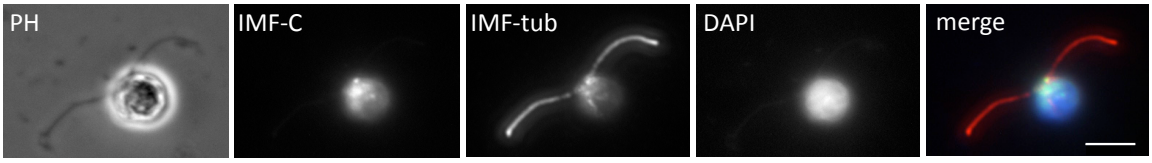

Figure 15. Indirect immunofluorescence of the *cw92* cells with anti-C-antibody. Cells were double labeled with anti-C antibody (1:300) (green) and anti-α-tubulin (1:200) (red). The nucleus was stained with DAPI (blue). PH stands for phase contrast image, IMF-C for immunofluorescence of anti-C antibody, IMF-tub for tubulin immunofluorescence, DAPI for nucleus. Scale bar, 5 μm.

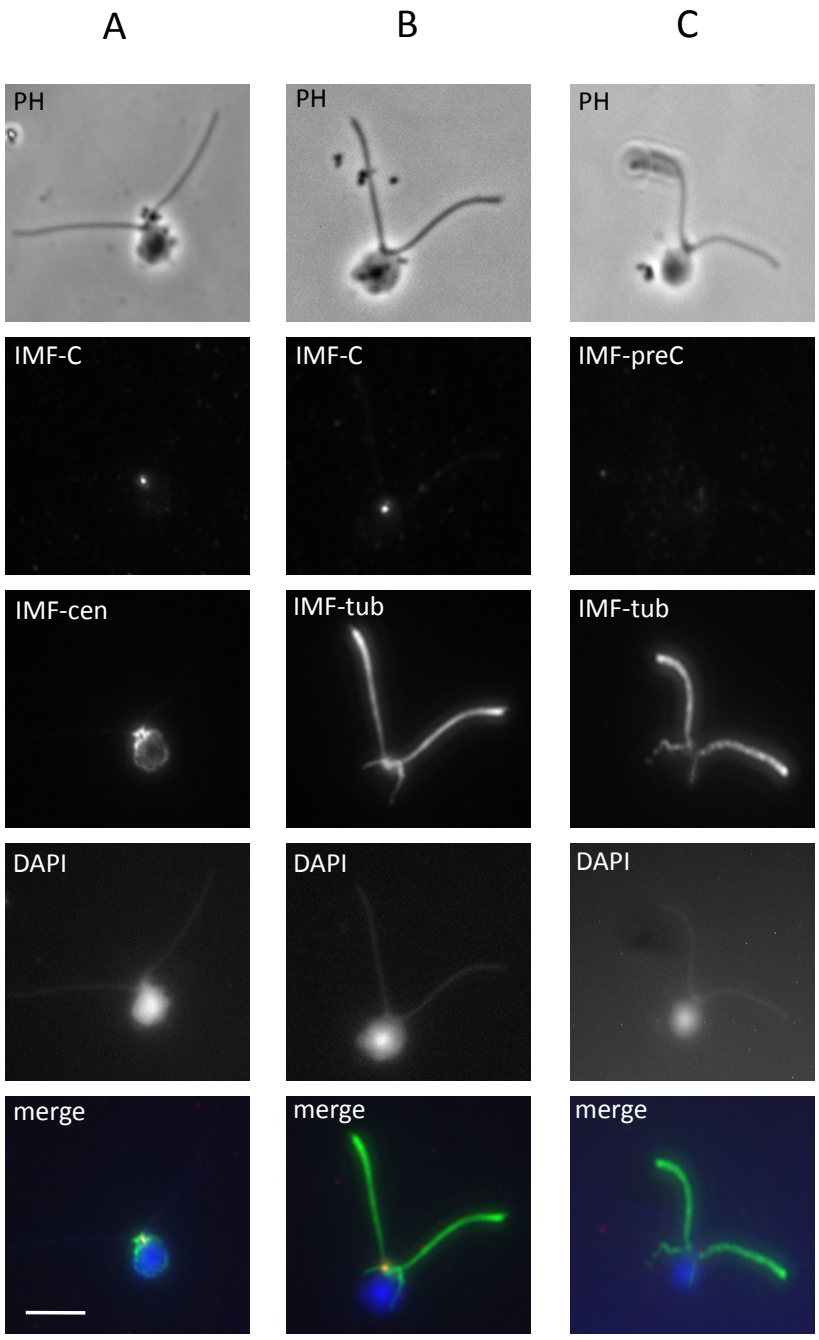

Figure 16. Colocalization using anti-C antibody and anti-centrin or anti-α-tubulin (B-5-1-2) on isolated cytoskeleton preparations.
(A) Colocalization of anti-C antibody (1:300) with anti-centrin antibody (1:50).
(B) Colocalization of anti-C antibody (1:300) with anti-α-tubulin (1:200) antibody.
(C) Colocalization of the preimmune IgGs (1:150) with anti-α-tubulin antibody. In all images the nucleus is stained with DAPI (1:200) (blue), PH stands for phase contrast image, IMF-C for fluorescence of anti-C antibody (red), IMF-tub for α–tubulin fluorescence (green), IMF-cen for the anti-centrin fluorescence (green). Scale bar, 5 µm.

3.3.3. The Western blotting detection of antigen N

The peptide polyclonal anti-N antibody was raised in only one rabbit. After affinity-purification by chromatography it was tested successfully by Western blotting against its own antigen (results not shown). Several experiments were performed to find out the optimal antibody dilution for the anti-N antibody. Based on the outcome of these experiments and considering the background and non-specific bands the optimal dilution for antibody C was determined as 1:10000. The anti-N antibody was tested on isolated cytoskeleton preparations. As it is shown in Figure 17 the antibody N detected not only the signal of expected size (175 kDa), but also a nonspecific band of molecular weight 50 kDa. The negative control (purified IgGs of preimmune serum) showed no signal.

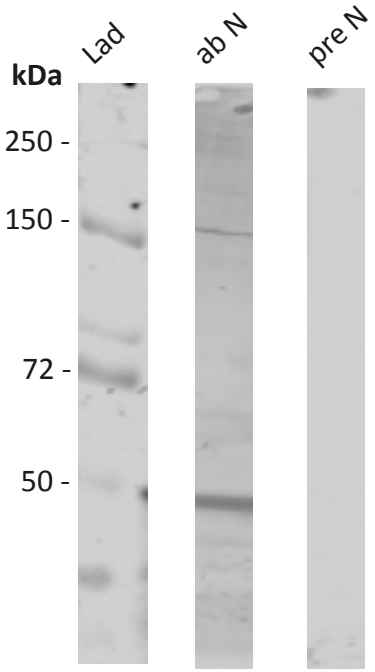

Figure 17. Western blotting with the antibody N. Testing the anti-N antibody (first lane right of the ladder) (1:10000) against isolated cytoskeleton preparations of *cw92.* A signal of the expected size (175 kDa) is detected in cytoskeleton preparations. Along with expected signal non-specific bands were present. IgGs from preimmune serum (second lane right of the ladder) detect no signal.

3.3.4. Immunolocalization of Bld10p using anti-N antibody

To examine the localization the Bld10p indirect immunofluorescence experiments on whole cells as well as isolated cytoskeletons were performed with affinity purified polyclonal peptide anti-N antibody. Double fluorescence labeling was utilized by visualizing either

centrin or α–tubulin together with anti-N antibody. As a secondary antibody for anti-N antibody goat anti-rabbit IgG FITC-conjugate and for anti-α-tubulin goat anti-mouse IgG Cy3-conjugate were used. The nucleus was stained with DAPI. The optimal dilution for the anti-N antibody was established as 1:500. Despite the chloroplast autofluorescence immunofluorescence on whole cells shows Bld10p localization at the position of basal bodies (Figure 18). However, it is difficult to determine the exact localization of Bld10p. The immunofluorescence analyses on isolated cytoskeletons in contrast showed localization to basal bodies (Figure 19A and 19B). Preimmune IgGs were used as a negative control. As a secondary antibody for anti-N antibody goat anti-rabbit IgG Cy3-conjugate and for anti-α-tubulin and anti-centrin goat anti-mouse IgG FITC-conjugate were employed. However, some background fluorescence was present. Also in case of antibody N one dot (rarely 2 dots) was visible in both colocalization experiments. This dot was as well usually positioned to the one basal/probasal body. Preimmune sera were used as negative control and as was expected showed no fluorescence at the basal bodies (Figure 19C).

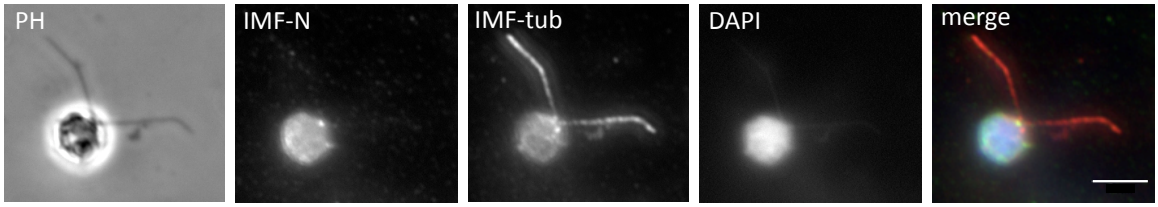

Figure 18. Indirect immunofluorescence with anti-N-antibody on *cw92* cells. Cells were double labeled with anti-N antibody (1:500) (green) and anti-α-tubulin (1:200) (red). The nucleus stained with DAPI (blue). PH stands for phase contrast image, IMF-N for immunofluorescence of anti-N antibody, IMF-tub for tubulin immunofluorescence, DAPI for nucleus. Scale bar, 5 µm.

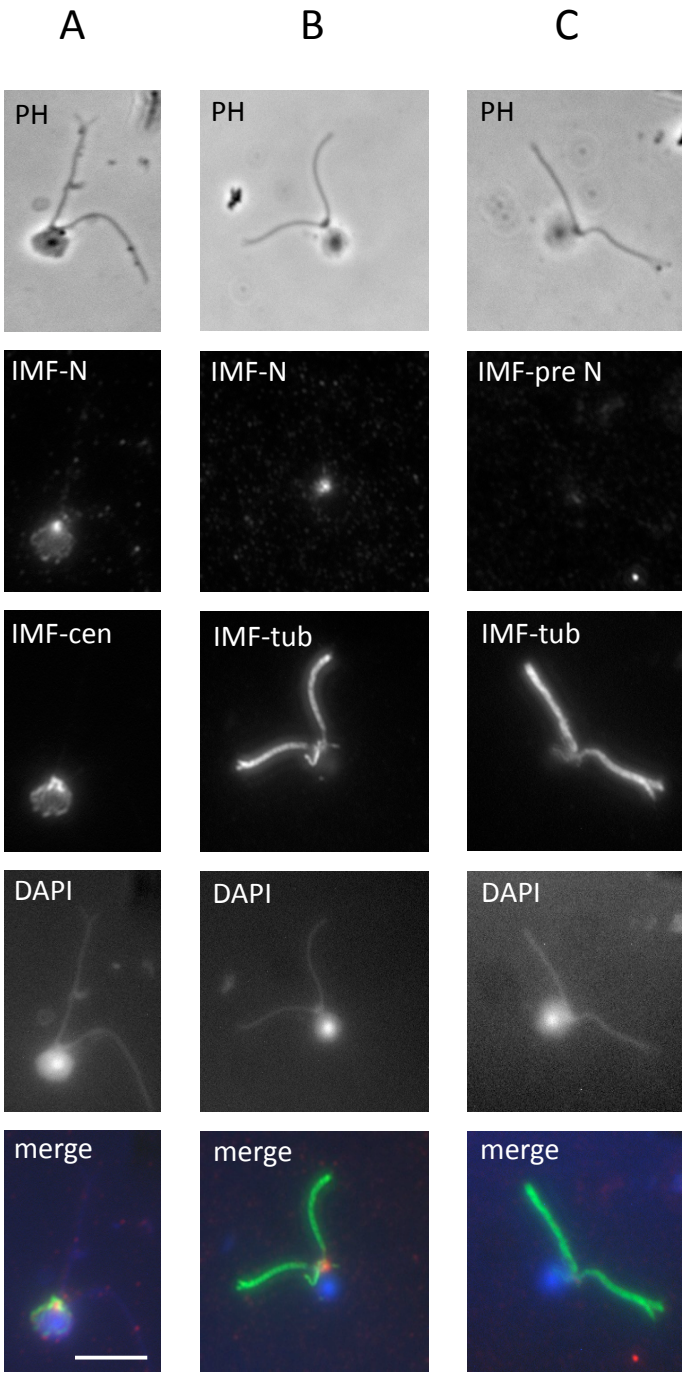

Figure 19. Colocalization using anti-N antibody with anti-centrin and anti-α-tubulin (B-5-1-2) on isolated cytoskeleton preparations.
(A) Colocalization of anti-N antibody (1:500) with anti-centrin antibody (1:50).
(B) Colocalization of anti-N antibody with anti-α-tubulin antibody (1:200).
(C) Colocalization of the preimmune IgGs (1:150) (negative control) with anti-α-tubulin antibody. In all images the nucleus is stained with DAPI (1:200) (blue), PH stands for phase contrast image, IMF-N for fluorescence of anti-N antibody (red), IMF-tub for α–tubulin fluorescence (green), IMF-cen for the anti-centrin fluorescence (green). Scale bar, 5 μm.

3.3.5. The Western blotting detection of antigen M

The peptide polyclonal anti-M antibody was as well raised in one rabbit. It was then affinity-purified by chromatography and tested successfully by Western blotting against its own antigen (results not shown). To find out the optimal antibody dilution for the antibody M Western blots were performed. Based on the outcome of these experiments the optimal dilution for anti-M antibody was determined as 1:1000. The specificity of the anti-M antibody was tested on isolated cytoskeleton preparations. As it is demonstrated in Figure 20 a weak signal of Bld10p by anti-M antibody was detected at the expected size of 175 kDa. The negative control (purified IgGs of preimmune serum) as it was expected, showed no signal.

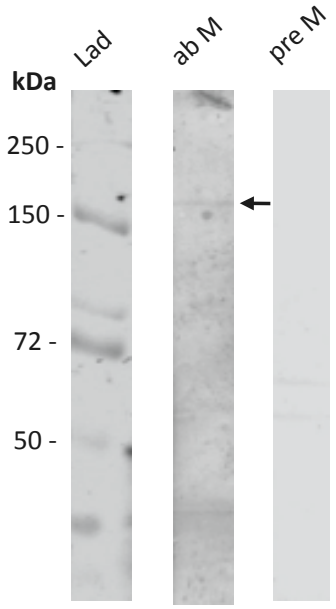

Figure 20. Western blotting with the antibody M. Testing the anti-M antibody (first lane right of the ladder) (1:1000) against isolated cytoskeleton preparations of *cw92.* A weak signal of expected size (175 kDa) was detected in cytoskeleton preparations (arrow). IgGs from preimmune serum (second lane right of the ladder) detect no signal.

3.3.6. Immunolocalization of Bld10p using anti-M antibody

Next, indirect immunofluorescence experiments on whole cells as well as isolated cytoskeletons were performed with affinity purified polyclonal anti-M antibody. Double fluorescence labeling was used by visualizing either centrin or α–tubulin together with anti-M antibody. As a secondary antibody for anti-M antibody in the experiment with whole cells goat anti-rabbit IgG FITC-conjugate and for anti-α-tubulin goat anti-mouse IgG Cy3-

conjugate were used. The nucleus was stained with DAPI. The optimal dilution for the anti-M antibody was determined as 1:50. Chloroplast autofluorescence was present also in this immunofluorescence experiment. Bld10p localization using anti-M antibody in cells showed not a distinct dot, but rather blurry big dot (Figure 21). Subsequently, localization studies were performed on isolated cytoskeletons. As a secondary antibody for anti-M antibody goat anti-rabbit IgG Cy3-conjugate and for anti-α-tubulin and anti-centrin goat anti-mouse IgG FITC-conjugate were employed. The immunofluorescence analyses on isolated cytoskeletons in contrast demonstrated localization to basal bodies (Figure 22A and 22B). However, some axoneme background fluorescence was present. One dot (rarely 2 dots) was visible in both anti-centrin and anti-α-tubulin colocalization experiments. This dot was as well usually positioned to the one basal/probasal body. Preimmune sera were used as a negative control.

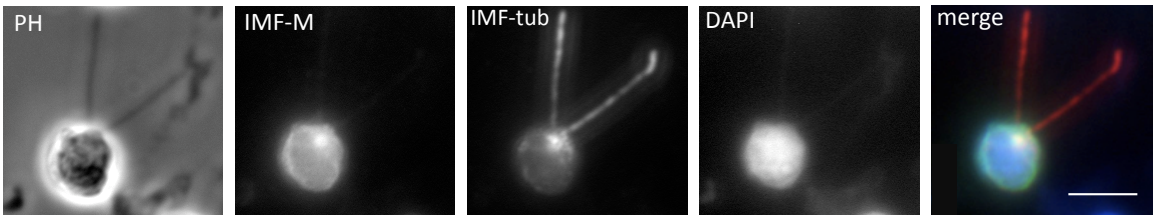

Figure 21. Indirect immunofluorescence with anti-M-antibody on *cw92* cells. Cells were double labeled with anti-M antibody (1:300) (green) and anti-α-tubulin (1:200) (red). The nucleus was stained with DAPI (1:200) (blue). PH stands for phase contrast image, IMF-M for immunofluorescence of anti-M antibody, IMF-tub for tubulin immunofluorescence, DAPI for nucleus. Scale bar, 5 µm.

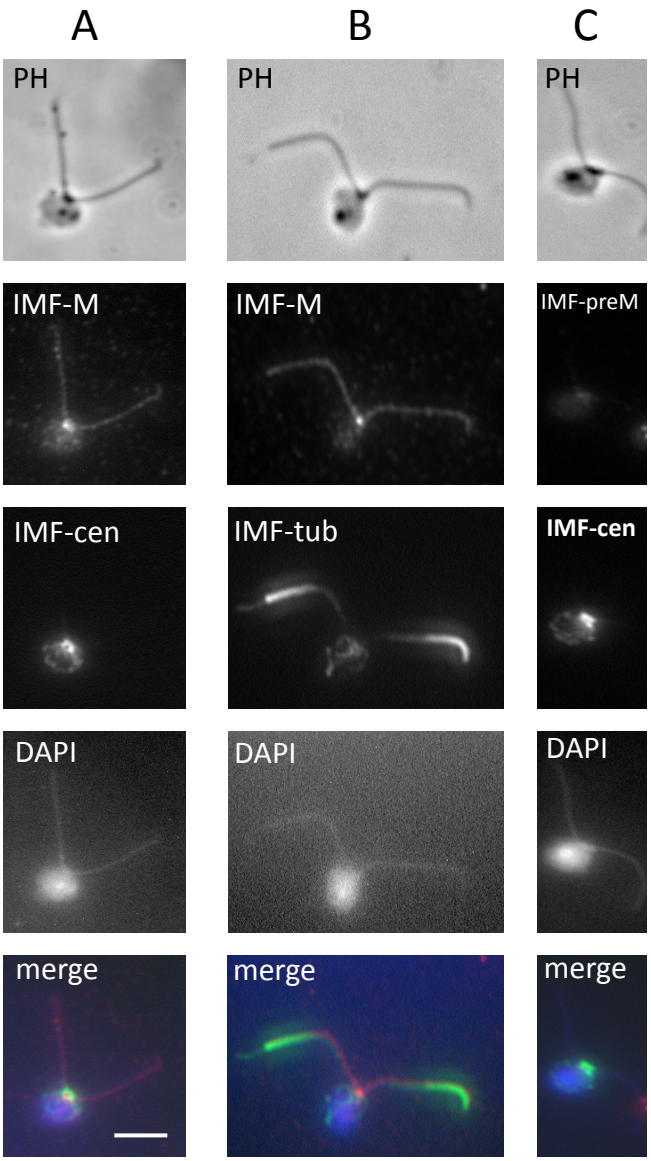

Figure 22. Colocalization using anti-M antibody with anti-centrin and anti-α-tubulin (B-5-1-2) on isolated cytoskeleton preparations.
(A) Colocalization of anti-M antibody with anti-centrin antibody.
(B) Colocalization of anti-M antibody with anti-α-tubulin antibody.
(C) Colocalization of the preimmune IgGs (negative control) with anti-α-tubulin antibody. In all images the nucleus is stained with DAPI (blue), PH stands for phase contrast image, IMF-M for fluorescence of anti-M antibody (red), IMF-tub for α–tubulin fluorescence (green), IMF-cen for the anti-centrin fluorescence (green). Scale bar, 5 μm.

3.4. Immunofluorescence of isolated deflagellated cytoskeletons indicates Bld10 localization to parental basal bodies

To observe the Bld10p localization from the top it was necessary to deflagellate the cells. The deflagellation was achieved by using pH shock. This allowed observing the basal apparatus from above without axonemes. Axonemes often overlay the basal bodies and make it difficult to recognize their fluorescence. More importantly, with the presence of axonemes only a side view of the basal apparatuses can be obtained. These experiments were performed using anti-C antibody, since it showed high specificity in Western blotting analyses and clear localization (without background) in indirect immunofluorescence microscopy results in comparison with the other two antibodies. As a secondary antibody for anti-C antibody goat anti-rabbit IgG Cy3-conjugate and for anti-α-tubulin and anti-centrin goat anti-mouse IgG FITC-conjugate were used. The DNA was labeled with DAPI. Interestingly, immunofluorescence examinations of the deflagellated cytoskeletons have shown infrequently one or three dots and often two dots. The advantage of this method was evident: it considerably improved the view of the Bld10p localization.

In the immunofluorescence of deflagellated cytoskeletons showed Bld10p localization to the parental basal bodies. Remarkably, one of the dots has a higher intensity in comparison with the other one (Figure 23B). This kind of pattern is often observed in the experiment with the deflagellated cytoskeletons. The presence of three fluorescing dots is indicated in Figure 23A. One of them (in the middle) intensely fluorescing, the other is weakly fluorescing and third one has a fluorescence of middle intensity. Remarkably, based on the position of the third dot it does not localize to the probasal body.

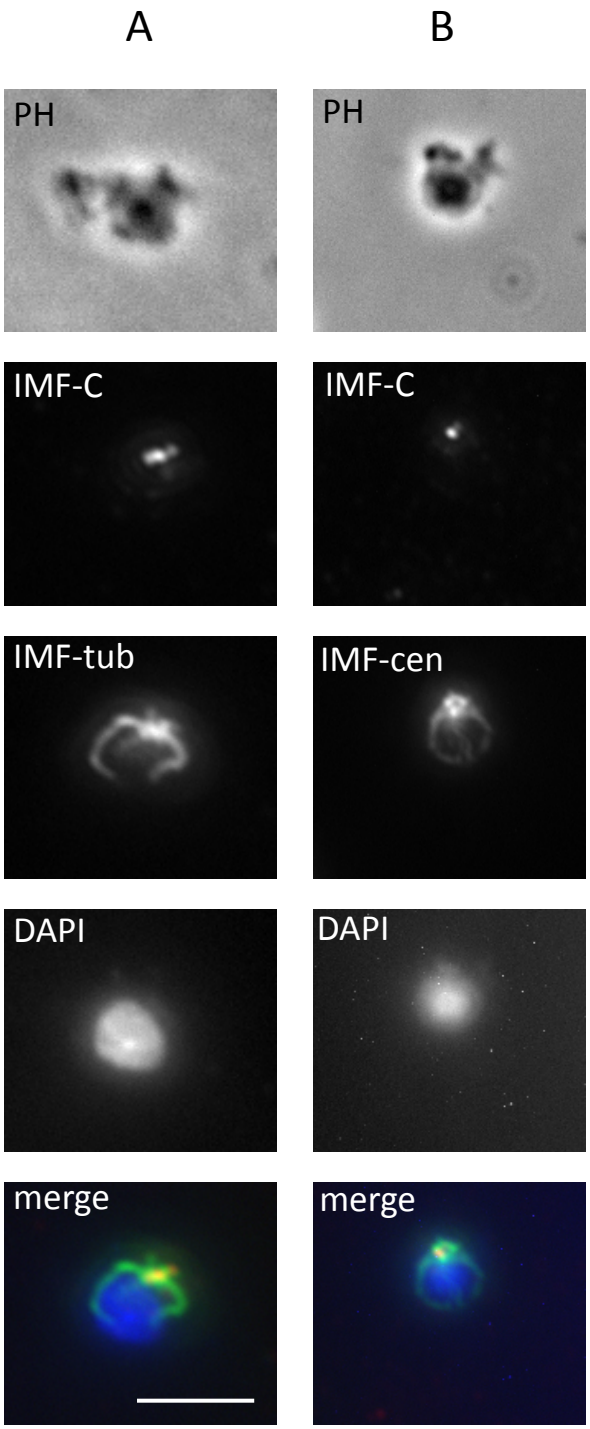

Figure 23. Colocalization using anti-C antibody with anti-α-tubulin and anti-centrin on the deflagellated cytoskeleton preparations.
(A) Colocalization with anti-α-tubulin (B-5-1-2) (green). Three dots are visualized with anti-C antibody (red).
(B) In colocalization with the anti-centrin antibody only one dot is observed.
(A, B) The nucleus is stained with DAPI (blue), PH stands for phase contrast image, IMF-M for fluorescence of anti-M antibody (red), IMF-tub for α–tubulin fluorescence (green), IMF-cen for the anti-centrin fluorescence (green). Scale bar, 5 µm.

3.5. Bld10 forms a protein complex

3.5.1. Far-Western blotting and co-immunoprecipitation did not detect Bld10p interacting partners

Physiological protein-protein interactions can be determined by different techniques, such as co-immunoprecipitation, Far-Western blotting, and separation of protein complexes by native electrophoresis. Individual protein constituents can be finally identified by mass spectrometric techniques. In this PhD study three methods were employed to find interacting partners of Bld10p.

The first parameter to be optimized in the analysis of protein interactions is the sample preparation method. The major limitation in these studies was to solubilize the cytoskeleton proteins. First, I intended to solubilize isolated cytoskeleton by Triton X-100. Because of its feature to form micelles Triton-X 100 helped to aggregate cytoskeleton components, which made it impossible to obtain proteins in a soluble phase. Experiments by using different chaotropic agents: sarkosyl (0,5%, 1%), potassium iodide (0,5 M, 1 M, 2 M), urea (2 M, 4 M, 8 M), guanidium chloride (4 M, 8 M) with different concentrations were performed to achieve total solubilisation of the cytoskeletons. The detection of Bld10p with the help of anti-C antibody confirmed localization in the soluble phase (results not shown). Because 8 M urea easily solubilized the cytoskeleton it was decided to use urea in further experiments. To identify protein interactions of Bld10p I employed the Far-Western technique. The Far-Western blotting technique is similar to Western blotting. In Far-Western blotting antigens C, M and N were employed to probe the protein of interest (Bld10) on the blot. In this technique antibody detectable “bait” protein is used to detect a target protein. The cytoskeleton sample containing the unknown “prey” protein was separated by the SDS-PAGE and then transferred to the membrane. After transfer the membrane is blocked and probed with the antigen C, N and M. Then the antigens were detected by using corresponding antibody. Subsequently, co-immunoprecipitation was performed. In co-immunoprecipitation the target antigen precipitated by the antibody co-precipitates a binding partner/protein complex from a lysate, i.e., the interacting protein is bound to the target antigen, which becomes bound by the antibody that becomes captured on the Protein A gel support. To confirm whether the Bld10p complex is eluted SDS-PAGE electrophoresis was performed,

which did not show any band. This result was confirmed by the Bradford protein determination technique (no detectable amount of the protein was observed) and by the Western blotting of the eluate (no detection of the antigens was observed). Thus, the coupling of the antibody to the resin happened as expected (almost 85% of the antibody was coupled), whereas the antigen complex coupling to the antibody was not successful. Using these techniques, I expected to identify binding partners of the Bld10 protein. Numerous attempts to optimize the conditions of the above-mentioned techniques to identify the interacting partners of Bld10p were not successful.

3.5.2. Blue native polyacrylamide gel electrophoresis reveals Bld10p complex

Blue Native Polyacrylamide Gel Electrophoresis (BN-PAGE) was initially developed to isolate membrane protein complexes from mitochondria (Schagger and von Jagow, 1991) Interestingly, no application of BN-PAGE using cytoskeleton preparations has been reported until now. For native electrophoresis a Bis-Tris native acrylamide gradient gel (4-16%) was used. Several components are required for the BN-PAGE, like for example Coomassie Briliant Blue G-250 dye, which imposes a negative charge to the proteins; Bis-Tris that stabilizes pH (7,0-7,5) in the native gel; 6-aminocaproic acid (zwitterionic compound) that improves solubilization; and a mild neutral detergent. For the experiment with cytoskeleton urea was used to solubilize the cytoskeleton proteins, instead of non- ionic detergents, like Triton X-100 or n-dodecyl-beta-D-maltoside (DDM)

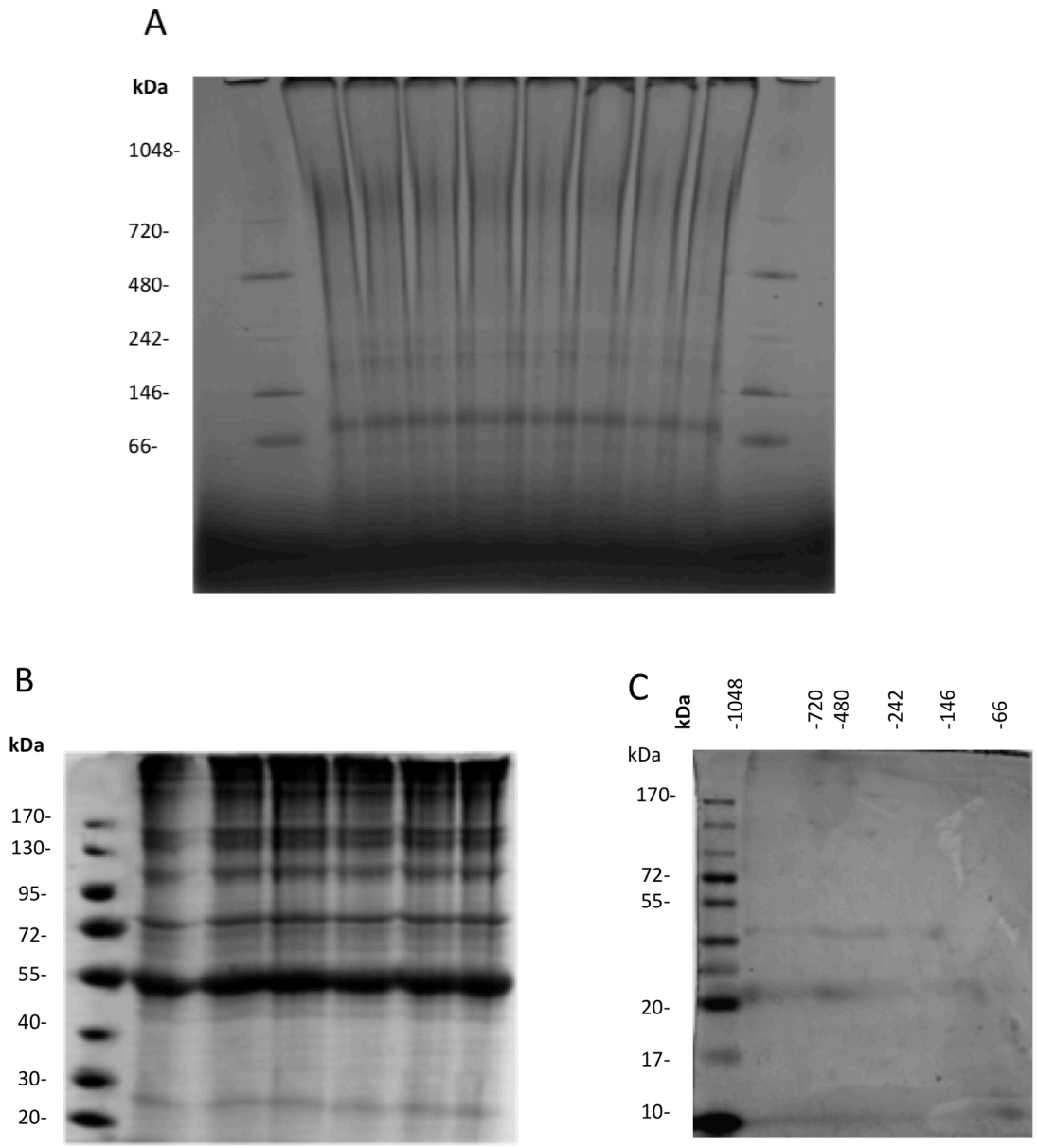

Figure 24. **Separation of solubilized cytoskeletons by 1D BN-PAGE (A), SDS-PAGE (B) and 2D BN/ SDS-PAGE (C).**

(A) 1D BN-PAGE (4-16%) of soluble phase of the isolated cytoskeletons. Approximately 30 µg of protein per lane were loaded on the gel. All lanes were loaded with the same sample. The gel was stained by Colloidal Coomasie.

(B) SDS-PAGE (12,5%) of solubilized cytoskeletons. All lanes were loaded with the same samples. The gel was stained by Colloidal Coomasie.

(C) Subunits of the protein complexes were separated by 2D BN/SDS electrophoresis (8%). The BN-gel slice was previously incubated in SDS-sample buffer with the reducing agent. The gel was silver stained.

Protease inhibitors were added as well when solubilization of cytoskeletons was performed. As it is shown on Figure 24A the protein complexes migrate as a blue non-focused bands. In contrast, SDS-PAGE shows clear separate bands (Figure 24B). To dissociate protein complexes into their individual proteins second dimension SDS-PAGE was employed. The lanes from the first dimensional BN PAGE were cut out and equilibrated with SDS-sample buffer. Then, the gel strip was placed into second dimension SDS-PAGE. The Figure 24C shows the silver stained second dimension BN-SDS-gel. Although clear separation was achieved, the amount of the protein seems to be too low, i.e. the spots were not intense enough for the further mass spectrometry analyses.

To identify Bld10p in the 1D-BN PAGE gel a Western blotting of the BN-gel has been performed using anti-C antibody. To remove Coomassie from the BN-gel and impose a negative charge to the proteins, the gel was incubated in SDS-running buffer. Before immunoblotting transfer, the gel had to be equilibrated with transfer buffer. The Western blotting analyses detected a strong signal of approximately 600 kDa (Figure 25).

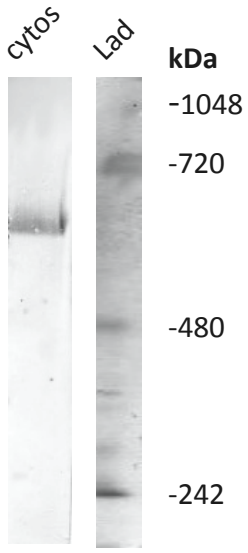

Figure 25. Western Blotting of the 1-D BN gel. The anti-C antibody (1:1000) detected Bld10p in a complex that has a molecular weigh of about 600 kDa**.**

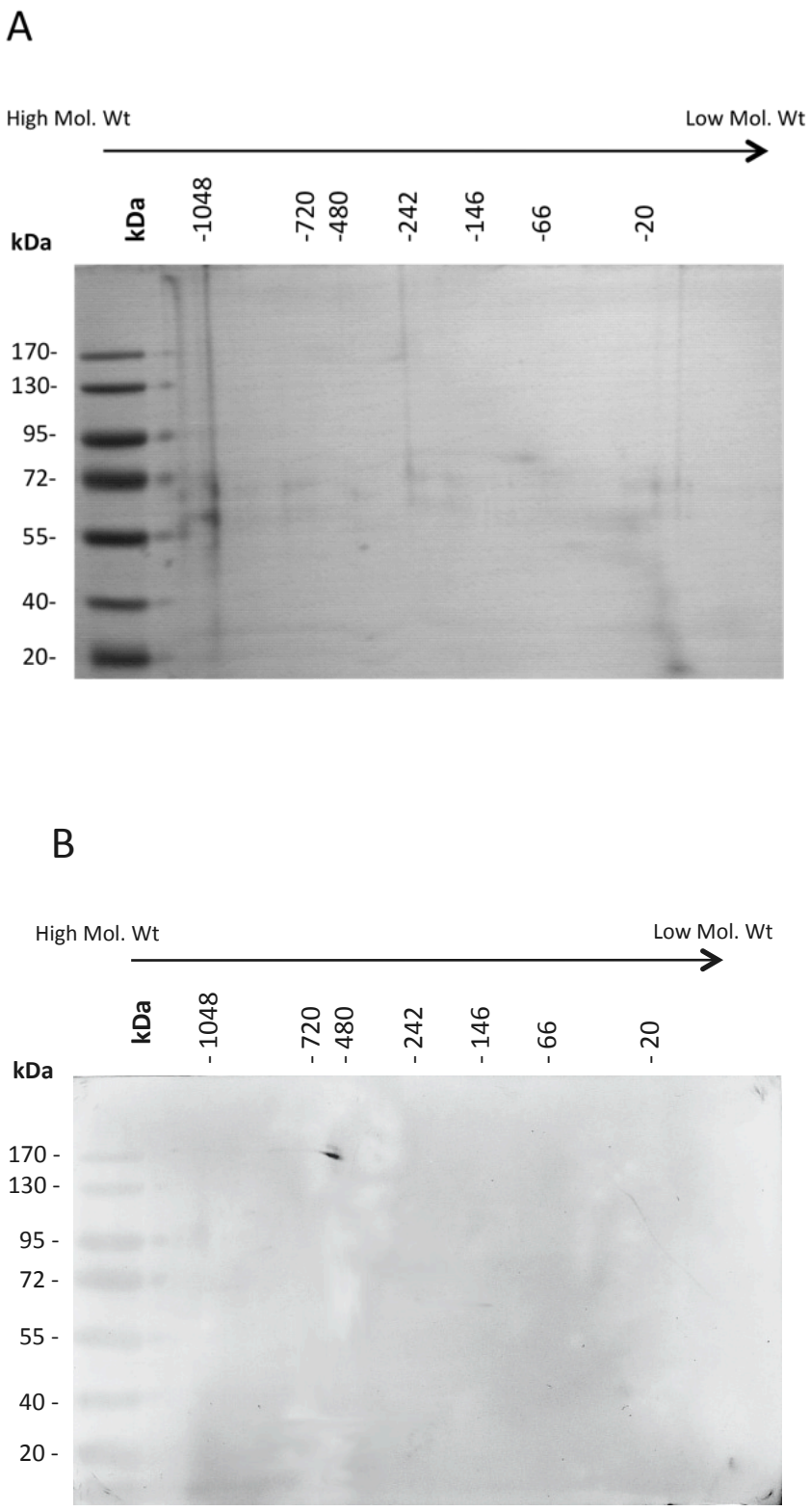

Figure 26. 2D BN/SDS PAGE and Western blotting of the 2D-BN/SDS gel.
(A) The second dimensional separation of the protein complexes from the BN-PAGE stained with colloidal Coomassie.
(B) Western blotting of the 2D-BN/SDS using anti-C antibody (1:1000) detects a signal at approximately 600 kDa.

This result demonstrates that Bld10p might either be associated with other proteins or forms a tetramer with itself. Later, this result was also confirmed by using anti-N and anti-M antibodies (results not shown). To test whether Bld10p can also be detected on the 2D BN/SDS-PAGE, Western blotting of the 2D BN/SDS PAGE was performed. Following 2D BN/SDS-PAGE (Figure 26A) the gel is electroblotted onto a PVDF membrane for protein detection with anti-C antibody. The experiment demonstrated the detection of one spot of the expected size on the Western membrane (Figure 26B). So, the previous finding in first dimensional blue native electrophoresis confirmed by the Western blotting of 2D-BN/SDS PAGE.

3.5.3. The immunogold electron microscopy shows Bld10 localization to cartwheel of basal bodies

To investigate the Bld10p localization at the ultrastructural level postembedding immunogold labeling was performed. In this experiment all three Bld10 antibodies were employed: anti-M antibody, anti-N antibody and anti-C antibody. Anti-M antibody (1:50) showed non-specific localization to the axonemes (results not shown), which is consistent with the fluorescence results of the anti-M antibody. Anti-N antibody (1:500) showed only few gold particles (results not shown). The immunogold electron microscopy of the anti-C antibody demonstrated the distribution of the gold particles at the proximal end of the basal bodies, where the cartwheel structure is positioned (Figure 27). Although the anti-C labeling seems to be specific some nuclear material was as well labeled with the gold particles (Figure 27). It is important to note that these data have not been yet evaluated quantitatively.

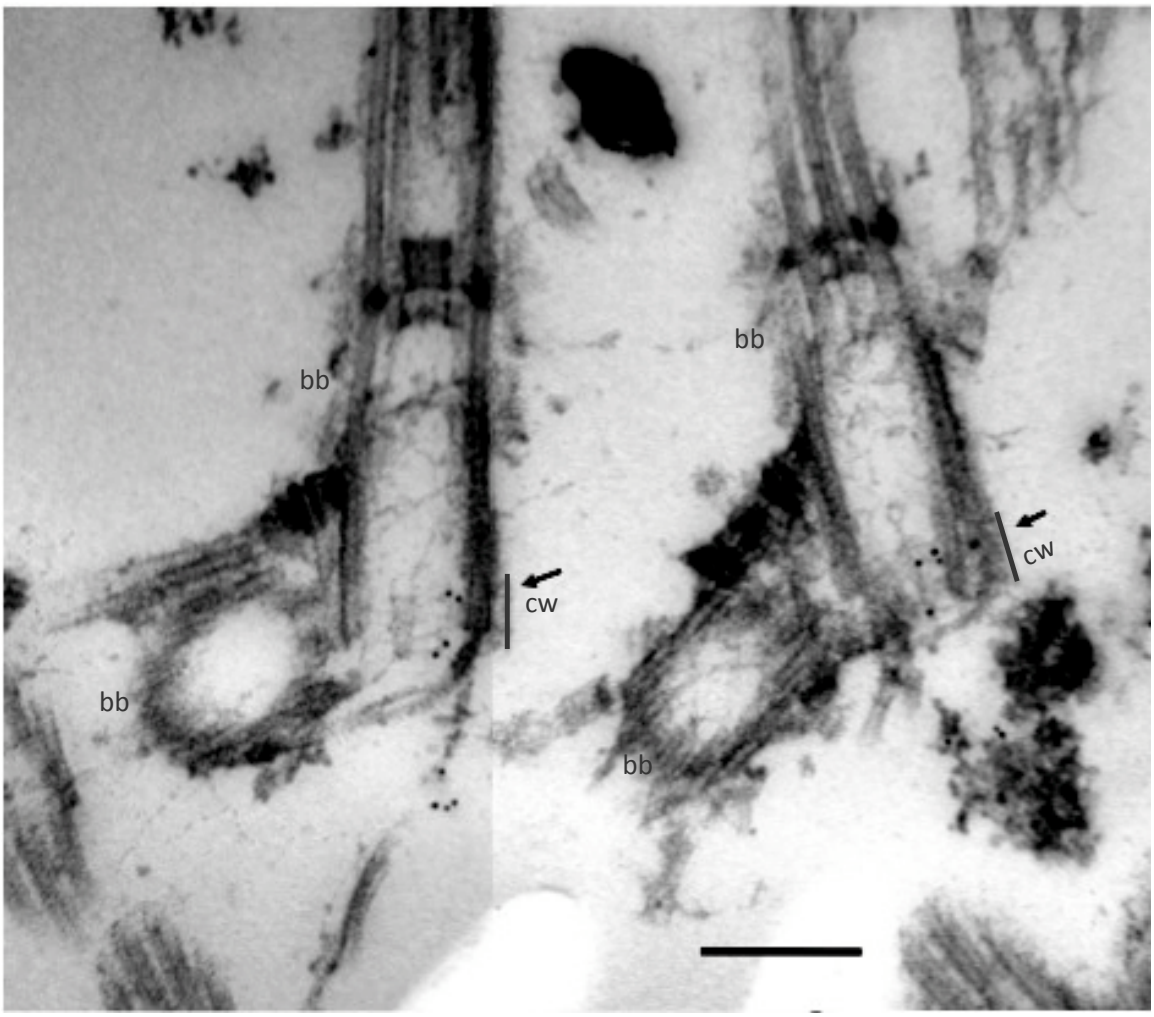

Figure 27. Immunogold electron microscopy analyses of the distribution of Bld10p using anti-C antibody. Longitudinal and the cross sections of the basal bodies (bb) are presented. The cartwheel (cw) structure is observed at the proximal end of the longitudinally sectioned basal bodies. The gold particles are mostly distributed at the cartwheel region. Scale bar, 200 nm.

4. Discussion

4.1. Developing an isolation protocol to purify the cartwheel structure

In my investigations I attempted to purify the cartwheel structure biochemically by isolating the probasal bodies. Here I would like to stress the importance of the biochemical purification of the cartwheel structure as a novel concept. The cartwheel with its characteristic ninefold symmetrical structure has a diameter of about 130 nm and is approximately 70 nm long (Cavalier-Smith, 1974). It has been shown that the number of the cartwheel tiers is higher in probasal bodies than in basal bodies (Geimer and Melkonian, 2004). Additionally, the statistical analyses of 53 longitudinal sections of probasal bodies demonstrated that the cartwheel of probasal bodies composed of four to seven tiers (Geimer and Melkonian, 2004). Since the cartwheel is such a miniature structure, by the isolation of the probasal bodies that primarily consist of the cartwheel we could possibly obtain pure cartwheel structure. Remarkably, until now there has been no report on cartwheel isolation and purification in eukaryotic cells. We speculate that the reason for that might be the difficulties one could encounter during the isolation. The advantages of the isolation method are evident: once the probasal bodies are purified they can be analyzed by electron microscopy where the cartwheel characteristic structure can be observed. Subsequently, this method would enable the examination of the cartwheel protein composition by mass spectrometry with the following verification of peptides using the JGI (Joint Genome Institute) *Chlamydomonas reinhardtii* genome database. Currently, two proteins are known to be localized to the cartwheel: Bld10 (Matsuura et al., 2004) and SAS-6 (Nakazawa et al., 2007) and both of them were identified by the screening of the *Chlamydomonas reinhardtii* mutants. Although insertional mutagenesis proved to be a valuable tool in *C. reinhardtii* functional genomics studies, we believe that a biochemical purification approach to isolate the cartwheel would provide a more direct way to study the whole cartwheel proteome at once.

To develop this strategy I tested three main parameters: suitable *Chlamydomonas* cell wall deficient mutants, buffers and detergents. The evaluation of the cell growth rate of the

investigated cell wall deficient mutants demonstrated the better growth in case of *cw92* compared to other mutants tested. From the tested detergents NP40 and Triton X-100 seem to be more suitable than the other tested detergents. As it is shown in the purification protocol of basal bodies modified in our lab ((Brachhold, 2007), the usage of TE (Tris-EDTA) buffer detaches probasal bodies from the basal bodies. Thus in EM whole mount preparations the probasal bodies are absent and only basal bodies are seen. In contrast, MT buffer, which is a microtubule-stabilizing buffer, might prevent probasal bodies from detachment of basal bodies. Recent immunofluorescence studies on the effect of these buffers (MT and TE) on the basal apparatus intact structure confirmed the above-mentioned observation (C. Wölwer, unpublished data). Thus, by using the MT buffer in all purification steps, the appropriate detergent (4% NP40 or Triton X-100) and *cw92* mutant it was possible to retain intact probasal bodies and cartwheel structure in basal bodies. The presence of probasal bodies as well as cartwheel structure of basal bodies was verified by electron microscopy in ultrathin sections of embedded cytoskeleton preparations.

While these advantages are important, some limitations were encountered. The major limitation I faced was probably difficulties by scaling up the experimental setup. Besides, due to the fact that these (probasal bodies) are very small components it was necessary to grow many liters of algal culture (presumably 300-400 liters). For an attempt to isolate probasal bodies I used cultures from 500 ml up to 10 liters. It is important to note that for the isolation of the basal bodies (modified in our lab) from 40 liters of culture only 20-25 µg of protein was obtained. Thus, we anticipated that for the isolation of the probasal bodies five to ten times more culture would be necessary.

Despite the progress made, success was not achieved towards isolation of the probasal bodies. As a consequence more studies are necessary to establish the comprehensive purification protocol to isolate probasal bodies, i.e. to obtain purified cartwheel structure.

4.2. Immunolocalization studies indicate Bld10p localization to the parental basal bodies

Here I conducted an investigation by taking a closer look at the localization of the cartwheel protein Bld10. Bld10p is shown to be the first cartwheel protein identified in *Chlamydomonas reinhardtii.* Immunoelectron microscopy localizes Bdl10p to the cartwheel, the structure with characteristic ninefold symmetry positioned at the proximal end of basal bodies (Matsuura et al., 2004).

Numerous ultrastructural studies of the basal bodies (Stubblefield, 1967; Dippell, 1968; Cavalier-Smith, 1974; Geimer and Melkonian, 2004) determined the following steps in the development of the basal body: it starts with fibrous structures or granules; then the first microtubular structures arise as a ring of nine microtubular singlets (A tubules), which are supported by the cartwheel; with the basal body elongation the B- and C-tubules are added and finally a cylinder which comprises nine triplets extended to the mature basal body/centriole. So, the cartwheel with the characteristic hub and spokes structure appeared to be the first ninefold symmetrical structure during basal body/centriole development.

Strikingly, despite the differences in microtubule number of centrioles in different organisms, the shape of the centrioles and ninefold symmetry are conserved even among evolutionary distantly related organisms (Delattre and Gonczy, 2004; Strnad and Gonczy, 2008). Matsuura *et al.* reported that indirect immunofluorescence microscopy studies of Bld10p show three or four dots at the position of the basal bodies, although only an IMF image with three dots (Figure 28) is presented in the publication (Matsuura et al., 2004). Authors imply that the existence of more than two dots suggest that Bld10p localizes also to the probasal bodies (Figure 29). Besides, the presence of the Bdl10p during the mitosis in the spindle poles suggests its localization to basal bodies throughout whole cell cycle (Matsuura et al., 2004).

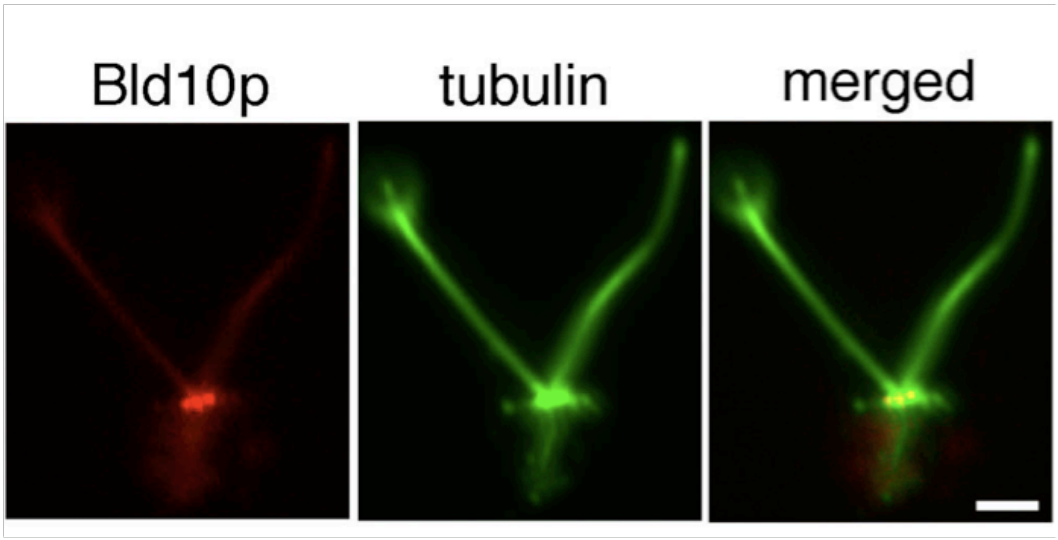

Figure 28. Immunofluorescence images of the nucleoflagellar apparatuses double stained with anti-Bld10p (red) and anti-α-tubulin antibody (green). Scale bar, 2 µm (Matsuura et al., 2004)

In contrast, my results of the immunolocalization studies of Bld10p using polyclonal antibodies often showed two dots, rarely one dot or three dots in a row (Figure 23). One bright dot was observed when immunofluorescence with cytoskeletons with flagella/axonemes was performed. Later immunofluorescence analyses of the deflagellated cytoskeleton showed the Bdl10p localization as two dots which have different fluorescence intensity: one is usually lighter and smaller than the other. Rarely three dots in a row were seen in deflagellated cytoskeletons. Because of the position of the third dot it cannot be localized to probasal bodies. A possible explanation why often one dot was observed in cytoskeleton preparations with flagella might be that the presence of axonemes did not allow to fully observe the basal apparatus. Moreover, in the preparation with axonemes only side view is possible, which makes it difficult to see the basal apparatus from the top.

Yet another question of interest for us was in which of the basal bodies - mature or immature - the protein localizes. This can be achieved by identifying positional relationship of the basal and probasal bodies to the X-shaped 4-2-4-2 microtubular flagellar root system (Ringo, 1967; Melkonian, 1980; Geimer and Melkonian, 2004). The basal bodies are positioned at the wide angle (obtuse angle), whereas the probasal bodies are positioned at the narrow angle (acute angle) (Figure 4). Therefore, the immunofluorescence of the deflagellated cytoskeletons using double labeling was performed. This method enabled a better view on the basal apparatuses. Results based on these experiments indicate Bld10p

localization to the parental basal bodies. These findings are very interesting and unexpected considering the fact that probasal bodies are mainly composed of cartwheel tiers. Moreover, it was reported that Bld10 is a principal cartwheel protein and plays a key role in stabilizing the ninefold symmetry (Hiraki et al., 2007).

Another interesting aspect is that despite the conserved character of the cartwheel, Bld10p has no homology or very little homology with other proteins. It is well-known that in *Chlamydomonas reinhardtii* basal body formation occurs in a very similar manner to the centriole assembly in other organisms. Surprisingly, *Chlamydomonas* Bdl10p shares only 25% identity in a limited region of the sequence with mammalian Cep135 protein and unknown mouse protein BC062951 (Matsuura et al., 2004). In addition, RNAi studies in cell culture demonstrated that Cep135 (human Bld10 ortholog) is required for pericentriolar material integrity (Ohta et al., 2002), for centrosomal cohesion through the recruitment of the centriolar C-NAP1 protein (Kim et al., 2008) and for the assembly of excess procentrioles in Plk4-overexpressing cells (Kleylein-Sohn et al., 2007). Moreover, recently it was reported that the Bld10 homolog in *Drosophila* is required for the assembly of the axoneme central pair of microtubules (Mottier-Pavie and Megraw, 2009). These authors believe that *Drosophila* Bld10p is a conserved centriolar protein and required for proper assembly of centrioles and basal bodies to achieve their normal length (Mottier-Pavie and Megraw, 2009).

Thus, despite the fact that cartwheel structure is found in *Drosophila* (Preble et al., 2000) Bld10p is not localized to the cartwheel. Indeed, such a variety in functions of this protein is very surprising and at the same time confusing, considering the conserved nature of the cartwheel. Hence, the Bld10 homologues have a different role in different organisms, which raises doubts about the role of Bld10 as a pivotal structural protein of the cartwheel.

	***Chlamydomonas* Bld10p**	**Human Cep135**
Full-length Drosophila Bld10	15% identical	22% identical
	28% similar	43% similar
Bld10 conserved domain	19% identical	24% identical
	41% similar	48% similar

Figure 29. Sequence similarities among Bld10 orthologs (Mottier-Pavie and Megraw, 2009). Protein sequences were aligned using the ClustalW program in MacVector 8.0 using the default parameters.

On the contrary, SAS-6 protein – the second cartwheel protein identified in *Chlamydomonas reinhardtii* seems to be very conserved. SAS-6 homologues appeared to be essential for procentriole formation and conserved among many organisms, such as *D. melanogaster* (Peel et al., 2007; Rodrigues-Martins et al., 2007), *C. reinhardtii* (Nakazawa et al., 2007), *Danio rerio* (Yabe et al., 2007) and *H. sapiens* (Strnad et al., 2007).

Obtained immunofluorescence results together with the Bld10p ortholog sequence similarity data (Figure 29) raise uncertainty about role of the Bld10p as a principal structural component of the cartwheel. In other words, this study contributes to the important question of whether Bld10p is a structural component of the cartwheel or it plays some other yet unknown role in the basal body/centriole development. To address the question about the role of the Bld10 more knowledge, i.e. more studies are required.

This study offers in-depth insight into the Bld10p localization. Taken together immunolocalization observations suggest Bld10 localization to parental basal bodies. Hence, as a result of these findings we question the role of Bld10p as a cartwheel principal structural protein. Besides, different intensity of the spots observed in the immunofluorescence analyses (one large spot and one small spot) leads to the conclusion that expression of the Bld10 protein could be developmentally regulated. Additionally, some insights are coming from the immunoelectron localization data of Bld10p. Although the

immunoelectron microscopy results have not been evaluated quantitatively, the Bld10 localization to the cartwheel is detected.

4.3. Bld10 protein forms a protein complex

In this PhD thesis I demonstrated that Bld10p forms a complex that has a size of about 600 kDa. This result was achieved by employing blue native polyacrylamide electrophoresis, an effective technique to detect protein complexes. It is well known that protein-protein interactions are fundamental for all biological processes, ranging from the formation of the cellular structures to the regulation of signaling pathways (Miernyk and Thelen, 2008). Physiological protein-protein interactions can be identified by different technologies, such as yeast-two hybrid screening, Far-Western blotting, co-immunoprecipitation, and separation of the protein complexes by native electrophoresis. Additionally, the generated polyclonal antibodies against cartwheel protein Bld10 could be employed to find interacting partners of the Bld10p.

Interestingly, in spite of the specificity of the antibodies, particularly the anti-C antibody, the affinity techniques like co-immunoprecipitation and Far-Western blotting did not produce any results i.e. did not reveal interacting partners of Bld10p. One of the possible explanations why immunoprecipitation did not work could be that the antibodies I used were either generated against partial protein or were peptide antibodies, which make it complicated to detect a protein in a native conformation. In contrast, in Western blotting proteins are denatured, i.e. molecules are linear that is why Bld10 can be detected by the polyclonal antibodies. In Far-Western method the problem could be the partial nature of the protein (antigen C), which should detect unknown interacting proteins. In this case proteins may not be able to interact, resulting in a failure to identify an interaction.

Interestingly, despite the fact that Bld10p was discovered about five years ago, no information about possible interacting partners of the protein is reported. However, a negative result obtained with these methods does not mean that the protein has no interacting partners. In some instances it is recommended to use more than one method to detect interacting partners of desired protein.

Therefore, Blue Native PAGE as another powerful approach to study protein interactions was employed. Blue Native PAGE as a technique, which enables separation of the protein complexes by their apparent molecular mass. The combination of mild detergents and Coomassie dye, substituting for the highly denaturing detergent sodium dodecyl sulfate (SDS) made it possible to separate intact respiratory complexes by electrophoresis (Schagger and von Jagow, 1991). Initially, Blue Native PAGE was developed to study mitochondrial proteins and since then was extensively used for the respiratory chain and the photosynthetic complexes in different organisms. Intriguingly, there is no report about the BN-PAGE application to study cytoskeleton protein complexes. Therefore, some components from the original Blue Native PAGE protocol (Schagger and von Jagow, 1991) were modified in order to adapt it to my purposes.

The choice of the detergent was very crucial in order to extract but not disrupt protein complexes. The usage of nonionic detergents like Triton X-100 was ruled out, because of their feature to form micelles and thus helping to aggregate cytoskeleton proteins. Instead the chaotropic agent urea was used. Although urea is a strong detergent and can dissociate many protein complexes, it was the only detergent that made it possible to solubilize cytoskeletons. So, cytoskeletons were treated with urea to solubilize the components of the cytoskeleton.

Instead of defined band in the BN-gel a smear of non-defined bands or the smear over the whole length of the gel was observed (Figure 24A). The smear might appear due to protein aggregation or the proteins are present as overlapping multiprotein complexes (Swamy et al., 2006). Besides, monovalent cations or other small molecules that negatively influence the electrophoresis might cause a poor separation. Despite the smear in the BN gel, the Western blotting using anti-C antibody detected a prominent band at about 600 kDa (Figure 25) Additionally, to identify and analyze protein complexes in more detail it was important to perform second dimension electrophoresis. Second dimension SDS-PAGE of the BN-gel was performed in order to detect the monomeric constituents of the complex. Besides, it would bring more understanding, since in BN-PAGE no clear band was observed. Although the second dimension gel showed spots, the amount of protein was too low for the further mass spectrometric analyses (Figure 24C). However, the Western blotting analyses of the second dimension BN/SDS-PAGE showed the same result: a prominent spot of a complex which has a size of about 600 kDa in a first dimension and 175 kDa in a second dimension

(the molecular weight of Bld10) (Figure 26B). Thus we can conclude that the Bld10 forms a complex. Whether with other unknown/known protein or itself still remains to be elucidated.

The major limitation in BN-PAGE was the amount of protein loaded on a gel. The difficulties with cytoskeleton solubilization made it impossible to solubilize the cytoskeletons in less amount of the solubilization buffer than it was used. Although almost 30 µg of the protein was loaded on a gel, some of the solubilized cytoskeletons precipitated in the gel pocket and wouldn't completely enter in a gel. This was the reason that in second dimensional gel electrophoresis only very small dots were visible.

Obviously, co-migration of the proteins on BN-gels is not the definite proof of native association since discrete complexes may have similar molecular weight and as a result may appear in the same band. However, the resolution of the BN-PAGE is much higher than standard gel filtration chromatography techniques and if the sample is well-fractionated to reduce complexity it is considered as a strong evidence for association (Eubel et al., 2005).

It is important to emphasize that for the first time there is the indication of the Bld10p being in a complex. Clearly, we cannot exclude the interaction of Bld10p with itself, but even this interaction might be interesting.

4.4. Future perspectives

In this PhD thesis two main findings were achieved. First, it has been shown that the cartwheel protein Bld10 forms a complex. Second, the immunolocalization data suggest Bld10p localization to parental basal bodies, rather than to probasal bodies.

The observations reported here provide key insight into details of the Bdl10 localization. Besides our immunoelectron microscopy studies have shown Bld10 localization to the cartwheel of the basal bodies.

The immunofluorescence results along with Bld10 orthologs sequence comparison supported the hypothesis that Bld10 is not an important structural protein of the cartwheel. However, to better understand the role of the cartwheel protein Bld10 detailed immunoelectron microscopical examinations are needed. In the future, it would be very interesting to investigate to what extend Bld10 contributes to the cartwheel composition.

5. References

Alvey, P. L. (1986). "Do adult centrioles contain cartwheels and lie at right angles to each other?" Cell Biol Int Rep **10**(8): 589-98.

Asamizu, E., K. Miura, K. Kucho, Y. Inoue, H. Fukuzawa, K. Ohyama, Y. Nakamura and S. Tabata (2000). "Generation of expressed sequence tags from low-CO2 and high-CO2 adapted cells of *Chlamydomonas reinhardtii*." DNA Res **7**(5): 305-7.

Asamizu, E. and Y. Nakamura (2004). "[System for expressed sequence tags (EST) analysis]." Tanpakushitsu Kakusan Koso **49**(11 Suppl): 1847-52.

Asamizu, E., Y. Nakamura, S. Sato, H. Fukuzawa and S. Tabata (1999). "A large scale structural analysis of cDNAs in a unicellular green alga, Chlamydomonas reinhardtii. I. Generation of 3433 non-redundant expressed sequence tags." DNA Res **6**(6): 369-73.

Azimzadeh, J. a. B., M. (2004). "The centrosome in evolution." Centrosomes in Development and Disease: 93-122.

Basto, R., J. Lau, T. Vinogradova, A. Gardiol, C. G. Woods, A. Khodjakov and J. W. Raff (2006). "Flies without centrioles." Cell **125**(7): 1375-86.

Batteiger, B., W. J. t. Newhall and R. B. Jones (1982). "The use of Tween 20 as a blocking agent in the immunological detection of proteins transferred to nitrocellulose membranes." J Immunol Methods **55**(3): 297-307.

Beech, P. and M. Melkonian (1993). "The basal apparatus of the quadriflagellate Spermatozopsis exsultans (Chlorophycea): numbering of basal body triplets reveals triplet individuality and developmental modifications." J Phycol **29**: 191-202.

Bendayan, M. and M. Zollinger (1983). "Ultrastructural localization of antigenic sites on osmium-fixed tissues applying the protein A-gold technique." J Histochem Cytochem **31**(1): 101-9.

Binarova, P., V. Cenklova, J. Prochazkova, A. Doskocilova, J. Volc, M. Vrlik and L. Bogre (2006). "Gamma-tubulin is essential for acentrosomal microtubule nucleation and coordination of late mitotic events in Arabidopsis." Plant Cell **18**(5): 1199-212.

Blacque, O. E., S. Cevik and O. I. Kaplan (2008). "Intraflagellar transport: from molecular characterisation to mechanism." Front Biosci **13**: 2633-52.

Bobinnec, Y., A. Khodjakov, L. M. Mir, C. L. Rieder, B. Edde and M. Bornens (1998). "Centriole disassembly in vivo and its effect on centrosome structure and function in vertebrate cells." J Cell Biol **143**(6): 1575-89.

Boletta, A. and G. G. Germino (2003). "Role of polycystins in renal tubulogenesis." Trends Cell Biol **13**(9): 484-92.

Bornens, M. (2002). "Centrosome composition and microtubule anchoring mechanisms." Curr Opin Cell Biol **14**(1): 25-34.

Boveri, T. (1901). "Zellen-Studien IV. Über die Natur der Centrosomen." Jena. Z. Med. Naturw. **28**: 1-220.

Boynton, J. E., N. W. Gillham, E. H. Harris, J. P. Hosler, A. M. Johnson, A. R. Jones, B. L. Randolph-Anderson, D. Robertson, T. M. Klein and K. B. Shark (1988). "Chloroplast transformation in Chlamydomonas with high velocity microprojectiles." Science **240**(4858): 1534-8.

Brachhold, K. (2007). "Das Basalapparat-Subproteom von *Chlamydomonas reinhardtii*." Dissertation, Botanical Institute, University of Cologne.

Bradford, M. M. (1976). "A rapid and sensitive method for the quantitation of microgram quantities of protein utilizing the principle of protein-dye binding." Anal Biochem **72**: 248-54.

Brazelton, W. J., C. D. Amundsen, C. D. Silflow and P. A. Lefebvre (2001). "The bld1 mutation identifies the Chlamydomonas osm-6 homolog as a gene required for flagellar assembly." Curr Biol **11**(20): 1591-4.

Broadhead, R., H. R. Dawe, H. Farr, S. Griffiths, S. R. Hart, N. Portman, M. K. Shaw, M. L. Ginger, S. J. Gaskell, P. G. McKean and K. Gull (2006). "Flagellar motility is required for the viability of the bloodstream trypanosome." Nature **440**(7081): 224-7.

Callaini, G., W. G. Whitfield and M. G. Riparbelli (1997). "Centriole and centrosome dynamics during the embryonic cell cycles that follow the formation of the cellular blastoderm in Drosophila." Exp Cell Res **234**(1): 183-90.

Cavalier-Smith, T. (1974). "Basal body and flagellar development during the vegetative cell cycle and the sexual cycle of Chlamydomonas reinhardii." J Cell Sci **16**(3): 529-56.

Cerutti, H. and J. A. Casas-Mollano (2006). "On the origin and functions of RNA-mediated silencing: from protists to man." Curr Genet **50**(2): 81-99.

Cole, D. G. (2003). "The intraflagellar transport machinery of Chlamydomonas reinhardtii." Traffic **4**(7): 435-42.

Coss, R. A. (1974). "Mitosis in Chlamydomonas reinhardtii basal bodies and the mitotic apparatus." J Cell Biol **63**(1): 325-9.

Dammermann, A., T. Muller-Reichert, L. Pelletier, B. Habermann, A. Desai and K. Oegema (2004). "Centriole assembly requires both centriolar and pericentriolar material proteins." Dev Cell **7**(6): 815-29.

Davies, D. R. and V. Lyall (1973). "The assembly of a highly ordered component of the cell wall: the role of heritable factors and of physical structure." Mol Gen Genet **124**(1): 21-34.

Davy, B. E. and M. L. Robinson (2003). "Congenital hydrocephalus in hy3 mice is caused by a frameshift mutation in Hydin, a large novel gene." Hum Mol Genet **12**(10): 1163-70.

Delattre, M. and P. Gonczy (2004). "The arithmetic of centrosome biogenesis." J Cell Sci **117**(Pt 9): 1619-30.

Dippell, R. V. (1968). "The development of basal bodies in Paramecium." Proc Natl Acad Sci U S A **61**(2): 461-8.

Doxsey, S. J., P. Stein, L. Evans, P. D. Calarco and M. Kirschner (1994). "Pericentrin, a highly conserved centrosome protein involved in microtubule organization." Cell **76**(4): 639-50.

Dutcher, S. K. (2003). "Elucidation of basal body and centriole functions in Chlamydomonas reinhardtii." Traffic **4**(7): 443-51.

Dutcher, S. K. (2007). "Finding treasures in frozen cells: new centriole intermediates." Bioessays **29**(7): 630-4.

Dutcher, S. K., N. S. Morrissette, A. M. Preble, C. Rackley and J. Stanga (2002). "Epsilon-tubulin is an essential component of the centriole." Mol Biol Cell **13**(11): 3859-69.

Dutcher, S. K. and E. C. Trabuco (1998). "The UNI3 gene is required for assembly of basal bodies of Chlamydomonas and encodes delta-tubulin, a new member of the tubulin superfamily." Mol Biol Cell **9**(6): 1293-308.

Ehrhardt, D. W. and S. L. Shaw (2006). "Microtubule dynamics and organization in the plant cortical array." Annu Rev Plant Biol **57**: 859-75.

Eubel, H., H. P. Braun and A. H. Millar (2005). "Blue-native PAGE in plants: a tool in analysis of protein-protein interactions." Plant Methods **1**(1): 11.

Feldman, J. L., S. Geimer and W. F. Marshall (2007). "The mother centriole plays an instructive role in defining cell geometry." PLoS Biol **5**(6): e149.

Fuller, S. D., B. E. Gowen, S. Reinsch, A. Sawyer, B. Buendia, R. Wepf and E. Karsenti (1995). "The core of the mammalian centriole contains gamma-tubulin." Curr Biol **5**(12): 1384-93.

Geimer, S., J. Clees, M. Melkonian and K. F. Lechtreck (1998(a)). "A novel 95-kD protein is located in a linker between cytoplasmic microtubules and basal bodies in a green flagellate and forms striated filaments in vitro." J Cell Biol **140**(5): 1149-58.

Geimer, S., K.-F. Lechtreck and M. Melkonian (1998(b)). "A novel basal apparatus protein of 90 kD (BAp90) from the flagellate green alga Spermatozopsis similis is a component of the proximal plates and identifies the d-(dexter)surface of the basal body." Protist **149**: 173-184.

Geimer, S. and M. Melkonian (2004). "The ultrastructure of the Chlamydomonas reinhardtii basal apparatus: identification of an early marker of radial asymmetry inherent in the basal body." J Cell Sci **117**(Pt 13): 2663-74.

Geimer, S. and M. Melkonian (2005). "Centrin scaffold in Chlamydomonas reinhardtii revealed by immunoelectron microscopy." Eukaryot Cell **4**(7): 1253-63.

Gibbons, I. R. and A. V. Grimstone (1960). "On flagellar structure in certain flagellates." J Biophys Biochem Cytol **7**: 697-716.

Gould, R. R. (1975). "The basal bodies of Chlamydomonas reinhardtii. Formation from probasal bodies, isolation, and partial characterization." J Cell Biol **65**(1): 65-74.

Graf, R., C. Daunderer and M. Schliwa (1999). "Cell cycle-dependent localization of monoclonal antibodies raised against isolated Dictyostelium centrosomes." Biol Cell **91**(6): 471-7.

Guan, P., I. A. Doytchinova, C. Zygouri and D. R. Flower (2003). "MHCPred: A server for quantitative prediction of peptide-MHC binding." Nucleic Acids Res **31**(13): 3621-4.

Harris, E. H. (1989). "The Chlamydomonas sourcebook." Acedemic Press, New York.

Harris, E. H. (2001). "Chlamydomonas as a Model Organism." Annu Rev Plant Physiol Plant Mol Biol **52**: 363-406.

Harris, E. H. (2008). "Chlamydomonas Sourcebook." **Volume 1**.

Henneguy, L. F. (1898). "Sur les rapports des cils vibratiles avec les centrosomes." Archives d'Anatomie Microscopique **1**: 481-496.

Hinchcliffe, E. H., F. J. Miller, M. Cham, A. Khodjakov and G. Sluder (2001). "Requirement of a centrosomal activity for cell cycle progression through G1 into S phase." Science **291**(5508): 1547-50.

Hiraki, M., Y. Nakazawa, R. Kamiya and M. Hirono (2007). "Bld10p constitutes the cartwheel-spoke tip and stabilizes the 9-fold symmetry of the centriole." Curr Biol **17**(20): 1778-83.

Huang, B., Z. Ramanis, S. K. Dutcher and D. J. Luck (1982). "Uniflagellar mutants of Chlamydomonas: evidence for the role of basal bodies in transmission of positional information." Cell **29**(3): 745-53.

Khodjakov, A., R. W. Cole, B. R. Oakley and C. L. Rieder (2000). "Centrosome-independent mitotic spindle formation in vertebrates." Curr Biol **10**(2): 59-67.

Khodjakov, A., C. L. Rieder, G. Sluder, G. Cassels, O. Sibon and C. L. Wang (2002). "De novo formation of centrosomes in vertebrate cells arrested during S phase." J Cell Biol **158**(7): 1171-81.

Kim, K., S. Lee, J. Chang and K. Rhee (2008). "A novel function of CEP135 as a platform protein of C-NAP1 for its centriolar localization." Exp Cell Res **314**(20): 3692-700.

Kindle, K. L. (1990). "High-frequency nuclear transformation of Chlamydomonas reinhardtii." Proc Natl Acad Sci U S A **87**(3): 1228-32.

Kindle, K. L., R. A. Schnell, E. Fernandez and P. A. Lefebvre (1989). "Stable nuclear transformation of Chlamydomonas using the Chlamydomonas gene for nitrate reductase." J Cell Biol **109**(6 Pt 1): 2589-601.

Kleylein-Sohn, J., J. Westendorf, M. Le Clech, R. Habedanck, Y. D. Stierhof and E. A. Nigg (2007). "Plk4-induced centriole biogenesis in human cells." Dev Cell **13**(2): 190-202.

Kozminski, K. G., K. A. Johnson, P. Forscher and J. L. Rosenbaum (1993). "A motility in the eukaryotic flagellum unrelated to flagellar beating." Proc Natl Acad Sci U S A **90**(12): 5519-23.

Kubo, A. and S. Tsukita (2003). "Non-membranous granular organelle consisting of PCM-1: subcellular distribution and cell-cycle-dependent assembly/disassembly." J Cell Sci **116**(Pt 5): 919-28.

Laemmli, U. K. (1970). "Cleavage of structural proteins during the assembly of the head of bacteriophage T4." Nature **227**(5259): 680-5.

Lambert, A. M. (1993). "Microtubule-organizing centers in higher plants." Curr Opin Cell Biol **5**(1): 116-22.

Lange, B. M. and K. Gull (1996). "Structure and function of the centriole in animal cells: progress and questions." Trends Cell Biol **6**(9): 348-52.

Lechtreck, K. F. and A. Grunow (1999). "Evidence for a direct role of nascent basal bodies during spindle pole initiation in the green alga Spermatozopsis similis." Protist **150**(2): 163-81.

Lechtreck, K. F. and M. Melkonian (1991). "Striated microtubule-associated fibers: identification of assemblin, a novel 34-kD protein that forms paracrystals of 2-nm filaments in vitro." J Cell Biol **115**(3): 705-16.

Lechtreck, K. F. and G. B. Witman (2007). "Chlamydomonas reinhardtii hydin is a central pair protein required for flagellar motility." J Cell Biol **176**(4): 473-82.

Lenhossek, M. (1898). "Über Flimmerzellen." Verhandl. der Anat. Gesel. **12**: 106-128.

Li, J. B., J. M. Gerdes, C. J. Haycraft, Y. Fan, T. M. Teslovich, H. May-Simera, H. Li, O. E. Blacque, L. Li, C. C. Leitch, R. A. Lewis, J. S. Green, P. S. Parfrey, M. R. Leroux, W. S. Davidson, P. L. Beales, L. M. Guay-Woodford, B. K. Yoder, G. D. Stormo, N. Katsanis and S. K. Dutcher (2004). "Comparative genomics identifies a flagellar and basal body proteome that includes the BBS5 human disease gene." Cell **117**(4): 541-52.

Lien, T. and G. Knutsen (1976). "Synchronized cultures of a cell wall-less mutant of Chylamydomonas reinhardii." Arch Microbiol **108**(2): 189-94.

Lingle, W. L., S. L. Barrett, V. C. Negron, A. B. D'Assoro, K. Boeneman, W. Liu, C. M. Whitehead, C. Reynolds and J. L. Salisbury (2002). "Centrosome amplification drives chromosomal instability in breast tumor development." Proc Natl Acad Sci U S A **99**(4): 1978-83.

Loncarek, J. and A. Khodjakov (2009). "Ab ovo or de novo? Mechanisms of centriole duplication." Mol Cells **27**(2): 135-42.

Lupas, A., M. Van Dyke and J. Stock (1991). "Predicting coiled coils from protein sequences." Science **252**(5009): 1162-1164.

Mansir, A. and J. L. Justine (1998). "The microtubular system and posttranslationally modified tubulin during spermatogenesis in a parasitic nematode with amoeboid and aflagellate spermatozoa." Mol Reprod Dev **49**(2): 150-67.

Marshall, W. F. (2004). "Human cilia proteome contains homolog of zebrafish polycystic kidney disease gene qilin." Curr Biol **14**(21): R913-4.

Marshall, W. F. (2007). "What is the function of centrioles?" J Cell Biochem **100**(4): 916-22.

Marshall, W. F. (2008). "The cell biological basis of ciliary disease." J Cell Biol **180**(1): 17-21.

Marshall, W. F., Y. Vucica and J. L. Rosenbaum (2001). "Kinetics and regulation of de novo centriole assembly. Implications for the mechanism of centriole duplication." Curr Biol **11**(5): 308-17.

Matsuura, K., P. A. Lefebvre, R. Kamiya and M. Hirono (2004). "Bld10p, a novel protein essential for basal body assembly in Chlamydomonas: localization to the cartwheel, the first ninefold symmetrical structure appearing during assembly." J Cell Biol **165**(5): 663-71.

McDonald, K. and M. K. Morphew (1993). "Improved preservation of ultrastructure in difficult-to-fix organisms by high pressure freezing and freeze substitution: I. Drosophila melanogaster and Strongylocentrotus purpuratus embryos." Microsc Res Tech **24**(6): 465-73.

Megraw, T. L., S. Kilaru, F. R. Turner and T. C. Kaufman (2002). "The centrosome is a dynamic structure that ejects PCM flares." J Cell Sci **115**(Pt 23): 4707-18.

Melkonian, M. (1980). "Ultrastructural aspects of basal body associated fibrous structures in green algae: a critical review." Biosystems **12**(1-2): 85-104.

Meraldi, P. and E. A. Nigg (2002). "The centrosome cycle." FEBS Lett **521**(1-3): 9-13.

Merchant, S. S., S. E. Prochnik, O. Vallon, E. H. Harris, S. J. Karpowicz, G. B. Witman, A. Terry, A. Salamov, L. K. Fritz-Laylin, L. Marechal-Drouard, W. F. Marshall, L. H. Qu, D. R. Nelson, A. A. Sanderfoot, M. H. Spalding, V. V. Kapitonov, Q. Ren, P. Ferris, E. Lindquist, H. Shapiro, S. M. Lucas, J. Grimwood, J. Schmutz, P. Cardol, H. Cerutti, G. Chanfreau, C. L. Chen, V. Cognat, M. T. Croft, R. Dent, S. Dutcher, E. Fernandez, H. Fukuzawa, D. Gonzalez-Ballester, D. Gonzalez-Halphen, A. Hallmann, M. Hanikenne, M. Hippler, W. Inwood, K. Jabbari, M. Kalanon, R. Kuras, P. A. Lefebvre, S. D. Lemaire, A. V. Lobanov, M. Lohr, A. Manuell, I. Meier, L. Mets, M. Mittag, T. Mittelmeier, J. V. Moroney, J. Moseley, C. Napoli, A. M. Nedelcu, K. Niyogi, S. V. Novoselov, I. T. Paulsen, G. Pazour, S. Purton, J. P. Ral, D. M. Riano-Pachon, W. Riekhof, L. Rymarquis, M. Schroda, D. Stern, J. Umen, R. Willows, N. Wilson, S. L. Zimmer, J. Allmer, J. Balk, K. Bisova, C. J. Chen, M. Elias, K. Gendler, C. Hauser, M. R. Lamb, H. Ledford, J. C. Long, J. Minagawa, M. D. Page, J. Pan, W. Pootakham, S. Roje, A. Rose, E. Stahlberg, A. M. Terauchi, P. Yang, S. Ball, C. Bowler, C. L. Dieckmann, V. N. Gladyshev, P. Green, R. Jorgensen, S. Mayfield, B. Mueller-Roeber, S. Rajamani, R. T. Sayre, P. Brokstein, I. Dubchak, D. Goodstein, L. Hornick, Y. W. Huang, J. Jhaveri, Y. Luo, D. Martinez, W. C. Ngau, B. Otillar, A. Poliakov, A. Porter, L. Szajkowski, G. Werner, K. Zhou, I. V. Grigoriev, D. S. Rokhsar and A. R. Grossman (2007). "The Chlamydomonas genome reveals the evolution of key animal and plant functions." Science **318**(5848): 245-50.

Miernyk, J. A. and J. J. Thelen (2008). "Biochemical approaches for discovering protein-protein interactions." Plant J **53**(4): 597-609.

Molnar, A., F. Schwach, D. J. Studholme, E. C. Thuenemann and D. C. Baulcombe (2007). "miRNAs control gene expression in the single-cell alga Chlamydomonas reinhardtii." Nature **447**(7148): 1126-9.

Moritz, M., M. B. Braunfeld, J. C. Fung, J. W. Sedat, B. M. Alberts and D. A. Agard (1995). "Three-dimensional structural characterization of centrosomes from early Drosophila embryos." J Cell Biol **130**(5): 1149-59.

Moritz, M., M. B. Braunfeld, V. Guenebaut, J. Heuser and D. A. Agard (2000). "Structure of the gamma-tubulin ring complex: a template for microtubule nucleation." Nat Cell Biol **2**(6): 365-70.

Mottier-Pavie, V. and T. L. Megraw (2009). "Drosophila bld10 is a centriolar protein that regulates centriole, basal body, and motile cilium assembly." Mol Biol Cell **20**(10): 2605-14.

Nakazawa, Y., M. Hiraki, R. Kamiya and M. Hirono (2007). "SAS-6 is a cartwheel protein that establishes the 9-fold symmetry of the centriole." Curr Biol **17**(24): 2169-74.

Neuhoff, V., K. Philipp, H. G. Zimmer and S. Mesecke (1979). "A simple, versatile, sensitive and volume-independent method for quantitative protein determination which is independent of other external influences." Hoppe Seylers Z Physiol Chem **360**(11): 1657-70.

O'Connell, K. F., C. Caron, K. R. Kopish, D. D. Hurd, K. J. Kemphues, Y. Li and J. G. White (2001). "The C. elegans zyg-1 gene encodes a regulator of centrosome duplication with distinct maternal and paternal roles in the embryo." Cell **105**(4): 547-58.

O'Toole, E. T., T. H. Giddings, J. R. McIntosh and S. K. Dutcher (2003). "Three-dimensional organization of basal bodies from wild-type and delta-tubulin deletion strains of Chlamydomonas reinhardtii." Mol Biol Cell **14**(7): 2999-3012.

Oakley, B. R., C. E. Oakley, Y. Yoon and M. K. Jung (1990). "Gamma-tubulin is a component of the spindle pole body that is essential for microtubule function in Aspergillus nidulans." Cell **61**(7): 1289-301.

Oakley, C. E. and B. R. Oakley (1989). "Identification of gamma-tubulin, a new member of the tubulin superfamily encoded by mipA gene of Aspergillus nidulans." Nature **338**(6217): 662-4.

Ohta, T., R. Essner, J. H. Ryu, R. E. Palazzo, Y. Uetake and R. Kuriyama (2002). "Characterization of Cep135, a novel coiled-coil centrosomal protein involved in microtubule organization in mammalian cells." J Cell Biol **156**(1): 87-99.

Ostrowski, L. E., K. Blackburn, K. M. Radde, M. B. Moyer, D. M. Schlatzer, A. Moseley and R. C. Boucher (2002). "A proteomic analysis of human cilia: identification of novel components." Mol Cell Proteomics **1**(6): 451-65.

Pascher, A. (1918). "Über die Beziehung der Reduktionsteilung zur Mendelschen Spaltung." Ber Otsch Bot Ges **36**: 163-168.

Pastuglia, M., J. Azimzadeh, M. Goussot, C. Camilleri, K. Belcram, J. L. Evrard, A. C. Schmit, P. Guerche and D. Bouchez (2006). "Gamma-tubulin is essential for microtubule organization and development in Arabidopsis." Plant Cell **18**(6): 1412-25.

Pazour, G. J., N. Agrin, J. Leszyk and G. B. Witman (2005). "Proteomic analysis of a eukaryotic cilium." J Cell Biol **170**(1): 103-13.

Pazour, G. J. and G. B. Witman (2003). "The vertebrate primary cilium is a sensory organelle." Curr Opin Cell Biol **15**(1): 105-10.

Peel, N., N. R. Stevens, R. Basto and J. W. Raff (2007). "Overexpressing centriole-replication proteins in vivo induces centriole overduplication and de novo formation." Curr Biol **17**(10): 834-43.

Piasecki, B. P. and C. D. Silflow (2009). "The UNI1 and UNI2 genes function in the transition of triplet to doublet microtubules between the centriole and cilium in Chlamydomonas." Mol Biol Cell **20**(1): 368-78.

Pickett-Heaps, J. D. (1969). "The evolution of the mitotic apparatus, an attempt at comparative ultrastructural cytology in dividing cell plants." Cytobios **1**: 257-280.

Preble, A. M., T. M. Giddings, Jr. and S. K. Dutcher (2000). "Basal bodies and centrioles: their function and structure." Curr Top Dev Biol **49**: 207-33.

Pröschold, T., E. H. Harris and A. W. Coleman (2005). "Portrait of a species: Chlamydomonas reinhardtii." Genetics **170**(4): 1601-10.

Randolph-Anderson, B. L., J. E. Boynton, N. W. Gillham, E. H. Harris, A. M. Johnson, M. P. Dorthu and R. F. Matagne (1993). "Further characterization of the respiratory deficient dum-1 mutation of Chlamydomonas reinhardtii and its use as a recipient for mitochondrial transformation." Mol Gen Genet **236**(2-3): 235-44.

Rao, P. N., J. Y. Zhao, R. K. Ganju and C. L. Ashorn (1989). "Monoclonal antibody against the centrosome." J Cell Sci **93 (Pt 1)**: 63-9.

Reynolds, E. S. (1963). "The use of lead citrate at high pH as an electron-opaque stain in electron microscopy." J. Cell. Biol. **17**: 208-212.

Ringo, D. L. (1967). "Flagellar motion and fine structure of the flagellar apparatus in Chlamydomonas." J Cell Biol **33**(3): 543-71.

Rodrigues-Martins, A., M. Bettencourt-Dias, M. Riparbelli, C. Ferreira, I. Ferreira, G. Callaini and D. M. Glover (2007). "DSAS-6 organizes a tube-like centriole precursor, and its absence suggests modularity in centriole assembly." Curr Biol **17**(17): 1465-72.

Rolland, N., A. Atteia, P. Decottignies, J. Garin, M. Hippler, G. Kreimer, S. D. Lemaire, M. Mittag and V. Wagner (2009). "Chlamydomonas proteomics." Curr Opin Microbiol.

Rosenbaum, J. L. and G. B. Witman (2002). "Intraflagellar transport." Nat Rev Mol Cell Biol **3**(11): 813-25.

Ruiz-Binder, N. E., S. Geimer and M. Melkonian (2002). "In vivo localization of centrin in the green alga Chlamydomonas reinhardtii." Cell Motil Cytoskeleton **52**(1): 43-55.

Sager, R. (1960). "Genetic systems in Chlamydomonas." Science **132**: 1459-65.

Salisbury, J. L. (1995). "Centrin, centrosomes, and mitotic spindle poles." Curr Opin Cell Biol **7**(1): 39-45.

Salisbury, J. L., A. Baron, B. Surek and M. Melkonian (1984). "Striated flagellar roots: isolation and partial characterization of a calcium-modulated contractile organelle." J Cell Biol **99**(3): 962-70.

Salisbury, J. L., K. M. Suino, R. Busby and M. Springett (2002). "Centrin-2 is required for centriole duplication in mammalian cells." Curr Biol **12**(15): 1287-92.

Salisbury, J. L., C. M. Whitehead, W. L. Lingle and S. L. Barrett (1999). "Centrosomes and cancer." Biol Cell **91**(6): 451-60.

Schagger, H. and G. von Jagow (1991). "Blue native electrophoresis for isolation of membrane protein complexes in enzymatically active form." Anal Biochem **199**(2): 223-31.

Schmidt, T. I., J. Kleylein-Sohn, J. Westendorf, M. Le Clech, S. B. Lavoie, Y. D. Stierhof and E. A. Nigg (2009). "Control of centriole length by CPAP and CP110." Curr Biol **19**(12): 1005-11.

Schmit, A. C. (2002). "Acentrosomal microtubule nucleation in higher plants." Int Rev Cytol **220**: 257-89.

Scholey, J. M. (2008). "Intraflagellar transport motors in cilia: moving along the cell's antenna." J Cell Biol **180**(1): 23-9.

Schrevel, J. and C. Besse (1975). "A functional flagella with a 6 + 0 pattern." J Cell Biol **66**(3): 492-507.

Schroda, M. (2006). "RNA silencing in Chlamydomonas: mechanisms and tools." Curr Genet **49**(2): 69-84.

Schulz-Raffelt, M., M. Lodha and M. Schroda (2007). "Heat shock factor 1 is a key regulator of the stress response in Chlamydomonas." Plant J **52**(2): 286-95.

Shrager, J., C. Hauser, C. W. Chang, E. H. Harris, J. Davies, J. McDermott, R. Tamse, Z. Zhang and A. R. Grossman (2003). "Chlamydomonas reinhardtii genome project. A guide to the generation and use of the cDNA information." Plant Physiol **131**(2): 401-8.

Silflow, C. D., M. LaVoie, L. W. Tam, S. Tousey, M. Sanders, W. Wu, M. Borodovsky and P. A. Lefebvre (2001). "The Vfl1 Protein in Chlamydomonas localizes in a rotationally asymmetric pattern at the distal ends of the basal bodies." J Cell Biol **153**(1): 63-74.

Silflow, C. D., B. Liu, M. LaVoie, E. A. Richardson and B. A. Palevitz (1999). "Gamma-tubulin in Chlamydomonas: characterization of the gene and localization of the gene product in cells." Cell Motil Cytoskeleton **42**(4): 285-97.

Sodeinde, O. A. and K. L. Kindle (1993). "Homologous recombination in the nuclear genome of Chlamydomonas reinhardtii." Proc Natl Acad Sci U S A **90**(19): 9199-203.

Spektor, A., W. Y. Tsang, D. Khoo and B. D. Dynlacht (2007). "Cep97 and CP110 suppress a cilia assembly program." Cell **130**(4): 678-90.

Strnad, P. and P. Gonczy (2008). "Mechanisms of procentriole formation." Trends Cell Biol **18**(8): 389-96.

Strnad, P., S. Leidel, T. Vinogradova, U. Euteneuer, A. Khodjakov and P. Gonczy (2007). "Regulated HsSAS-6 levels ensure formation of a single procentriole per centriole during the centrosome duplication cycle." Dev Cell **13**(2): 203-13.

Stubblefield, E. a. B., B. (1967). "Architecture and function of the mammalian centriole." In: Formation and Fate of Cell Organelles, Ed. Warren, K.B: 175-218.

Sueoka, N. (1960). "Mitotic Replication of Deoxyribonucleic Acid in Chlamydomonas Reinhardi." Proc Natl Acad Sci U S A **46**(1): 83-91.

Swamy, M., G. M. Siegers, S. Minguet, B. Wollscheid and W. W. Schamel (2006). "Blue native polyacrylamide gel electrophoresis (BN-PAGE) for the identification and analysis of multiprotein complexes." Sci STKE **2006**(345): pl4.

Towbin, H., T. Staehelin and J. Gordon (1979). "Electrophoretic transfer of proteins from polyacrylamide gels to nitrocellulose sheets: procedure and some applications." Proc Natl Acad Sci U S A **76**(9): 4350-4.

Tsang, W. Y., A. Spektor, S. Vijayakumar, B. R. Bista, J. Li, I. Sanchez, S. Duensing and B. D. Dynlacht (2009). "Cep76, a centrosomal protein that specifically restrains centriole reduplication." Dev Cell **16**(5): 649-60.

Uetake, Y., Y. Terada, J. Matuliene and R. Kuriyama (2004). "Interaction of Cep135 with a p50 dynactin subunit in mammalian centrosomes." Cell Motil Cytoskeleton **58**(1): 53-66.

Urbani, L. and T. Stearns (1999). "The centrosome." Curr Biol **9**(9): R315-7.

Vogel, J. M., T. Stearns, C. L. Rieder and R. E. Palazzo (1997). "Centrosomes isolated from Spisula solidissima oocytes contain rings and an unusual stoichiometric ratio of alpha/beta tubulin." J Cell Biol **137**(1): 193-202.

Ward, S., Y. Argon and G. A. Nelson (1981). "Sperm morphogenesis in wild-type and fertilization-defective mutants of Caenorhabditis elegans." J Cell Biol **91**(1): 26-44.

Wiese, C. and Y. Zheng (2006). "Microtubule nucleation: gamma-tubulin and beyond." J Cell Sci **119**(Pt 20): 4143-53.

Wright, R. L., J. Salisbury and J. W. Jarvik (1985). "A nucleus-basal body connector in Chlamydomonas reinhardtii that may function in basal body localization or segregation." J Cell Biol **101**(5 Pt 1): 1903-12.

Yabe, T., X. Ge and F. Pelegri (2007). "The zebrafish maternal-effect gene cellular atoll encodes the centriolar component sas-6 and defects in its paternal function promote whole genome duplication." Dev Biol **312**(1): 44-60.

Zimmerman, W. and S. J. Doxsey (2000). "Construction of centrosomes and spindle poles by molecular motor-driven assembly of protein particles." Traffic **1**(12): 927-34.

Zorin, B., Y. Lu, I. Sizova and P. Hegemann (2009). "Nuclear gene targeting in Chlamydomonas as exemplified by disruption of the PHOT gene." Gene **432**(1-2): 91-6.

6. List of abbreviations

aa	amino acid
Ab	antibody
AP	alkaline phosphatase
APS	ammonium persulfate
bp	base pair
BBS	Bardet-Biedl Syndrome
BSA	bovine serum albumin
°C	Grad Celcius
ca.	circa
cDNA	complementary DNA
C-Terminus	carboxyl-terminus
cw	cartwheel
Da	dalton
DAPI	4',6' diamidino-2 phenylindole
dcf	distal connecting fiber
ddH_20	bidistilled water
DDM	n-dodecyl-beta-D-maltoside
DMSO	dimethilsulfoxide
DNA	deoxyribonucleic acid
dNTP	deoxynukleosid-5'-triphosphate
DTT	dithiothreitol
E	Einstein
EDTA	ethylenediaminitetraacetic acid
EGTA	ethyleneglycol tetraacetic acid
e.g.	*exempli gratia* - for example
et al.	*et alii* - and others
etc.	*et cetera* - and other things
EM	electron microscope
EST	expressed sequenced tag
FITC	fluorescein isothiocyanate

g	gramm
g	gravity units
i.e.	*id est* – that is
GFP	green fluorescent protein
HPLC	high performance liquid chromatography
HSM	high salt concentration medium
IFT	intraflagellar transport
IgG	immunoglobulin G
IPTG	isopropyl-1-thio-beta-D-galactoside
JGI	Joint Genome Institute
kb	kilobase
kDA	kilodalton
l	liter
M	mole
max	maximal
MW	molecular weight
min	minute
miRNA	micro RNA
mpcf	median proximal connecting fiber
mRNA	messenger RNA
mt	mating type
MT	microtubule
MT-buffer	microtubule stabilizing buffer
MTOC	microtubule organizing center
N	normality
NBBC	nucleus-basal body connector
NBT	4-nitro-blue-tetrazolium chloride
NP-40	nonidet P-40
OD	optical density
PAGE	polyacrylamide gel electrophoresis
PCM	pericentriolar material
PCD	primary cilia dyskinesia

PCR	polymerase chain reaction
pH	potentia hydrogenii
PKD	polycystic kidney disease
PVDF	polyvinilidendifluorid
RNA	ribonucleic acid
rpm	revolutions per minute
RT	room temperature
sec	seconds
SDS	sodium dodecyl sulfate
siRNA	small interfering RNA
SMAF	striated microtubule associated fiber
SPB	spindle pole body
TCP	total cellular protein
TEMED	N,N,N',N-Tetramethylethylendiamine
tf	transitional fiber
Tm	melting temperature
tr	transitional region
U	unit
V	volt
vfl	variable flagella number (mutants)
v/v	volume/volume
w/v	weight/volume
W	Watt

7. Acknowledgements

Here I would like to express my gratitude to all those people who helped me to accomplish this work.

First of all, I want to thank my supervisor Prof. Michael Melkonian. His enormous devotion and commitments to science inspired me all the way through my PhD study. Without his encouragement, support and guidance this work would not be possible.

I extend my special thanks to Prof. Maria Leptin and Prof. Siegfried Roth not only for advising me during my PhD study as thesis committee members, but also for their active participation in numerous Graduate School organized activities.

I thank all members in our lab for creating warm and friendly working environment. To all these people I am grateful for my German proficiency and for never letting me feel that I am away from my country.

I thank Kerstin Brachhold for the helpful tips and the scrupulous proofreading of my thesis.

I would like to address my gratitude to Burkhard Becker for his interest and valuable scientific advises.

Thanks are due to Stefan Geimer for ultrathin sectioning and immunogold labeling, Christina Wölwer and Kristina Siliunas for the fruitful collaborations, Sebastian Hess for the help with microscopic photo imaging, CCAC (Culture Collection of Algae at the University of Cologne) for the *Chlamydomonas* mutant strains.

I would like to acknowledge Graduate School in Genetics and Functional Genomics (IGSGFG) for the funding, for the multicultural atmosphere, for all soft skills courses and many other things. I greatly appreciate the comprehensive work of the IGSGFG staff, in particular Isabell Witt and Brigitte von Wilcken-Bergmann. Their constant care and support was accompanying me over the last years.

I want to thank my husband for his love, patience and understanding at mostly happy, but sometimes heavy moments during these years and continuous help on completing this dissertation.

I want to express my gratitude to my family who live in a beautiful country Armenia for their mental support and encouragement, for having always stayed behind me. My mother and father I want to thank for giving me the best of gifts ever - education. My brother I would like to thank for his love and care and my baby-niece for her lovely inspirational smile that I could experience through the Internet.

Erklärung

Ich versichere, dass ich die von mir vorgelegte Dissertation selbständig angefertigt, die benutzten Quellen und Hilfsmittel vollständig angegeben und die Stellen der Arbeit – einschließlich Tabellen, Karten und Abbildungen – , die anderen Werken im Wortlaut oder dem Sinn nach entnommen sind, in jedem Einzelfall als Entlehnung kenntlich gemacht habe; dass diese Dissertation noch keiner anderen Fakultät oder Universität zur Prüfung vorgelegen hat; dass sie noch nicht veröffentlicht worden ist sowie, dass ich eine solche Veröffentlichung vor Abschluss des Promotionsverfahrens nicht vornehmen werde. Die Bestimmungen dieser Promotionsordnung sind mir bekannt. Die von mir vorgelegte Dissertation ist von Prof. Dr. M. Melkonian betreut worden.

Köln, den 22.08.2009

(Nelli Vardanyan)